

PDF hosted at the Radboud Repository of the Radboud University Nijmegen

The following full text is a publisher's version.

For additional information about this publication click this link.

<http://hdl.handle.net/2066/27452>

Please be advised that this information was generated on 2017-12-05 and may be subject to change.

Hemangioblastomas

Studies on the molecular genetic background

Thesis Radboud University Nijmegen, The Netherlands

ISBN: 90-9020587-X

Copyright © J.M.M. Gijtenbeek, 2006

Lay-out: Martien Frijns, Doetinchem

Cover design: Dr. Karl Brasse, Eyeland Design Network, Vreden, Germany

Printed by: PrintPartners Ipskamp, Enschede

The publication of this thesis was financially supported by:

GlaxoSmithKline B.V., Mundipharma Pharmaceuticals B.V., Novartis

Oncology, Pfizer B.V., Sanofi-Aventis B.V., Schering-Plough B.V.,

UCB Pharma B.V.

Hemangioblastomas

Studies on the molecular genetic background

Een wetenschappelijke proeve op het gebied van de
Medische Wetenschappen

Proefschrift

ter verkrijging van de graad van doctor
aan de Radboud Universiteit Nijmegen
op gezag van de Rector Magnificus, prof. dr. C.W.P.M. Blom,
volgens besluit van het College van Decanen
in het openbaar te verdedigen op dinsdag 20 juni 2006
des namiddags om 3.30 uur precies

door

J.M.M. Gijtenbeek

geboren op 30 juli 1962 te Halsteren

Promotor: Prof. dr. G.W.A.M. Padberg

Copromotores: Dr. P. Wesseling
Dr. J.W.M. Jeuken

Manuscriptcommissie: Prof. dr. A.H.M. Geurts van Kessel
Prof. dr. J.W.M. Lenders
Prof. dr. M.J. van den Bent (Erasmus MC/
Daniel den Hoed kliniek, Rotterdam)

Voor mijn ouders

Table of contents

Chapter 1	General introduction <i>Outline of the thesis</i> <i>Review of the clinical, histopathological, and molecular genetic features</i> <i>Molecular genetic techniques</i>	11
Chapter 2	Characteristic chromosomal aberrations in sporadic cerebellar hemangioblastomas revealed by comparative genomic hybridization <i>Journal of Neuro-Oncology 2001;52:241-247</i>	39
Chapter 3	Comparative genomic hybridization and von Hippel-Lindau mutation analysis in sporadic and hereditary hemangioblastomas: possible genetic heterogeneity <i>Journal of Neurosurgery 2002;97:977-982</i>	49
Chapter 4	Array-based comparative genomic hybridization analysis of sporadic hemangioblastomas <i>Submitted</i>	61
Chapter 5	Cyclin D1 genotype and expression in sporadic hemangioblastomas <i>Journal of Neuro-Oncology 2005;74:261-266</i>	73
Chapter 6	Molecular analysis as a tool in the differential diagnosis of VHL disease-related tumors <i>Diagnostic Molecular Pathology 2005;14:115-120</i>	85

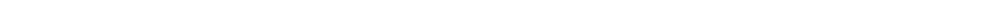
Chapter 7	Three-dimensional reconstruction of tumor micro-vasculature: Simultaneous visualization of multiple components in paraffin-embedded tissue <i>Angiogenesis 2005;8:297-305</i>	99
Chapter 8	Summary and general discussion	117
	References	131
	Nederlandse samenvatting	147
	Dankwoord	159
	Curriculum vitae	163
	List of publications	165

Abbreviations

BAC	bacterial artificial clones
CGH	comparative genomic hybridization
CNS	central nervous system
CT	computer tomography
<i>CCND1</i>	cyclin D1 gene
EGFR	epidermal growth factor receptor
GBM	glioblastoma multiforme
HB	hemangioblastoma
HIF	hypoxia-inducible factor
LOH	loss of heterozygosity
MRI	magnetic resonance imaging
PCR	polymerase chain reaction
PDGF	platelet-derived growth factor
pVHL	VHL protein
RCC	clear cell renal cell carcinoma
TGF	transforming growth factor
TSG	tumor suppressor gene
VEGF	vascular endothelial growth factor
VHL	Von Hippel-Lindau disease
WHO	World Health Organization

Chapter 1

General introduction



Introduction

A couple of years ago, a case of a hemangioblastoma (HB) that we encountered triggered a long and animated discussion with our neuropathologist. The issues raised and the questions posed regarding the intriguing histopathological and molecular genetic features of HBs inspired us to the studies described in this thesis.

HBs are highly vascularized benign tumors predominantly located in the cerebellum. They occur as sporadic tumors and as a manifestation of von Hippel-Lindau (VHL) disease, a hereditary tumor syndrome that results from a germline mutation in the *VHL* tumor suppressor gene (TSG).¹ We chose to focus our studies especially on sporadic HBs as the majority of HBs occur sporadically and the genetic background of sporadic tumors has not been elucidated. Our initial investigations suggested the involvement of multiple chromosomes in sporadic HBs. We extended our studies in that direction and compared the chromosomal abnormalities of sporadic and hereditary HBs in order to further clarify the genetic background of the sporadic tumors.

Molecular genetic changes in the *VHL* TSG have been reported in sporadic tumors as well. The identification of the *VHL* gene, and the subsequent unraveling of the functions of the VHL protein (pVHL), has given insight in the mechanisms leading to the rich vascular network of HBs. The exceptionally high vascularity is a histopathological hallmark of these tumors. However, *VHL* gene inactivation and loss of pVHL does not fully explain the mechanisms of tumor initiation.² Thus, even in VHL-associated HBs, inactivation of the *VHL* gene alone is probably not sufficient to initiate tumors, and other genes may act in collaboration with *VHL*. The identification of chromosomal abnormalities may help to detect the genes involved in the development of sporadic HBs, as well as additional genes involved in hereditary HBs. Unraveling of the genetic pathways of HBs may give insight in oncogenic mechanisms in general, and may lead to the identification of new therapeutic targets.

Aim and outline of the thesis

The aim of our studies was to elucidate the genetic background of sporadic HBs.

At the time we started our investigations, molecular genetic studies in sporadic HBs had been focused on mutations or loss of the *VHL* gene on chromosome 3p. The few cytogenetic studies of HBs had not revealed any additional chromosomal abnormalities.

Our first aim of study was to screen the genome of sporadic HBs in order to identify chromosomal regions of interest (in addition to 3p25-26), which might contain genes involved in the oncogenesis of these tumors. For this purpose, we used comparative genomic hybridization (CGH). With this technique, screening of the whole genome of a tumor is possible in a single experiment. CGH analysis assesses chromosomal imbalances, e.g. loss or gain of (part of a) chromosome(s). A lost chromosome may contain a TSG, while a gain of chromosome may indicate the presence of an oncogene.

The chromosomal imbalances identified by CGH in 10 sporadic HBs are described in **Chapter 2**. We suggested a specific sequence of chromosomal abnormalities in sporadic HBs, and compared our CGH results with the genetic pathways as reported in sporadic renal cell carcinomas (RCCs) and pheochromocytomas, two other tumor types that are relatively frequent in VHL disease. The finding of multiple chromosomal abnormalities in addition to loss of chromosome 3 supported our suggestion that the genetic pathways leading to sporadic HBs differ from the pathways involved in VHL-associated HBs.

Based on these results, we extended our studies to a larger group of sporadic HBs and to VHL-associated HBs, in order to compare the chromosomal aberrations detected by CGH in both tumor types (**Chapter 3**). Since the importance of the *VHL* gene in the oncogenesis of sporadic HBs has not been elucidated, we also performed mutation analysis of the *VHL* gene in all tumors. Genetic heterogeneity between sporadic and hereditary HBs was also suggested in this second study.

The results of the study described in Chapter 3 prompted us to screen five sporadic HBs with 32K array CGH. Array CGH allows for detailed screening of the genome, as its resolution is much higher than conventional CGH. Microdeletions and micro-amplifications can be detected by array CGH. The results are described in **Chapter 4**.

A couple of years ago, the cyclin D1 (*CCND1*) gene has been reported as an important target gene of pVHL. The *CCND1* gene is an oncogene, and overexpression of its protein cyclin D1 has been reported in multiple tumors. Moreover, a common polymorphism of the *CCND1* gene has been associated with prognosis of various cancers. The *CCND1* genotype has also been suggested as a genetic modifier in VHL disease.

We assessed cyclin D1 expression and the influence of *CCND1* genotype in sporadic HBs in **Chapter 5**.

During our studies we were confronted with an intriguing patient with VHL disease. The value of molecular analysis, including CGH, loss of heterozygosity (LOH), and *VHL* mutation analysis, as a tool in the differential diagnosis of VHL-associated tumors, is demonstrated in this patient in **Chapter 6**.

The exceptionally high vascularity of HBs is illustrated in 3D images of the tumor vasculature (**Chapter 7**). We describe a new technique for 3D reconstruction of the microvasculature (and other microscopic structures) of both normal and pathological tissue. This technique also allows for simultaneous visualization of different components of the vessel wall (e.g. endothelial cells and activated pericytes).

In **Chapter 8** the results of all of the described studies are summarized and discussed in the light of recent advantages in the field of sporadic HBs.

This thesis starts with a review of the current knowledge of the clinical, histopathological, and molecular genetic aspects of sporadic and VHL-associated HBs. A brief description of the molecular genetic techniques used in our studies, e.g. LOH, CGH, and array CGH follows at the end of this chapter.

Review of the clinical, histopathological, and molecular genetic features of hemangioblastomas

Clinical features

Definition

The formal introduction of capillary HBs as a cystic or solid cerebellar tumor category dates from the classic publications by Arvid Lindau (1926), and by Harvey Cushing and Percival Bailey (1928).³⁻⁵ Cushing and Bailey first coined the word hemangioblastoma, and defined pathological criteria to separate these tumors from vascular malformations. However, the first description of a cerebellar HB was made more than fifty years earlier.^{4,5} In the World Health Organization (WHO) Classification of Tumors of 2000, HBs are classified as grade 1 (benign) tumors of uncertain histogenesis.⁶

The Swedish pathologist Arvid Lindau was the first to link the cerebellar and spinal tumors to retinal vascular malformations, as described by the German ophthalmologist Eugen von Hippel in 1911, and to cysts of the kidneys, pancreas, and epididymis.³ He called this syndrome 'Angiomatosis des Zentralnervensystems'.^{3,5} The syndrome is nowadays known as von Hippel-Lindau (VHL) disease and recognized as an autosomal dominant inherited tumor syndrome.¹ VHL disease is characterized by a predisposition to form HBs of the retina and central nervous system (CNS), clear cell renal cell carcinomas (RCCs), pheochromocytomas, neuroendocrine pancreatic tumors, endolymphatic sac tumors (ELSTs), and cyst(adenoma)s in the kidney, pancreas, epididymis and broad ligament. Although HBs are a major manifestation of VHL disease, the majority of HBs occur as sporadic tumors. The histopathological and clinical features of VHL-associated and sporadic HBs are identical in most aspects and are therefore reviewed together. Where appropriate, differences are specified (Table 1).

Location

HBs account for 1-2.5% of all intracranial neoplasms.^{4,7,8} They occur predominantly in the cerebellum (75%), are less commonly seen in the brainstem (10%), and spinal cord (15%), and rarely occur supratentorial.^{9,10} The majority of sporadic HBs is located in the cerebellum, whereas VHL-

associated HBs are often multiple, and located at various sites. Tumors located in the cerebellum are mainly found in the hemispheres, and less frequently in the vermis.^{4,8} Brainstem tumors are located in the medulla oblongata, particularly at the area postrema.^{4,11} Spinal HBs account for about 5% of all spinal tumors, are mostly located in the posterior half of the spinal cord, and are found in diminishing frequency from cervical to lumbar areas.^{4,11} HBs can even be found at the lumbosacral nerve roots and at the filum terminale.¹² Extradural HBs are rare.^{4,13} Hemangioblastomatosis, dissemination to spinal cord and subarachnoid space, is extremely rare but has been reported in sporadic HBs.¹⁴

Table 1 Differences between sporadic and hereditary HBs

	% of all HBs	Solitary tumor	Predominant location	Mean age of onset (years)	Recurrence after treatment
Sporadic HB	75%	Often	Cerebellum	45 y	Rare
Hereditary HB	25%	Rare	Various CNS sites	33 y	More often

HB=hemangioblastoma; CNS=central nervous system. Ref ^{1,4,10,15-17}

Symptoms

Clinical symptoms depend on the site and size of the CNS HB.¹⁰⁻¹² In sporadic HBs, symptoms generally present in the 5th and 6th decade,^{15,16} whereas VHL-associated HBs present at an earlier age.¹ HBs occur rarely under the age of 18.¹⁸ Symptoms of increased intracranial pressure predominate in patients with cerebellar lesions. Headache is the most frequent initial symptom in these patients (12-21%), followed by nausea, vomiting, gait ataxia, dysmetria, dysarthria, diplopia, and vertigo.^{4,10,11} Hydrocephalus may result in rapid decompensation with papilledema. Gait ataxia, dysphagia, motor deficits, and sensory deficits, are described in patients with brain stem lesions.^{4,10,11} Pain and paresthesia are the most common symptoms in spinal HB, followed by sensory and motor deficits, and urine incontinence.^{10,11} Neurological

examination is normal in patients with small lesions. Despite the high vascularity of HBs, subarachnoid or intra-parenchymal hemorrhage is rare.^{4,10,19}

Symptoms are related to a mass effect, and most symptomatic cerebellar and brainstem HBs are associated with a cyst, whereas asymptomatic tumors have cysts in only 13% of cases.^{11,20,21} Symptomatic spinal tumors are often associated with syringomyelia.^{4,20} The cerebellar cysts are usually much larger than the tumor itself. The tendency of HBs to form expanding cysts can cause life-threatening complications, such as hydrocephalus, raised intracranial pressure, and brain herniation. HBs frequently show a pattern of growth in which they enlarge for a period of time (growth phase) and then enter a period of arrested growth (quiescent phase), which may last several years. Symptomatic HBs grow faster than asymptomatic tumors, and cysts enlarge faster than the solid part of the tumor.¹¹ However, no threshold tumor size or threshold rate of growth has been identified that reliably predicts an association with either symptoms or a cyst. Such an association would be of value to determine the optimal timing to start treatment. The role of possible modifiers of tumor growth, such as genetic factors, puberty, pregnancy, menopause, aging, and hormonal therapy is not yet clear.¹¹

Neuroimaging

The diagnostic method of choice for HBs of the cranialspinal axis is gadolinium-enhanced T1-weighted MRI.^{4,22}

The tumors can easily be identified by MRI. T2-weighted or FLAIR (fluid-attenuated inversion recovery) MRI is used to quantify cysts and peritumoral edema. Both angiography and CT scan have been replaced by MRI. Radiologically, cerebellar HBs are traditionally described in four types: type 1 (5%) is a simple cyst without a macroscopic nodule; type 2 is a cyst with a mural nodule (60%) (Figure 1); type 3 is a solid tumor (26%); and type 4 is a solid tumor with small internal cysts (9%).^{9,23}

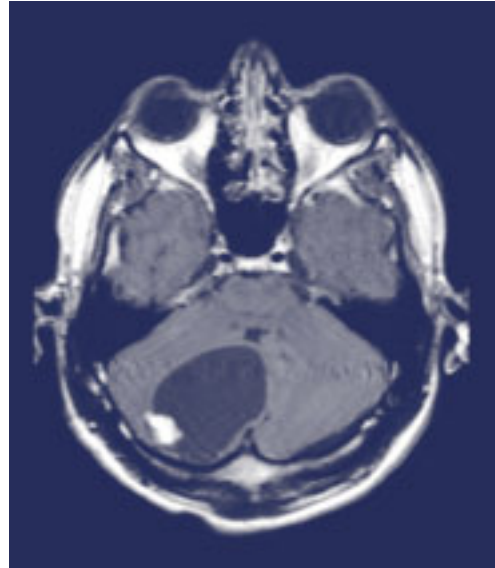


Figure 1 Typical hemangioblastoma with contrast-enhancing nidus and large cyst (T1-weighted MRI). Compression of the fourth ventricle induced hydrocephalus. The patient experienced right-sided ataxia, progressive headache, nausea, and vomiting.

Clinical criteria of von Hippel-Lindau disease

In approximately 25% of patients a HB is a manifestation of VHL disease.^{4,10,12} HBs of the CNS are the most common tumors in VHL disease, affecting 60-80% of all patients.^{11,12,24} VHL disease is a hereditary disorder, with a birth incidence of 1: 36.000, and more than 90% penetrance by 65 years of age.^{25,26} The diagnosis is often based on clinical criteria, including the family history. Typical VHL-associated tumors are HBs of the retina or CNS, clear cell RCCs, pheochromocytomas, ELSTs, and multiple pancreatic cysts. Renal or epididymal cysts occur frequently in the normal population, and are therefore less specific for VHL disease.

The clinical diagnosis of VHL disease is established in a patient with a typical VHL-associated tumor and a positive family history for VHL disease. Patients with no relevant family history must have two or more HBs, or one HB in combination with another typical VHL-associated tumor, to meet the diagnostic criteria.^{1,27}

Specific correlations of genotype and phenotype have been demonstrated in VHL families. Type 1 families have a reduced risk of pheochromocytomas, whereas they can develop all other VHL-associated tumor types. Type 2 families develop pheochromocytomas, in combination with either a low-risk (type 2A) or high-risk (type 2B) for clear cell RCCs, or pheochromocytomas alone (type

2C). Most families have VHL type 1, while type 2B is the most common type in families with pheochromocytomas (Table 2).²⁸⁻³³

Table 2 Clinical classification of VHL phenotypes

VHL type	Retinal HB	CNS HB	RCC	Pheo
1	+	+	+	-
2A	+	+	-	+
2B	+	+	+	+
2C	-	-	-	+

HB=hemangioblastoma;
RCC= clear cell renal cell carcinoma;
Pheo=pheochromocytoma

Management of patients

Screening of patients with a hemangioblastoma

Since HBs are the presenting manifestation in 40% of VHL patients, all patients with a HB require screening for VHL disease. As VHL-associated HBs present at a mean age of 33 years, and occur often at multiple sites along the craniospinal axis, young patients with multiple tumors are particularly at risk to have VHL disease.^{11,12,15} HBs are together with clear cell RCC the leading cause of morbidity and mortality in VHL disease. Early detection and treatment of VHL-associated tumors improve the prognosis of VHL patients. Therefore, clinical and radiological screening programs are recommended at regular intervals for VHL patients, as well as for patients at risk for VHL disease (Table 3).^{1,34}

Table 3 Recommended periodic screening in individuals at risk for VHL disease
Adapted from Hes et al,³⁴ with permission

Test	Start age, frequency
Medical history	10 years, yearly
Clinical examination, blood pressure	10 years, yearly
Blood counts and serum chemistry (creatinine)	10 years, yearly
24 h urinary metanephrines	10 years, yearly
Ophthalmoscopy	5 years, yearly
Ultrasound abdomen: kidneys, pancreas, liver	10 years, 1-yearly*
MRI abdomen	10 years, 2-yearly*
MRI (with gadolinium) craniospinal axis	15 years, 2-yearly
MRI internal auditory canals	On indication**
Audiogram	On indication**
Neurological examination	On indication***

* every year either ultrasound or MRI abdomen;

** symptoms: hearing loss, tinnitus, vertigo;

*** neurological symptoms, or tumors on MRI craniospinal axis.

Moreover, genetic screening for germline mutations is recommended in all HB patients younger than 50 years, because 4-14% of patients without clinical, radiological, or familial evidence for VHL disease appears to be carrier of a *VHL* gene mutation.³⁵⁻³⁸ After genetic screening is performed, monitoring can be directed at those patients carrying a mutation (Table 4).

Table 4 Recommended screening for germline mutation of *VHL* gene. Adapted from Hes et al,³⁹ with permission from the Endocrine Society

-
- Patients with a classical VHL-syndrome, fulfilling clinical criteria, and/or their first-grade relatives
 - A member of a family with a known *VHL* germline mutation
 - A patient with a high-risk for VHL, e.g.
 - Multiple VHL-tumors in an organ
 - Bilateral VHL-tumors
 - Two or more VHL-organ systems involved
 - One VHL-tumor at an early age (< 50 year for HB and pheochromocytomas, and < 30 year for RCC)
 - A patient with one VHL-tumor and from a family with only HBs, or RCCs, or pheochromocytomas
-

Surgery

The standard treatment is complete surgical removal of the solid part of the HB.^{10,11,15,40} Curation is the goal of surgery, and although postoperative mortality was as high as 10% in earlier years, most HBs of the craniospinal axis can be safely completely removed nowadays.^{1,15,41} However, even after microsurgical removal recurrences occur in 6-12% after a median time of 11 years (range 3- 35 years), and mortality is high in these patients.^{15,17}

Stereotactic radiosurgery is an alternative treatment for brainstem or cerebellar tumors, especially for patients with limited surgical options.⁴²⁻⁴⁴ A solitary small or medium sized tumor (diameter < 1-2 cm) usually shrinks or stops growing after radiosurgery, and a margin dose of 20 Gray is likely to be sufficient. However, an associated cyst often does not respond to radiosurgery of the solid part of the tumor, and formation of a de novo cyst after treatment is possible. In some cases repeated surgical evacuation of the cyst is required. Therefore, for a single sporadic cystic HB surgical removal is recommended.⁴²

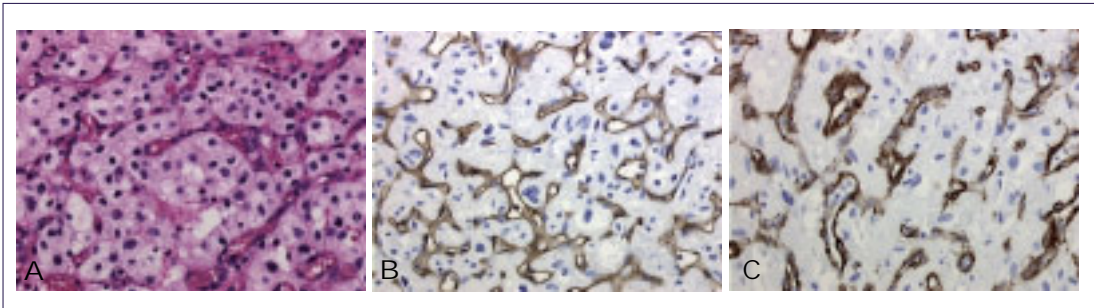


Figure 2 Histological features of HBs. Stromal cells with ample clear, vacuolated cytoplasm (HE) (A). Immunostaining of endothelial cells with anti-CD34 (B). Immunostaining of activated pericytes with α -smooth muscle actin (C).

Histopathological features

HBs are generally well-circumscribed tumors that appear bright red at macroscopy.⁴⁵ Histologically, HBs are characterized by two main components: vacuolated, often large tumor cells (stromal cells) and a rich capillary network. Intratumoral hemorrhages and cysts are common. The numerous lipid-containing vacuoles of the stromal cells account for the typically clear cell morphology (Figure 2).

The clear cell morphology can sometimes lead to differential diagnostic problems with metastatic clear cell RCC, especially since this renal cancer is also part of VHL disease. The stromal cells represent the neoplastic component of the tumor.^{46,47}

The abundant vascular network of a HB consists of numerous, often delicate, capillaries with endothelium surrounded by pericytes. Pericytes stabilize vessel walls and regulate several endothelial functions, such as permeability, proliferation, and vascular branching. Activated pericytes are found in vessels participating in angiogenesis. The amount of activated pericytes on vessels in different tumor types is variable, and has been reported to range from 30-97% (mean 69%) in HBs.^{48,49}

Most symptomatic HBs are associated with a cyst, which is usually larger than the associated tumor.^{11,20} Symptomatic spinal tumors are often associated with syringomyelia.^{4,11} The mechanisms underlying cyst development are only recently understood.²¹ Cyst formation is initiated by increased tumor vascular permeability and increased interstitial pressure in the tumor, leading to plasma

extravasation into surrounding tissue. When the capacity of the surrounding tissue to absorb extravasated fluid is exceeded, peritumoral edema and subsequent cyst formation occurs. In a recent study, the mean time required for peritumoral edema to evolve into a cyst in HBs was 36 +/-23 months.²¹

Origin

The origin of the neoplastic stromal cells in HBs is still matter of debate. No similar cell type has been described in the developing or adult CNS, and studies to determine the histogenesis of these cells by using electronmicroscopy and immunohistochemistry have reported conflicting results. Lindau originally suggested an angiomesenchymal misdevelopment at the third month of fetal life. At that time, vascular mesenchym is situated on the posterior medullary velum, and as cerebellar hemispheres also begin to develop, part of the vascular mesenchym might be drawn into the cerebellum, and represent the origin of subsequent tumor development.⁵⁰ This theory has given the tumor its name. The suggestion that stromal cells share a common angioblastic/mesenchymal ancestry with endothelial cells and pericytes supports the theory of Lindau.⁵¹⁻⁵³ However, astrocytic, pericytic/smooth muscle cell, fibrohistocytic, and neuroendocrine origin have been proposed as well.⁵⁴⁻⁵⁷ In 2000, the WHO classified HBs as tumors of uncertain histogenesis.⁶ Recently, new evidence for a developmental, angiomesenchymal origin, confirming the originally hypothesis of Lindau, has been provided.^{58,59}

Molecular genetic features

Von Hippel-Lindau disease

VHL disease is an autosomal dominant inherited syndrome, which results from a germline mutation in the *VHL* tumor suppressor gene (TSG). This gene is located on chromosome 3p25-26, and was first identified in 1993.⁶⁰ The *VHL* gene is a relatively small gene of approximately 14,500 basepairs. The protein coding region is divided into three exons, and the protein product (pVHL) contains 213 aminoacids.⁶⁰

Identification of germline mutations is possible in up to 100% of VHL families, and more than 150 different germline *VHL* mutations linked to VHL disease

have been reported so far.^{29,30,61-63} Mutations leading to loss of function of pVHL, e.g. (micro) deletions, insertions, splice site or nonsense mutations, are mostly found in VHL type 1 families. VHL type 2 families (with pheochromocytomas) almost invariably harbor specific missense (substitution of only one aminoacid) mutations, leading to an altered function of pVHL.^{28-33,39} It is presumed that the genotype-phenotype correlations reflect the degree to which the functions of pVHL are quantitatively or qualitatively altered by different *VHL* mutations; development of pheochromocytomas requires at least partial pVHL function.⁶⁴

Because of the variability in expression of VHL disease in and between families, it has been suggested that in addition to the germline mutation external factors, such as environmental or life style factors, or additional genes, play a role.⁶⁵

Knudson's two-hit hypothesis

Most patients with VHL disease inherit a germline mutation of the gene from an affected parent, and a normal (wild-type) gene from the unaffected parent. VHL disease is considered to fit Knudson's two-hit hypothesis of TSGs; inactivation of both alleles of a TSG is required to initiate tumor formation (Figure 3).⁶⁶ The *VHL* germline mutation is present in all cells of a VHL patient. However, only the cells in the specific VHL target organs that undergo somatic inactivation of the remaining wild-type allele develop tumors.^{61,67,68} Somatic inactivation of the remaining *VHL* allele can occur by mutation of the *VHL* gene, loss of the chromosome part containing this gene, or promoter hypermethylation inhibiting the transcription of the *VHL* gene.^{61,67} Deletions of part of a chromosome are often analyzed by loss of heterozygosity (LOH) analysis. This technique is described briefly at the end of this chapter.

The *VHL* gene in sporadic tumors

In most VHL-associated tumors the germline mutation is combined with LOH at 3p.^{61,68} Inactivation of the *VHL* gene also plays a role in the oncogenesis of the sporadic counterparts of VHL-tumors;^{2,16} LOH at 3p is found in up to 84-98% of sporadic clear cell RCCs, somatic *VHL* gene mutations are reported in 46-57%,⁶⁹⁻⁷¹ and hypermethylation in approximately 5-19%.^{2,72,73} According to Knudson's two-hit hypothesis, inactivation of both alleles of a TSG is required

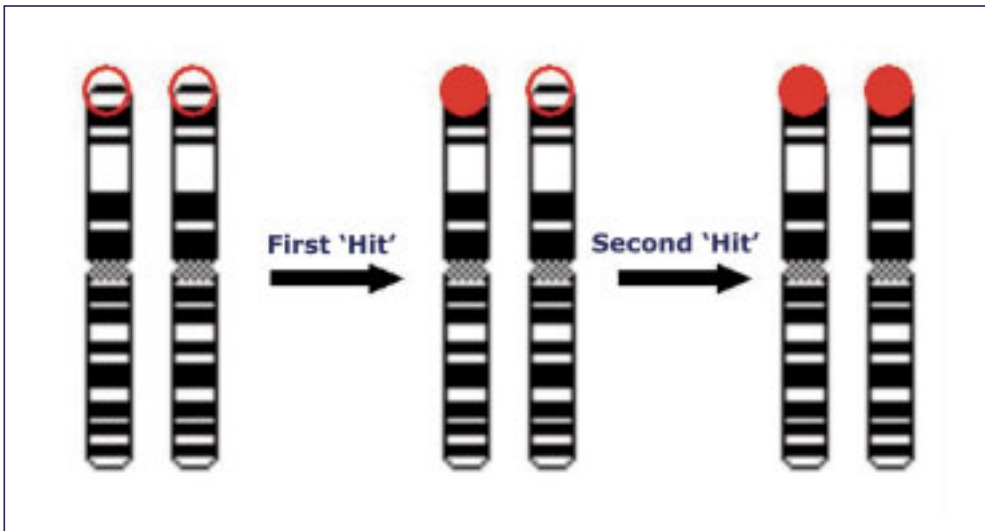


Figure 3 Knudson's two-hit model for tumor suppressor genes (TSGs).⁶⁶ A normal cell contains two intact alleles of a TSG (left). All cells from carriers of a germline mutation already contain one abnormal allele of the gene (middle), and only one additional somatic hit is required for inactivation of the TSG and initiation of tumorigenesis (right). In a tumor cell from patients with a sporadic tumor two separate somatic hits are required.

to inactivate the gene. However, in most studies the frequency of biallelic inactivation is not determined. In one study of sporadic clear cell RCCs inactivation of both alleles of the *VHL* gene by LOH, somatic inactivation, or hypermethylation, was found in only 44%.⁷⁴ Somatic mutation of the *VHL* gene combined with LOH at 3p has been reported in 33-46% of sporadic RCCs.^{69,70} In sporadic HBs, somatic mutations of the *VHL* gene were detected in 10-41% (mean 25%), and LOH at 3p was found in 20-53%.^{38,61,75-77} In two studies on sporadic HBs hypermethylation of the *VHL* gene promoter was not found.^{61,77} Inactivation of both alleles of the *VHL* gene was detected in only one (8%) of 13 sporadic HBs compared with 13 (62%) of 21 *VHL*-associated tumors.⁶¹ Somatic *VHL* mutations are rare in sporadic pheochromocytomas, the frequency of LOH at 3p is relatively low (24%), and hypermethylation has not been reported.^{2,78}

Other tumor suppressor genes

Since inactivation of both alleles of the *VHL* gene is infrequently found in sporadic tumors, the function of *VHL* may not be completely lost in the majority of these tumors and other TSGs on chromosome 3p or elsewhere in the genome may be important in the development of these tumors as well. A role for TSGs at 3p12-14 and 3p21.3 in the tumorigenesis of sporadic and *VHL*-associated clear cell RCCs has been proposed, but involvement of these putative TSGs in HBs has not been reported so far.^{73,79,80}

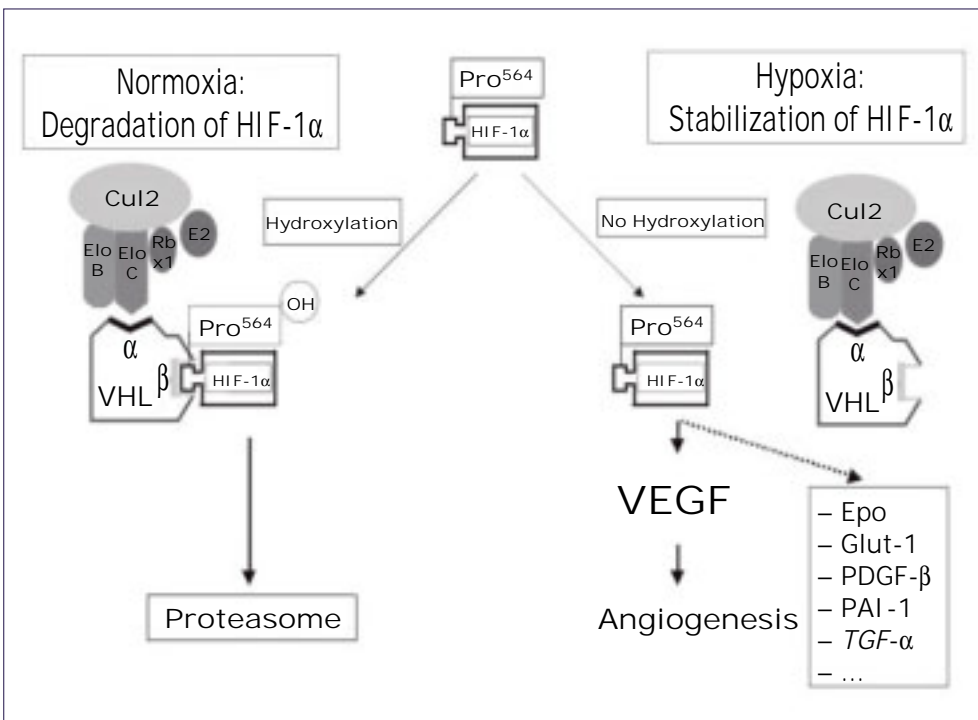


Figure 4 The oxygen-dependent degradation of HIF-1 α by pVHL. The pVHL contains two functional domains (α and β). The α -domain binds to a multiprotein complex, containing Elongin B and C, Cul2, RBx1, and E2. The β -domain binds directly to its substrate, HIF-1 α . VHL protein inhibits HIF activity under normal oxygen conditions (normoxia) by targeting the HIF-1 α subunit for ubiquitination. The polyubiquitinated HIF-1 α is destroyed by the proteasome. Under hypoxic conditions, hydroxylation of HIF does not take place, and the nonhydroxylated HIF-1 α subunits are not recognized by pVHL. Consequently, HIF-1 α is stabilized and activates transcription of its target genes. Damage or loss of function of pVHL also leads to upregulation of HIF target genes, and resembles the hypoxia pathway. Adapted from Hes et al,³⁹ with permission from the Endocrine Society.

Genes located at chromosomes other than chromosome 3 may be involved in sporadic VHL-tumors. In sporadic and VHL-associated clear cell RCCs, DNA copy number changes of several chromosomes have been found, including loss of 1q, 4q, 6q, 8p, 9p,14q, and 19, and gain of 5q, 7, 17q, and Xq.⁸¹⁻⁸⁸ In pheochromocytomas, besides loss of chromosome 3, loss of chromosome 11 is found in VHL-associated tumors, and loss of 1q, and 3q in sporadic tumors.^{89,90} At the start of our studies, no cytogenetic abnormalities in HBs had been reported.^{91,92}

Function of VHL protein

Lack of pVHL induces intracellular metabolic changes that closely resemble changes observed in oxidative stress. The α -domain of pVHL binds to a protein called elongin C, which binds to a complex containing elongin B, cullin-2 (CUL2), Rbx, and E2 to form an ubiquitin ligase complex which targets specific proteins for polyubiquitylation and subsequent proteosomal degradation.^{64,93-96}

Many of the genes that are regulated by hypoxia, including vascular endothelial growth factor (VEGF) and erythropoietin (Epo), are under the control of a transcription factor called hypoxia-inducible factor (HIF). The pVHL-elongin-CUL2 complex directs the polyubiquitylation, and hence destruction, of the α -subunits of HIF-1 and HIF-2 in the presence of oxygen.^{64,93} In hypoxic conditions, the HIF- α subunits accumulate and activate transcription of hypoxia-inducible genes, many of which are important in regulating angiogenesis, cell growth, and cell survival (Figure 4).

Cells lacking pVHL are unable to degrade HIF- α subunits, irrespective of changes in oxygen, and upregulation of HIF target gene occurs.^{97,98} HIF target genes include VEGF, Epo, plasminogen activator inhibitor 1 (PAI-1), glucose transporter 1 (Glut1), glycolytic enzymes, carbonic anhydrases (CA-9 and -12), platelet-derived growth factor (PDGF), and transforming growth factor (TGF- α and $-\beta$).⁹⁹⁻¹⁰² In HBs, expression of HIF-1 and 2 α and its target genes VEGF, PDGF-B, Epo, Glut1, CA-9 and -12, TGF- α and epidermal growth factor receptor (EGFR), fibroblast growth factor (FGF), and placental growth factor (PIGF) has been reported.^{48,99,100,103-107}

VHL inactivation in tumors

Although the *VHL* gene and its principal target HIF-1 α are expressed in all tissues, VHL inactivation is linked to only a small subset of tumors (e.g. HBs, RCCs, pheochromocytomas), and tumorigenesis appears to depend on tissue context (e.g. CNS, kidney, adrenals). The mechanisms for the organ-specific tumorigenesis in VHL disease remain to be elucidated. Stromal and endothelial cells in HBs express a number of (angiogenic) growth factors and their receptors, e.g. VEGF and VEGF-receptor (VEGFR)-1 and 2, and TGF- α and EGFR, suggesting paracrine as well as autocrine growth-factor loops.^{47,103-105,108} Overexpression of VEGF and PDGF-B is likely responsible for the hypervascularity of HBs, as these factors are potent mitogens for endothelial cells and pericytes, respectively.¹⁰⁹ VEGF also increases the permeability of endothelium (hence its alternative name Vascular Permeability Factor, VPF) and the tendency of HBs to form cysts is linked to this function of VEGF.^{21,103}

In the kidney of VHL patients, the epithelial cells lining of pre-neoplastic renal cysts show loss of pVHL function and overexpression of HIF and HIF target genes.¹¹⁰ As in HBs, VEGF and PDGF-B account for the highly vascular nature of these tumors. Moreover, the renal tubular epithelial cells are particularly sensitive to the mitogenic effects of TGF- α /EGFR, and overproduction of TGF- α has been linked to renal cyst formation.^{64,111} However, additional genetic alterations are probably required for conversion of the cysts to RCCs, while the *VHL* gene serves as a gatekeeper TSG.² The role of pVHL and HIF in pheochromocytomas remains to be elucidated, as regulation of HIF seems normal in these tumors.³⁹

Alternative functions of pVHL

Upregulation of angiogenic growth factors by the activated HIF pathway provides an explanation for the angiogenic phenotype of the VHL-associated HBs and RCCs. It has been demonstrated that HIF activation occurs at a very early stage in the evolution of renal tumors. However, it remains to be clarified how the loss of *VHL* triggers oncogenesis and whether HIF mediates it.¹¹⁰

Genotype-phenotype correlations in VHL disease suggest that pVHL has functions independent of its role in HIF regulation. In type 2C VHL disease (pheochromocytomas only), the ability to polyubiquitylate the HIF- α subunits is retained, and thus development of pheochromocytomas is likely linked to a

pVHL loss of function unrelated to HIF.^{2,112} It has been suggested that a gain of function of pVHL may be involved in VHL type 2C tumors.³⁹ Furthermore, *VHL* mutants linked to type 2A and type 2B (low vs high risk for RCC, resp) are both unable to properly regulate HIF, suggesting that the risk of RCC is modified by a different and additional pVHL function.²

A number of putative pVHL functions involving cellular processes have been identified including fibronectin binding and extracellular matrix assembly, interaction with atypical protein kinase C (a regulator of cell polarity and cell growth) among other substrates, regulation of mRNA stability, cytoskeletal stability, cell cycle exit control, and differentiation.^{2,98,113-118} Whether some of these functions are HIF-dependent is still unclear. Cells lacking pVHL do not deposit a proper extracellular fibronectin matrix, secrete higher levels of metalloproteases, are more invasive, and because epithelial cell behavior is influenced by interactions with the extracellular matrix, show increased proliferation compared to cells with normal pVHL.^{2,113,118} In this way, altered extracellular matrix production may contribute to tumorigenesis after pVHL inactivation.

VHL protein targets; cyclin D1

The identification of novel pVHL targets using gene expression analysis might provide further insights into mechanisms of pVHL tumor suppressor activity. The pVHL targets include genes that are regulated by HIF and hypoxia, as well as other genes that control cell growth, cellular metabolism, differentiation, extracellular matrix breakdown, and angiogenesis.¹¹⁹⁻¹²³ One of these genes is the *CCND1*, that encodes a protein (cyclin D1) that plays a critical role in the control of the cell cycle at the G1 (resting phase)/S (DNA synthesis) checkpoint.¹²⁴ Overexpression of cyclin D1 releases a cell from its normal cell cycle controls and facilitates transformation to a tumor cell. Overexpression of cyclin D1 is a feature of many cancers.¹²⁵ It has been shown that inactivation of pVHL induces upregulation of cyclin D1. Whether this occurs by a HIF and/or hypoxia-dependent pathway is not yet clear.^{120,123,126,127} The finding in some studies that *CCND1* is hypoxia-inducible in RCC cell lines but not in other tumor cell lines, has led to the suggestion that a distinct hypoxia-related signaling pathway exists in renal cells, which contributes to the tissue selectivity of VHL-associated tumors.^{120,123,128} Overexpression of cyclin D1 in cells lacking pVHL might explain

why tumor cells are not capable to exit the cell cycle.¹¹⁷ Although the (putative) functions of the majority of the novel pVHL target genes suggest a contribution of these genes to tumor development after pVHL inactivation, the exact mechanisms are still speculative.

CCND1 genotype

In VHL disease, both inter- and intrafamilial variability in tumor expression is well recognized and differences in tumor-susceptibility have been attributed to allelic heterogeneity; e.g. specific missense germline mutations confer a high risk for pheochromocytoma, whereas large deletions or protein-truncating mutations confer a low risk. However, susceptibility to retinal and CNS HBs and most RCCs are not influenced by the type of underlying germline mutation.⁶⁵ It has been suggested that in these cases genetic and/or environmental modifier effects account for the phenotypic variation.^{65,123} One of the potential genetic modifiers is the *CCND1* genotype.

The *CCND1* gene contains a common G→A polymorphism (870 G>A) within the splice donor region of exon 4 that modulates mRNA splicing. This polymorphism has been reported to influence susceptibility to various cancers.¹²⁹⁻¹³² In VHL disease, the G-allele was associated with an increased number of retinal HBs, and a trend to an earlier onset of CNS HBs, whereas no increased susceptibility to RCCs was found.¹²³

Targeted therapy

Agents that are directed against HIF responsive growth factors such as VEGF, PDGF-B, and TGF- α , and their receptors, have been investigated as potential treatment for HBs and RCCs.¹³³ Most preclinical and early clinical studies are performed in RCCs, and VEGF antagonists and EGFR inhibitors have shown activity in these studies.⁶⁴ A significant, although modest, prolongation in time to progression of metastatic RCC has been shown in a clinical randomized trial of bevacizumab, a VEGF neutralizing antibody. However, only 10% of patients had partial tumor response, and a survival benefit was not observed. Mild toxic effects were reported, with hypertension and proteinuria predominating.¹³⁴ There have been case reports on the use of targeted therapy for VHL-associated HBs. One VHL patient with an optic nerve HB had a dramatic and sustained

improvement in visual acuity following treatment with SU5416, which is an inhibitor of the VEGF receptor. Tumor regression was not observed, however, and clinical improvement might be attributed to blocking of the vascular permeability effects of VEGF resulting in decreased peritumoral edema.¹³⁵ In three patients with CNS HBs who were also treated with SU5416, no significant reduction in tumor size was noted. However, these patients unexpectedly developed polycythemia, which might be due to an increased production of Epo, increased susceptibility of red blood cell precursors to Epo, or an interaction of SU5416 with other receptors critical for erythropoiesis.¹³⁶ One patient with multiple cerebellar and spinal cord HBs and leptomeningeal spread after surgery was treated with a small molecule inhibitor of the EGFR tyrosine kinase (OSI-774; Tarceva™). This patient showed subjective improvement in neurological symptoms, and a minor reduction in size of two cerebellar HBs.¹³⁷ Other agents with antiangiogenic properties, such as thalidomide and interferon- 2α , also showed no tumor shrinkage in patients with HBs, although tumor progression was halted during treatment.^{138,139}

These studies suggest that VEGF inhibition alone is unlikely to cause regression of established, mature blood vessels, and future treatments should consider pathways other than that mediated by VEGF.¹³³ Compounds targeting (mature) endothelial cells and pericytes might cause regression of established tumors. Combinations of antiangiogenic agents with agents that block tumor cell autocrine loops, such as TGF- α / EGFR might be promising alternatives.^{133,134,140} In conclusion, as yet no therapeutic agent or combination of agents is available for use against HBs or RCCs in general clinical practice.

Molecular genetic techniques

Several techniques can be used to detect abnormalities of chromosomes or genes in tumors. Some methods are especially used for screening purposes, others are performed when more detailed information of (part of) a specific chromosomal region or gene is required. In this section the methods that were used in the molecular genetic studies described in this thesis are briefly discussed.

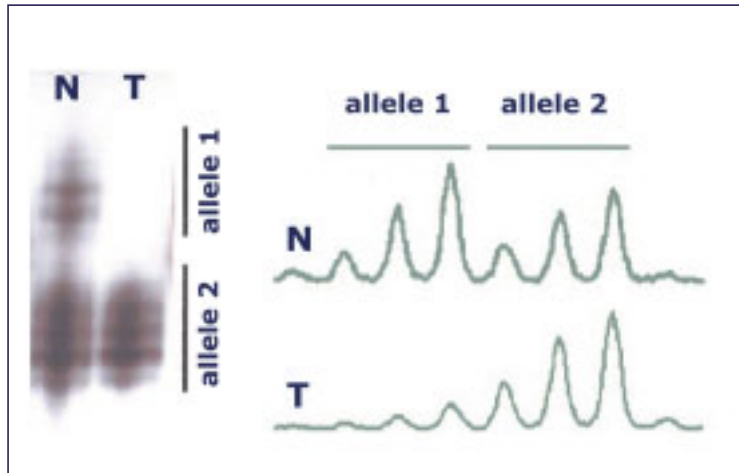


Figure 5 Loss of heterozygosity (LOH) analysis. PCR fragments are separated by either polyacrylamide gel-electrophoresis and visualized by autoradiography (left) or by capillary gel-electrophoresis after using fluorescent primers (right). Normal (N) and tumor (T) DNA of the same patient are compared and only one of both alleles was present in the tumor. Adapted from¹⁴¹, with permission.

Loss of heterozygosity

Loss of parts of chromosomes (loss of alleles) is a frequent event in tumors, and loss of heterozygosity (LOH) analysis is often used to detect these allelic imbalances. For LOH, tumor DNA as well as matched control/normal DNA (blood) of the patient is generally required. PCR (polymerase chain reaction) is used for amplification of a DNA fragment containing a highly polymorphic microsatellite repeat, for example a CA-repeat. The size of this fragment depends on the amount of CA's and differs within the population. Usually, a difference exists in fragment length of the paternal and maternal allele. The amplified PCR fragments are separated by gel-electrophoresis (Figure 5). When only one fragment is detected in the matched control DNA both alleles are of the same size (homozygous) and the marker is considered to be non-informative. Allelic loss can only be identified for heterozygous loci as it is detected by an imbalance between both alleles in the tumor DNA in comparison to the matched control DNA. In an alternative LOH procedure, paired normal DNA is not a necessity when a set of highly polymorphic markers is analyzed, the rationale being that the use of a set of these markers dramatically reduces

the possibility that detection of a single allele for all markers is caused by similar sizes of both alleles.¹⁴¹ By LOH only one locus of interest can be analyzed per experiment.

Mutation analysis

A sensitive method for analysis of gene mutations is direct sequencing. The sequence of the four nucleotides (A, C, T, or G) of the DNA fragment containing the region of interest is analyzed and compared to the normal sequence to detect deletions, insertions, or mutations. For direct sequencing a single primer is used (either forward or reverse) that is adjacent to the region to be sequenced. During PCR amplification the polymerase enzyme adds dNTPs (deoxynucleotide-triphosphates; either C, G, A, or T) to the free end of the primer (3' hydroxyl group) extending it along the template and forming covalent bonds between the dNTP subunits. Additionally, in a sequence reaction dideoxynucleotides (ddNTPs) are present for all four bases each labeled with a specific fluorochrome. The significance of such a modified base is that polymerization is halted when the modified base is incorporated into the growing DNA strand synthesized from the template. The result is a population of fragments of different sizes. The size of each fragment corresponds to the distance from the terminating base of the primer. When all fragments are separated by size, and the fluorescent-labeled nucleotide at the end of each fragment is detected by a laser, the original sequence can be reconstructed. Depending on the size of the fragment to be sequenced different (overlapping) primer sets are usually required. A change in the nucleotide-sequence of the gene can induce a substitution of an aminoacid and subsequently alter the function of the protein (Figure 6).

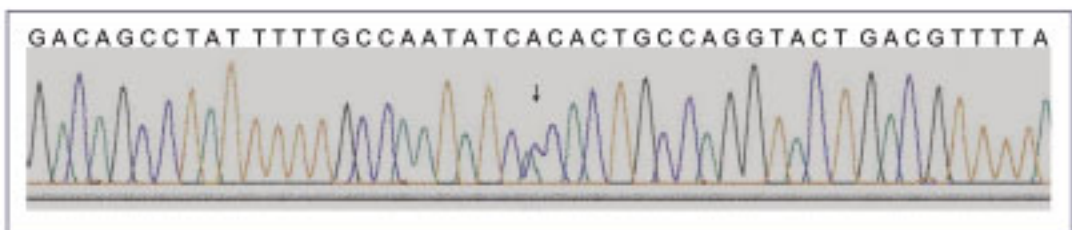


Figure 6 Sequence-analysis. The sequence of the bases of a DNA fragment is determined by the colored spike-pattern. The normal nucleotide sequence is indicated above. This sample contains at position 667 (arrow) a substitution of C for A (667A→C), leading to a change in an aminoacid (Threonine to Proline). A=adenine;T=thymine;G=guanine;C=cytosine.

Comparative genomic hybridization

CGH has the advantage that screening of the entire genome is allowed in a single experiment. Moreover, CGH does not require prior knowledge about the genetic constitution of the tumors, this in contrast to other molecular genetic techniques such as LOH. CGH is based on the comparison of two genomic DNA populations; one derived from the tumor to be analyzed and one from a karyotypic normal reference (Figure 6).

Tumor and reference DNA are differentially labeled (e.g. reference in red and tumor in green) with fluorochromes (direct labeling), or haptens (indirect labeling), which are later visualized by fluorescence. Both DNAs are mixed in a 1:1 ratio in the presence of repetitive DNA (COT-1-DNA) and are in situ hybridized to normal human metaphase chromosomes. During this co-hybridization, tumor and reference DNA compete for the same targets on normal metaphase chromosomes. The relative amount of tumor and reference DNA bound to a given chromosomal region is dependent on the relative abundance of these sequences in both DNA samples. Therefore, intensity differences in the fluorescent hybridization patterns of tumor (green) and reference (red) DNA can be interpreted as copy number differences between both genomes (e.g. gains will show in green, losses in red, and regions that are normally present will show in yellow).

The presence and localization of chromosomal imbalances can be detected and quantified by analyzing the ratio of the fluorescence intensities of tumor and reference DNA (green/red). These ratios show which chromosomal regions in the tumor genome are over- or under-represented relative to the reference genome. As ratio profiles are calculated along all chromosomes in the normal metaphase, an overview of the chromosomal imbalances throughout the entire genome is provided (Figure 7).

The CGH protocol we used has been fully described.¹⁴² In our laboratory this protocol results in reliable and sensitive CGH experiments. In adequate conventional CGH experiments, chromosomal imbalances as small as 2-5 Mb can be detected.

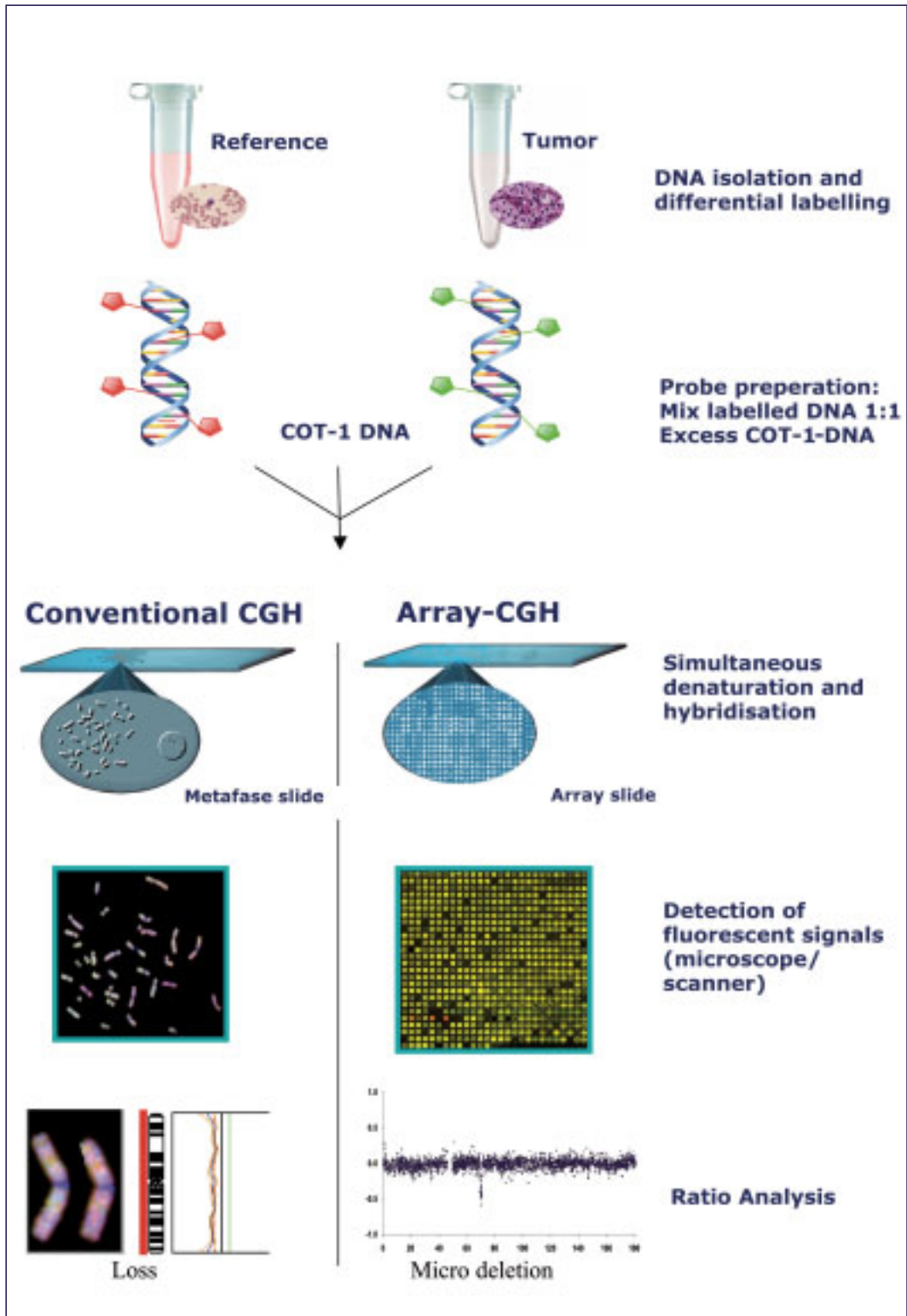


Figure 7. Loss of (part of) chromosome 3 identified by CGH and array CGH. Mixed differential labeled normal and tumor DNA are in situ hybridized to normal human metaphase chromosomes (CGH) or mapped genomic clones (array CGH). A copy number loss (loss of a whole chromosome 3) is shown in red (CGH; left). Array CGH shows a micro-deletion on chromosome 3 (right).

Array-based CGH

The problem of a limited resolution as described for conventional CGH can be overcome by hybridizing differentially labeled reference and tumor DNAs to an array of mapped sequences instead of chromosomes (Figure 7).¹⁴³⁻¹⁴⁵ Such CGH based micro-array analyses have been described as array CGH, matrix CGH, or genomic array analysis. For micro-array analysis hundred to thousands of DNA sequences are printed at a designated position on a microscopic glass slide using a robotic "arrayer".¹⁴³ Different types of DNA sequences can be spotted on a slide such as cDNAs, oligonucleotides, or (large) DNA fragments cloned into yeast artificial chromosomes (YACs), bacterial artificial chromosomes (BACs), P1-derived artificial chromosomes (PACs), cosmids, or other vectors. The resolution of array experiments depends on the size of the inserted fragments and the genomic spacing of the spots. The large amount of data obtained by array analysis require standardized storage systems as well as thorough statistical tools for normalization and automated detection of chromosomal imbalances. The array CGH used in Chapter 4 contains over 32,000 BAC clones, which allow for detection of chromosomal microdeletions and microamplifications at a resolution of approximately 100 kb.

Chapter 2

Characteristic chromosomal aberrations in sporadic cerebellar hemangioblastomas revealed by comparative genomic hybridization

Sandra H.E. Sprenger¹, Johanna M.M. Gijtenbeek², Pieter Wesseling¹, Raf Sciot³, Frank van Calenbergh³, Martin Lammens¹, Judith W.M. Jeuken¹

¹ Department of Pathology, Nijmegen Centre for Molecular Life Sciences,

² Department of Neurology, Radboud University Nijmegen Medical Centre, The Netherlands

³ Department of Neurosurgery, University Hospital K.U. Leuven, Belgium

Abstract

Hemangioblastomas (HBs) of the central nervous system (CNS) are benign tumors and occur as sporadic tumors (75%) or as a manifestation of von Hippel-Lindau (VHL) disease (25%). VHL disease is an autosomal dominant disorder characterized by HBs of the CNS and retina, renal cell carcinoma (RCC), pheochromocytoma, islet tumors of the pancreas, and endolymphatic sac tumors as well as cysts and cystadenoma in the kidney, pancreas and epididymis. In VHL patients a large spectrum of germline mutations in the *VHL* gene has been detected. In sporadic HBs *VHL* alleles are reported to be inactivated in up to 50% of the tumors. To our knowledge the involvement of other genes in sporadic HBs has not been investigated. To elucidate the oncogenesis of sporadic HBs, we performed CGH on 10 sporadic HBs to screen for chromosomal imbalances throughout the entire tumor genome. Aberrations most frequently detected are losses of chromosomes 3 (70%), 6 (50%), 9 (30%) and 18q (30%) and a gain of chromosome 19 (30%). Based on these frequencies and the co-occurrence of these aberrations in the analyzed tumors we hypothesize that loss of chromosome 3 (harboring the *VHL* gene) is an early event in the oncogenesis of sporadic HBs, followed by loss of 6, and then losses of chromosomes 9, 18q and gain of chromosome 19. Comparison of the chromosomal imbalances in sporadic HBs to those previously reported in RCCs and pheochromocytomas reveals that the pathway of sporadic HBs shows similarities to both the RCCs and pheochromocytomas.

Introduction

Hemangioblastomas (HBs) are benign, highly vascularized neoplasms of the central nervous system (CNS), which account for only 1-2% of all intracranial tumors. The origin of the tumor cells in sporadic HBs is still unknown.¹⁴⁷ HBs occur as sporadic tumors (75%) or as part of von Hippel-Lindau disease (VHL-associated HBs, 25%). VHL disease is an autosomal dominant disorder characterized by HBs of the CNS and retina, renal cell carcinoma (RCC), pheochromocytoma, islet tumors of the pancreas, and endolymphatic sac tumors as well as cysts and cystadenomas in the kidney, pancreas and epididymis.^{45,148} A large spectrum of germline mutations in the *VHL* tumor suppressor gene (TSG), located at chromosome 3p25-26 has been detected in VHL patients.^{35,38,60,75,76} The VHL protein (pVHL) is involved in transcription elongation and in regulation of stability of hypoxia-inducible factors such as vascular endothelial growth factor (VEGF).^{149,150} Inactivation of the *VHL* gene also plays a role in part of the sporadic counterparts of the tumors observed in VHL disease. In the stromal component of sporadic HBs somatic mutations of the *VHL* gene have been reported in up to 50% and a loss of heterozygosity (LOH) including the *VHL* region is reported in approximately 50%.^{35,38,75,76} To our knowledge the involvement of other genes in sporadic HBs has not been investigated. We used comparative genomic hybridization (CGH) to screen for chromosomal imbalances throughout the entire tumor genome of sporadic HBs to elucidate which chromosomal regions are important in the oncogenesis of cerebellar sporadic HBs.^{151,152} In addition we compared these results to those previously reported in non-papillary clear cell RCCs and pheochromocytomas, because co-occurrence of these tumors in VHL disease suggests a common oncogenic pathway.^{82,85,87,89}

Material and Methods

Surgical specimens of the tumors selected for the present study (Table 1) were obtained from 10 patients treated in the Radboud University Nijmegen Medical Centre, The Netherlands (patients N240-N244), and the University Hospital in Leuven, Belgium (patients N245-N249). All tumors were histopathologically classified as HBs according to the World Health Organization (WHO)

classification.⁴⁵ During surgery part of the tumor was snap-frozen in liquid nitrogen and stored at -80°C. Clinically, the tumors were diagnosed as sporadic cerebellar HBs based on neurological examination, negative family history of VHL disease, negative ophthalmological examination and unremarkable abdominal ultrasound and MRI of the brain and spinal cord. The mean patient age at operation was 52,3 years (range 31-72). CGH was performed on all sporadic HBs as previously described by Jeuken et al.¹⁵³ Briefly, DNA was extracted by a salting out procedure.¹⁵⁴ Control and tumor DNA were labeled by nick-translation with digoxigenin-dUTP and biotin-dUTP, respectively (Roche Molecular Biochemicals, The Netherlands), and precipitated in the presence of human COT-1-DNA (Gibco BRL Life Technologies, Inc., Gaithersburg, MD, USA) and herring sperm DNA. The probe and the metaphase slides were denatured simultaneously. After hybridization and post-hybridization washes, biotin and digoxigenin were detected using streptavidin-FITC and sheep-anti-digoxigenin-TRITC (Roche Molecular Biochemicals). The chromosomes were counterstained with 4,6'-diamino-2-phenylindole-dihydrochloride (DAPI) (Merck, Darmstadt, Germany) and the slides were mounted in Fluoroguard (Biorad, Veenendaal, The Netherlands). To test the quality of the CGH hybridizations, a negative and a positive control experiment were included in each series of CGH hybridizations.¹⁵³ Chromosomal imbalances of the X chromosome could only be detected if CGH was performed using tumor and control DNA of the same gender. For CGH analysis Quips CGH software (Applied Imaging, United Kingdom) was used. Detection thresholds for losses and gains were set at 0.8 and 1.2, respectively.

The frequency of gains and losses involving the individual chromosome arms detected by CGH in the sporadic HBs analyzed in this study, was compared with the frequency in RCCs^{82,85,87,155} and pheochromocytomas⁸⁹ previously reported by others in the literature. For RCCs we only included non-papillary, clear cell RCCs as seen in VHL patients.^{82,85,87} A large CGH study on RCCs only listing the most frequently found aberrations was included separately in the RCC figure.¹⁵⁵ In this overview we did not distinguish between complete and partial imbalances of chromosome arms.

Results

Comparative genomic hybridization

The chromosomal imbalances detected using CGH in 10 sporadic HBs are summarized in Table 1 and visualized in Figure 1. Losses (22/33, 67%) were more frequently detected than gains (11/33, 33%). Although the partial aberrations of the positive control were all clearly detected, we only detected aberrations of complete chromosomes or chromosome arms. Aberrations most frequently detected were losses of chromosomes 3 (70%), 6 (50%), 9 (30%) and 18q (30%) and a gain of chromosome 19 (30%). Two of the tumor samples did not contain any aberrations detectable by CGH. Aberrations of the X-chromosome were clearly detected if a sex mismatch was introduced confirming the quality of the CGH. The frequency of chromosomal imbalances of the chromosome arms in sporadic HBs and RCCs and pheochromocytomas is summarized in Figure 2.

Table 1 Chromosomal imbalances detected by CGH in sporadic hemangioblastomas

Tumor	Chromosomal imbalances						Other imbalances
	-3	→ -6	→ (+19	-18q	-9) →	+17	
N243	*	*	*	*	*	*	+4, +5, +7, +16, -18p, -22
N244	*	*	*	*	*	*	-18p
N240	*	*	*				
N246	*	*		*			+1q, -10, -14q
N242	*						
N241	*						
N245	*						
N248		*			*		-8, +15q
N247							
N249							

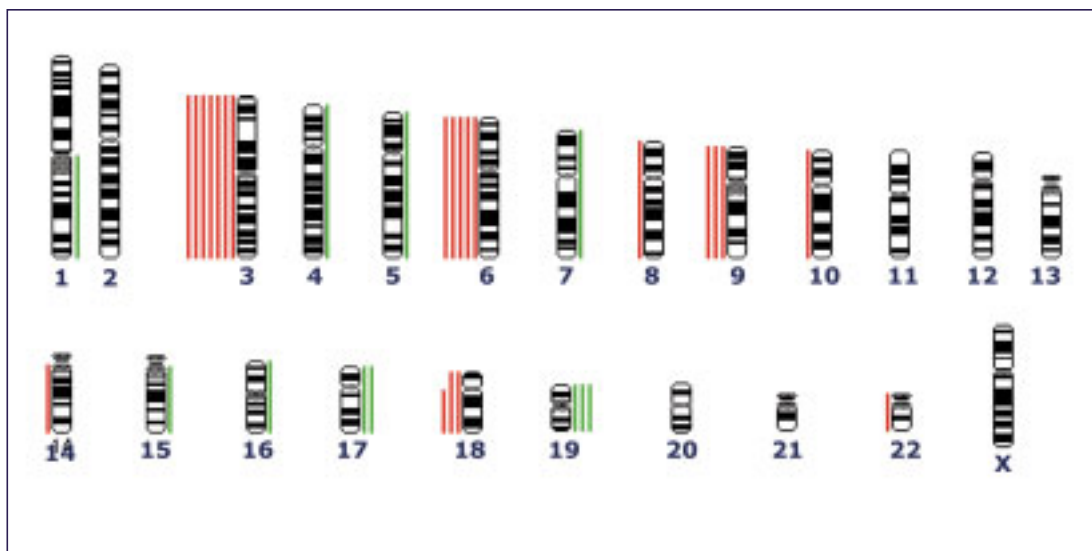


Figure 1 Diagram containing a summary of chromosomal imbalances detected by CGH in sporadic hemangioblastomas. Lines on the left and right of the chromosome indicate losses and gains of these chromosomal regions, respectively. The sexchromosomes were not analyzed.

Discussion

We performed CGH on 10 sporadic HBs to elucidate which chromosomal regions are involved in their oncogenesis. We found a relatively large amount of aberrations in this benign and slow growing tumor (WHO grade I). Aberrations most frequently detected were loss of chromosome 3 (70%) and 6 (50%), whereas a loss of chromosome 9 and 18q, and a gain of chromosome 19 were detected in 30% of the tumors. Our results (Table 1) suggest that there is a sequence of chromosomal imbalances in sporadic HBs in which loss of chromosome 3 is the initiating event for HBs, which is followed by loss of chromosome 6 and losses of 18(q) and/or 9, and/or a gain of chromosome 19. Next to these aberrations others might be present.

Although all sporadic HBs with a loss of chromosome 3 show complete loss of this chromosome, a review on DNA copy number losses in human neoplasms in general most frequently reported a loss of chromosome 3p.¹⁵⁶ Four regions have been reported to harbor a (putative) TSG, 3p12, 3p14.2, 3p21.3, and 3p25. At 3p25-26 the *VHL* gene has been identified which is reported to be

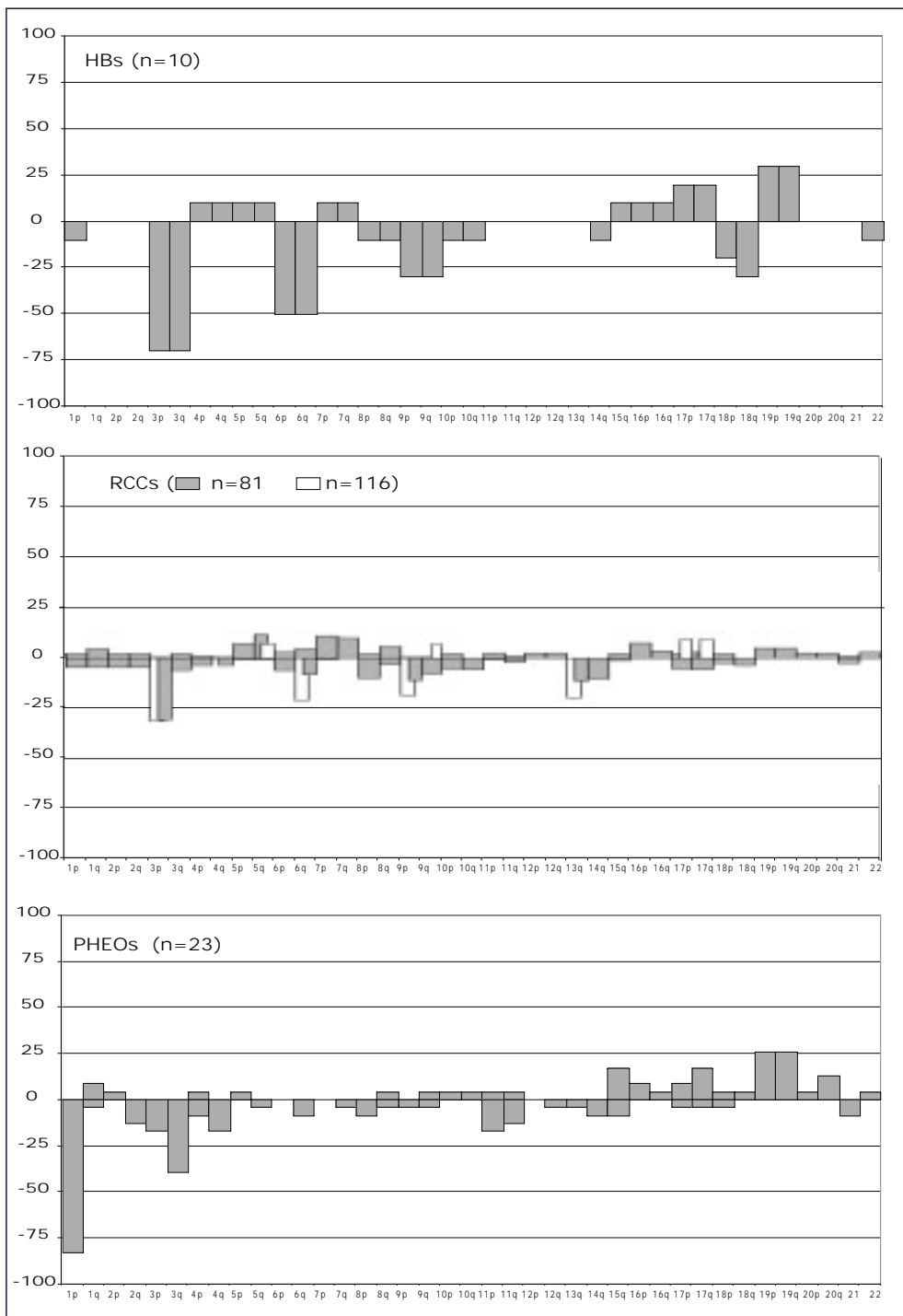


Figure 2 Bar graphs showing an overview of the frequency of chromosomal imbalances in our sporadic hemangioblastomas (HBs), and in renal cell carcinomas (RCCs)^{82,85,87,155} and pheochromocytomas (PHEOs)⁸⁹ previously reported by others in the literature. In the bar graph showing the RCCs, the gray boxes represent three studies^{82,85,87} which listed all aberrations found and the white boxes represent a large CGH study only listing the most frequently found aberrations.¹⁵⁵ A positive percentage on the y-axis represents the frequency of a gain, whereas a negative percentage represents the frequency of a loss. The chromosome arms are indicated on the x-axis.

involved in HB oncogenesis;⁶⁰ 1) germline mutations of the *VHL* gene cause VHL disease predisposing to multiple tumors, most frequently including HBs, 2) aberrations involving the *VHL* gene are frequently detected by mutation, SSCP, or LOH analysis in 10% to 50% of the sporadic HBs,^{36,38,75-77} 3) hypermethylation of a normally unmethylated CpG island of the *VHL* gene has been reported as an inactivating mechanism in HBs without *VHL* mutations.⁷² Since *VHL* aberrations are reported in up to 50% of sporadic HBs,⁷⁵ other (p)TSGs located on 3p or 3q might be involved in HB oncogenesis. In tumor N248 CGH did not detect a loss involving chromosome 3, but small losses undetectable by CGH might be present or alternative other mechanisms such as hypermethylation might affect genes on chromosome 3 initiating HB oncogenesis. Interestingly, this tumor is the only tumor containing a loss of chromosome 8 on which the gene for elongin C is located. pVHL binds to elongin C which additionally binds elongin B and cullin-2 (CUL2) forming the VCB complex. This complex induces degradation of their substrates and is involved in transcription elongation.¹⁴⁹ Aberrations of either VHL or elongin C might result in destabilizing the VCB-complex.

Similar to chromosome 3, in some sporadic HBs the complete chromosome 6 is lost while in human neoplasms in general a loss of only 6q is most frequently reported.¹⁵⁶ (p)TSGs have been suggested at 6p21.2, 6q23-25, and 6q24-35.¹⁵⁶ Next to TSGs, other genes such as VEGF (6p12) and ezrin (6q25-26) might be important in HBs. Upregulation of VEGF (transcript and protein) has been reported in the stromal cells and of the corresponding receptors in the tumor endothelium suggesting an paracrine mechanism responsible for angiogenesis in HBs.^{47,103} Normally, the VCB complex induces degradation of a transcription factor for hypoxia-inducible factors (HIF) and destabilization of this complex results in the upregulation of VEGF. As we frequently detected a loss of chromosome 6 in sporadic HBs, this might suggest that the remaining VEGF allele is sufficient for upregulation of VEGF. Another gene, Ezrin, located on 6q25-26 might be important in HBs. The ezrin protein has a diffuse cytoplasmatic expression in the stromal cells of HBs in contrast to its normal localization close to the plasma membrane.¹⁵⁷ This might be caused by overexpression of the protein or by expression of an aberrant ezrin protein with deficient binding to the membrane or cytoskeleton.¹⁵⁷

Losses of chromosomes 18q and 9, detected in 30% of the sporadic HBs, were reported in respectively 37% and 48% of human neoplasms and several known

or putative TSGs have been located on these chromosomes.¹⁵⁶ A gain of chromosome 19, detected in 30% of the sporadic HBs, is reported in 2 to 36% of a large variety of tumors.¹⁵⁸

Two of the HB samples did not contain aberrations detectable by CGH, indicating that no aberrations larger than 2 Mb are present in these samples. However, since it was reported that HBs consist of both neoplastic stromal cells and non-neoplastic cells, including vessels, macrophages, and reactive astrocytes^{46,76} it is also possible that aberrations were not detected due to the high percentage of normal DNA. Similarly, it was reported that the presence of non-neoplastic cells might obscure LOH scoring in HB tumor samples.⁷⁶

Since patients with germline mutations in the *VHL* gene are predisposed to multiple tumors including HBs, clear cell RCCs and pheochromocytomas, a close correlation between the oncogenesis of these tumors is to be expected. The overview of the frequency of aberrations detected by CGH in these tumors shows that although HBs contain a complete loss of chromosome 3, RCCs most frequently lost 3p whereas pheochromocytomas lost 3q. Losses of chromosomes 6 and 9, frequently occur in RCCs but not in pheochromocytomas. On the other hand, a gain of chromosome 19 is frequently reported for pheochromocytomas but less frequently for RCCs. Loss of chromosome 18 is rare in both tumors. Our results show that RCCs and pheochromocytomas show different frequencies of chromosomal imbalances implying different oncogenic pathways. In HBs chromosomal imbalances characteristic for either RCCs or pheochromocytomas are both detected. Since HBs do not harbor either loss of 3p or loss of 3q, but a loss of the complete chromosome 3, there seems to be one pathway for the oncogenesis of HBs, which show similarities to both the pathways for RCCs and pheochromocytomas.

In conclusion

Losses of chromosomes 3 and 6 were the most frequently detected chromosomal imbalances in sporadic HBs. Our results suggest that there is a characteristic pathway of chromosomal imbalances in which loss of chromosome 3 (harboring the *VHL* gene) and loss of chromosome 6 occur as sequential events, followed by a loss of 9 and/or a loss of 18q and/or a gain of 19. This pathway shows similarities to those of the RCCs and

pheochromocytomas. To further elucidate the oncogenesis of sporadic HBs, more sporadic HBs should be analyzed and additionally genes located on these chromosomal regions should be investigated.

Chapter 3

Comparative genomic hybridization and von Hippel-Lindau mutation analysis in sporadic and hereditary hemangioblastomas: possible genetic heterogeneity

Johanna M.M. Gijtenbeek¹, Bram Jacobs¹, Sandra H.E. Sprenger², Marc J. Eleveld³, Ad H.M. Geurts van Kessel³, Johan M. Kros⁴, Raf Sciot⁵, Frank van Calenbergh⁵, Pieter Wesseling², Judith W.M. Jeuken²

¹ Department of Neurology

² Department of Pathology and ³Department of Human Genetics, Nijmegen Centre for Molecular Life Sciences, Radboud University Nijmegen Medical Centre, The Netherlands

⁴ Department of Pathology, Erasmus University Medical Center, Rotterdam, The Netherlands

⁵ Department of Neurosurgery, University Hospital K.U. Leuven, Belgium

Abstract

Hemangioblastomas (HBs) occur sporadically or as a manifestation of von Hippel-Lindau (VHL) disease. In the majority of VHL-associated HBs inactivation of the *VHL* tumor suppressor gene (TSG), which is located on chromosome 3p25-26, is found. The *VHL* gene is assumed to be involved also in the development of sporadic HBs. In a previous study of chromosomal aberrations of sporadic HBs, multiple chromosomal imbalances were found in the majority of tumors. The aim of this study was to analyze further both sporadic HBs and VHL-associated HBs to determine if these histopathologically identical tumors have a different genetic background.

Sixteen sporadic HBs and seven VHL-associated HBs were identified by clinical criteria and analyzed. Comparative genomic hybridization (CGH) was used to screen for chromosomal imbalances throughout the entire HB genome. Additionally, mutation analysis of the *VHL* gene was performed by direct sequencing.

Loss of chromosome 3 and multiple other chromosomal imbalances were found in the sporadic HBs, although only one imbalance, a loss of chromosome 3, was detected in the seven VHL-associated HBs. Somatic *VHL* gene mutations were found in one-third of sporadic HBs, whereas a mutation of the *VHL* gene was detected in all VHL-associated HBs.

These results indicate that the molecular mechanisms underlying sporadic HBs and VHL-associated HBs are different. Inactivation of the *VHL* gene is probably not the most important event in the tumorigenesis of sporadic HBs. Other mechanisms of inhibition of VHL protein function, or inactivation of other TSGs, on chromosome 3(p) or on other chromosomes, might be important in the development of sporadic HBs.

Introduction

Hemangioblastomas (HBs) of the central nervous system (CNS) are rare, benign tumors (WHO Grade 1) that account for 1 to 2% of all intracranial tumors.^{10,45} They occur predominantly in the cerebellum, and typically appear on neuroimaging studies as contrast-enhancing nodules with associated cysts.⁴⁵ Symptoms often arise from an increase in intracranial pressure caused by impaired cerebrospinal fluid flow. The standard treatment is surgical removal; radiosurgery is an alternative for deeply located, small HBs.^{15,40}

HBs occur in sporadic form (75%) or as a manifestation of VHL disease (VHL-associated HBs, 25%).^{4,10} An autosomal dominant inherited disorder, VHL disease is caused by a germline mutation of the *VHL* tumor suppressor gene (TSG), and is characterized by one or more of the following tumors: HBs of the cerebellum, spinal cord, and retina; clear cell renal cell carcinomas (RCCs); pheochromocytomas; and endolymphatic sac tumors. Additionally, cysts in the pancreas, kidney, and epididymis are frequently found.²⁷ In approximately 40% of patients with VHL, an HB is the first manifestation of VHL disease.⁹ Therefore, clinical and radiological screening for other VHL-associated tumors is recommended in patients presenting with an HB.^{9,35,37}

Histologically, HBs are composed of neoplastic stromal cells and abundant capillaries.⁴⁵ The origin of the neoplastic stromal component is still subject of debate.^{7,45} The angiogenic phenotype of HBs has been explained by the involvement of the VHL protein (pVHL) in degradation of the HIFs (HIF-1 α and HIF-2 α) by ubiquitination.¹⁵⁹ The pVHL forms, with elongin B, elongin C, and cullin-2, the VCB-CUL2 complex, which targets the HIFs for degradation under normoxic conditions.^{94,95,97} In hypoxia, the HIFs are stabilized and induce angiogenesis by upregulation of angiogenic factors such as vascular endothelial growth factor (VEGF). Because of inactivation of the *VHL* gene, the HIFs are not degraded under normoxic conditions, and subsequently abundant vessel formation occurs.^{97,103} Nevertheless, the overexpression of angiogenic factors does not fully explain the tumorigenesis of HBs. Other factors with growth-inducing properties may also be important in the development of VHL-associated tumors.¹¹¹ Furthermore, the VHL protein may control gene expression by other mechanisms, for instance by regulation of transcription elongation,¹⁴⁹ although this latter function of the VHL protein has recently been disputed.¹⁵⁹

The *VHL* gene maps to chromosome 3p25-26,⁶⁰ and a broad spectrum of germline mutations has been reported in 63 to 100% of families in which VHL disease has been identified.^{29,30,61,62} In concordance with Knudson's two-hit hypothesis,⁶⁶ the majority of VHL-associated tumors show the germline mutation, and loss of heterozygosity (LOH) at 3p, small intragenic mutations, or hypermethylation of the other allele.^{61,67} Conflicting results of the importance of VHL hypermethylation have been reported in HBs of the CNS.^{61,67,77}

Inactivation of the *VHL* gene has also been reported to play a role in the sporadically occurring counterparts of the tumors observed in VHL disease.⁶⁹⁻⁷¹ Up to 50% of sporadic HBs showed LOH at 3p, whereas somatic mutations of the *VHL* gene have been found, on average, in 25%.^{38,61,75-77} Biallelic inactivation, however, was found in only one of 13 sporadic HBs investigated by Gläsker, et al,⁶¹ and they suggested that inactivation of other TSGs on chromosome 3p might be crucial for the development of sporadic HBs. Other chromosomes might be involved in the tumorigenesis of sporadic HBs, as indicated by our previous study,¹⁶⁰ in which we used comparative genomic hybridization (CGH) to screen for chromosomal imbalances throughout the entire tumor genome of 10 sporadic HBs. In the present study, we analyzed chromosomal imbalances by using CGH, and aberrations of the *VHL* gene by mutation analysis in sporadic HBs and VHL-associated HBs to elucidate further the molecular genetic differences in these histopathologically identical tumors.

Material and Methods

Twenty-three tumor samples of HBs of the CNS were obtained in 20 patients who were treated at the Radboud University Nijmegen Medical Centre, The Netherlands (Tumors N240-N244, N298, N341, N342, N379, and N380), the Erasmus University Medical Center, Rotterdam, The Netherlands (Tumors N364-N368, and N370), or the University Hospital Leuven, Belgium (Tumors N245-N249, N373, and N378). One sporadic HB was a recurrence (Tumors N298 and N243), and two patients with VHL had two different VHL-associated HBs (Tumors N379 and N380, and Tumors N364 and N368). Samples of 21 HBs were collected during surgery, snap-frozen, and stored at -80°C. In two cases (Tumors N341 and N342) no frozen tissue was available and, therefore, formalin-fixed and paraffin-embedded tissue was analyzed. Clinical criteria

provided by the Dutch National VHL Working Group, based on international guidelines, were used to establish VHL disease.^{27,35} Criteria for VHL disease include a single HB and a positive family history of VHL disease, at least two HBs (including retinal or spinal), or a single HB in association with other typical VHL-associated tumors such as clear cell RCC or pheochromocytoma.²⁷ All tumor samples were histopathologically diagnosed according to the criteria of the World Health Organization (WHO).⁴⁵

The CGH was performed as previously described by Jeuken et al.¹⁵³ Briefly, DNA was extracted by a salting out procedure.¹⁵⁴ Control and tumor DNA were labeled by nick-translation with digoxigenin-dUTP and biotin-dUTP, respectively. The DNA isolated from paraffin-embedded tissue (Tumors N341 and N342) was labeled with a rhodamine universal linkage system as described by the manufacturer, with minor modifications. Labeled DNA was precipitated in the presence of human COT-1-DNA and herring sperm DNA. Target metaphase spreads were prepared using standard procedures; the probe and the metaphase slides were denatured simultaneously. After hybridization and posthybridization washes, biotin and digoxigenin were detected using streptavidin-fluorescein isothiocyanate and sheep-antidigoxigenin-tetramethyl rhodamine isothiocyanate. The chromosomes were counterstained with 4,6'-diamino-2-phenylindole-dihydrochloride and were finally mounted in Fluoroguard. Negative and positive control experiments were included in each series of CGHs to monitor CGH quality. For CGH analysis, commercially available software was used and detection thresholds for losses and gains were set at 0.8 and 1.2, respectively.

Analysis of *VHL* gene mutations was performed by direct sequencing, as described by Bodmer, et al.¹⁶¹ In summary, five primer sets were used to amplify exons 1 (three overlapping primer sets), 2, and 3 of the *VHL* gene from tumor tissue DNA. The polymerase chain reaction (PCR) products were purified and subsequently sequenced, after which the sequence products were analyzed.

Sources of Supplies and Equipment. The digoxigenin-dUTP and the biotin-dUTP used in the nick-translations were purchased from Roche Molecular Biochemicals, Almere, The Netherlands, as were the streptavidin-fluorescein isothiocyanate and sheep-antidigoxigenin-tetramethyl rhodamine isothiocyanate. The rhodamine universal linkage system (model ULS/Ulysis) was acquired from Kreatech Biotechnology, Amsterdam, The Netherlands. The

human COT-1-DNA was supplied by Gibco-BRL Life Technologies, Inc., Gaithersburg, MD. The 4,6'-diamino-2-phenylindole-dihydrochloride was purchased from Merck, Darmstadt, Germany, and the Fluoroguard was acquired from Biorad, Veenendaal, The Netherlands. The Quips CGH software was purchased from Applied Imaging, Newcastle upon Tyne, UK. The PCR purification kit (QIAquick) was supplied by Qiagen, Westburg, The Netherlands. The ABI PRISM BigDye Terminator Cycle sequencing kit was acquired from Applied Biosystems, Foster City, CA, as was the ABI PRISM DNA analyzer (model 3700).

Results

In Table 1 we have summarized the clinical characteristics of the patients and tumors, chromosomal imbalances detected by CGH in the tumors, and *VHL* mutations detected by direct sequencing in the tumors. Clinical evaluation identified 16 sporadic HBs and seven *VHL*-associated HBs. The 16 sporadic HBs (obtained in 11 male and four female patients; mean age at surgery 50 years, range 14-69 years) included one recurrence and one spinal HB. All patients with *VHL* disease (two men and three women; mean age at surgery 33 years, range 21-47 years) harbored multiple cerebellar and/or spinal HBs, in two patients there were also multiple pancreatic and epididymal (Tumors N379 and 380) or renal (Tumor N378) cysts, in one patient there was a retinal HB (Tumor N370), and in two patients there was a positive family history for *VHL* disease (Tumors N373 and N378).

The CGH results are depicted in Figure 1. The chromosomal imbalances most frequently detected in 16 sporadic HBs were loss of chromosome 3 (designated -3) in 11 tumors (69%); -6 in seven (44%); -18(q) in five (31%); and -9 in four (25%); and gain of chromosome 19 (designated +19) in four sporadic HBs (25%). In three sporadic HBs (19%) no abnormalities were detected using CGH. In the seven *VHL*-associated HBs only one aberration (-3) was found on CGH (14%). This patient (Tumor N370) had multiple cerebellar and spinal HBs and a retinal HB.

Sequencing of the *VHL* gene identified three somatic frameshift mutations and two missense mutations in the sporadic HBs (five (31%) of 16; Table 1). These mutations, to our knowledge, have not been previously

Table 1 Patient and tumor characteristics and results of CGH and mutation analysis

Tumor nr	Age/sex	Tumor location	Chromosomal imbalances					Other imbalances	Mutation VHL gene tumor	
			-3	-6	-18	-9	+19		Nucleotide change	Mutation name
Sp HBs										
N241	34, F	cerebellar	*							
N242	56, M	Spinal	*							
N245	31, M	Cerebellar	*							
N341	61, M	Cerebellar	*				+4q, +6q, -16p, -19, -20q, -22			
N240	47, M	Cerebellar	*	*						
N246	56, M	Cerebellar	*	*	*		+1q, -10, -14q			
N243	49, M	Cerebellar	*	*	*	*	+4, +5, +7, +16, +17, -22	400 del C	400delC	frameshift
N298 [†]	52, M	Cerebellar	*	*	*	*	+4q, -22			
N244	60, F	Cerebellar	*	*	*	*	+17	528 ins GCGGCC	528insGCGGCC	frameshift
N366	69, M	Cerebellar	*	*	*	*	-8, -10, -11			
N365	14, M	Cerebellar	*				-8			
N248	52, M	Cerebellar	*	*		*	-8, +15q	392 del GGCC	392delGGCC	frameshift
N342	49, F	Cerebellar	*	*			-10, -14q	490 G to C	G93R	Gly to Arg
N247	72, F	Cerebellar								
N249	66, M	Cerebellar								
N367	42, M	Cerebellar						233 A to C	N71	Asn to Ile
VHL-HBs										
N379 [†]	28, M	Cerebellar								
N380 [†]	28, M	Cerebellar						667 A to C	T152P	Thr to Pro
N364 [§]	46, M	Spinal						667 A to C	T152P	Thr to Pro
N368 [§]	47, M	Cerebellar						453 T to G	S80R	Ser to Arg
								453 T to G	S80R	Ser to Arg
								homozygous del exon 2 [#]		
N370	47, F	Cerebellar	*					685 C to G	L158V	Leu to Val
N373	21, F	Spinal						446 A to G	N78S	Asn to Ser
N378	26, F	cerebellar								

*N246; -18q; [#]the deletion could not be confirmed by Southern blotting because of insufficient DNA.

[†]recurrence of N243; [‡]different HB, same patient; [§]different HB, same patient

described.^{32,35,38,61,67,75-77,162} Mutations were identified in six (86%) of seven VHL-associated HBs (Table 1). These mutations are not germline mutations per se; blood was available for only two VHL-associated HBs (Tumors N379 and N380) in which the germline mutation T152P was confirmed. To our knowledge, the mutation T152P has not been reported previously.^{30,62,162} All were missense mutations, of which S80R, L158V, and N78S were previously described as germline mutations.^{30,162} In one VHL-associated HB a homozygous deletion of exon 2 was found (Table 1). We could not confirm this deletion by Southern blotting due to the small amount of DNA available. Germline homozygous deletions have been reported in VHL disease.¹⁶²

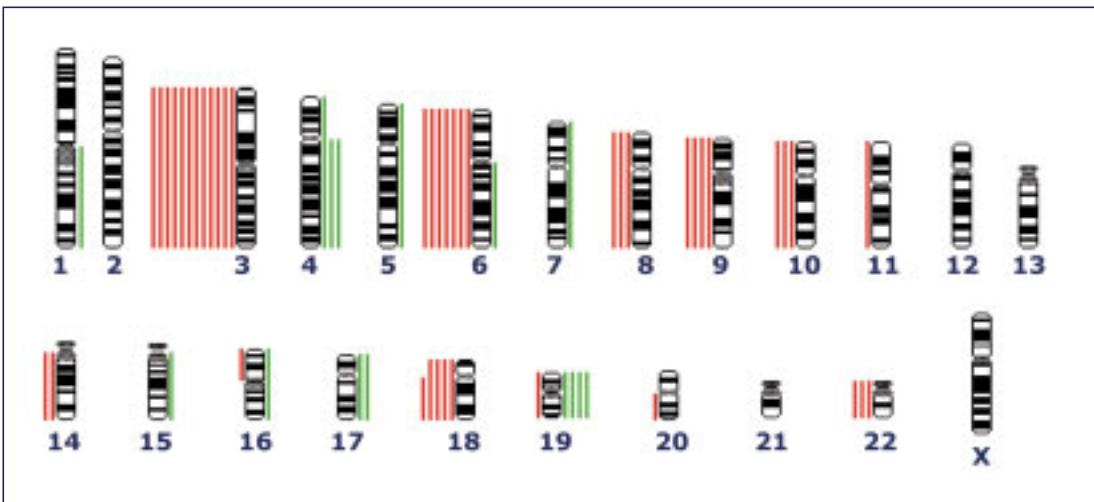


Figure 1 Map showing chromosome imbalances detected using CGH in sporadic hemangioblastomas (HBs) and VHL-associated HBs. Lines on the left side of the chromosomes represent regions that are underrepresented in the tumor genome (losses), whereas lines on the right side of the chromosomes represent regions that are overrepresented (gains). Only one chromosomal imbalance was detected in the VHL-associated HBs, a loss of chromosome 3. The other imbalances were detected in sporadic HBs.

Discussion

Loss of chromosome 3 and mutations of the *VHL* gene

A complete loss of chromosome 3 (designated -3) was found in 11 (69%) of 16 sporadic HBs, whereas -3 was detected in only one (14%) of seven of VHL-

associated HBs, and multiple other chromosomal imbalances were detected in most sporadic HBs, but not in VHL-associated HBs. Furthermore, mutations of the *VHL* gene were identified in only five (31%) of 16 sporadic HBs, but in all seven VHL-associated HBs (Table 1). Thus, these results show genetic differences in sporadic compared with VHL-associated HBs. Inactivation of the *VHL* TSG at 3p25-26 is considered to be a common oncogenic mechanism in VHL-associated tumors,^{61,67} and germline mutations of this gene are reported to be present in up to 100% of VHL-associated HBs.^{30,61,62} Until recently, it was generally assumed that the *VHL* TSG was also involved in the tumorigenesis of the sporadic counterparts of the VHL tumors,^{38,75-77} as was shown in clear cell RCCs.⁶⁹⁻⁷¹ Somatic mutations of the *VHL* gene have been reported, however, in only 25% of sporadic HBs (17 of 69; range 10-41%),^{38,61,75-77} whereas LOH at 3p has been found in 52% of tumors (16 of 31 overall; range 50-53%).^{61,76,77} Furthermore, in a recent study inactivation of both alleles of the *VHL* gene was found in only one (8%) of 13 sporadic HBs compared with 13 (62%) of 21 VHL-associated HBs, suggesting that biallelic inactivation of the *VHL* gene plays a minor role in tumorigenesis of sporadic HBs.⁶¹ These latter findings corroborate our suggestion that the *VHL* gene might be involved in only a subset of sporadic HBs and that other TSGs on chromosome 3p might be important in the development of sporadic HBs.

Although according to Knudson, inactivation of both alleles of a TSG is required to cause tumor development.⁶⁶ TSGs may also cause tumors by giving rise to dominant negative mutations or haploinsufficiency.^{163,164} Dominant negative mutations inhibit the function of the wild-type allele and the production of wild-type protein. Haploinsufficiency is caused by a relative shortage of the wild-type protein as a direct result of loss of one of the alleles. Such mechanisms might be involved in the tumorigenesis of sporadic HBs. As the detection limit of CGH is 2 to 5 Mb, smaller losses and gains may be present in these tumors.

Putative TSGs on chromosome 3

The frequent loss of chromosome 3 in sporadic HBs suggests a prominent role for genes located on this chromosome in the development of sporadic HBs. In a review of DNA copy number losses in various human neoplasms it was reported that a complete or partial loss of chromosome 3p is often found by LOH and CGH analysis, whereas losses of chromosome 3q are relatively rare.¹⁵⁶

Putative TSGs have been suggested at several regions on 3p: at 3p12-14 containing, among others, the *fragile histidine triad* gene; at 3p21.3-p22 containing the *lung cancer TSG region 1*; and in the *VHL* gene region 3p25-26 containing, among others, the DNA repair gene *Xeroderma pigmentosum C*.^{73,79,80,156} An important role for TSGs at 3p12-14 and 3p21.3 in the tumorigenesis of sporadic and *VHL*-associated RCCs has already been suggested,^{73,79,80} but the involvement of these putative TSGs in sporadic HBs or *VHL*-associated HBs has not yet been reported.

In three of the sporadic HB samples (Tumors N247, N249, and N367) no chromosomal aberrations were detected with CGH. Because the detection limit of CGH is 2 to 5 Mb, these HBs may contain small aberrations not detectable using this method. It is also possible that chromosomal aberrations were not detected because the percentage of normal DNA was too high. Nevertheless, because the *VHL*-associated HBs and sporadic HBs are phenotypically identical, there is no reason to assume that the percentage of normal DNA in the sporadic HBs and the *VHL*-associated HBs is different.

Involvement of other chromosomes in sporadic HBs

Genes located on other chromosomes may also play a role in the genesis of sporadic HBs. As reported in our previous study,¹⁶⁰ and confirmed by analyzing this larger group of sporadic HBs, the frequency of the aberrations and their occurrence in individual sporadic HBs might indicate a pathway of sequential events in sporadic HBs (see Table 1): -3 may be a primary event, followed by -6, -18, and -9, and/or +19. Interestingly, a loss of chromosome 8 was detected in three sporadic HBs, two of them with a normal constitution of chromosome 6. The third sporadic HB containing -8 was a tumor with multiple imbalances but with a normal chromosome 3. Therefore, eight of 10 sporadic HBs with multiple chromosomal aberrations had two of the following imbalances: -3, -6, or -8.

In human tumors, (putative) TSGs and oncogenes have been reported on chromosomes 6, 8, 9, 18, and 19.¹⁵⁶ Whether these genes are involved in the development of sporadic HBs is currently unknown. Other imbalances were less frequently found in sporadic HBs (Table 1). Some of these imbalances were also infrequently detected in *VHL*-associated and sporadic clear cell RCCs.^{68,88,165} Because of the angiogenic phenotype of HBs, some genes on

chromosome 6 and 8 are particularly interesting. *Brain-specific angiogenesis inhibitor 3*, a gene with angiogenesis-inhibiting properties specifically expressed in the CNS, is mapped to 6q12.¹⁶⁶ Theoretically, inactivation of this gene in sporadic HBs might contribute to the abundant vessel formation in HBs. Two of the sporadic HBs without -6 had -8. Chromosome 8 contains two genes encoding antiangiogenic factors; *brain-specific angiogenesis inhibitor 1* is mapped to 8q24, and *angiopoietin 2* is mapped to 8p21.¹⁶⁶ Angiopoietin 2 is a tyrosine kinase receptor antagonist and is expressed at sites of vascular remodeling and maturation, where it can have both angiogenic and antiangiogenic properties.¹⁶⁷

Further investigation of the genes located on the chromosomes that show imbalances in sporadic HBs may help elucidate the pathogenesis of the enigmatic HB.

In conclusion

As detected by CGH, chromosome 3 was lost in the majority of sporadic HBs, whereas loss of chromosome 3 was found in only one VHL-associated HB. Additionally, losses of chromosome 6, 9, and 18, and gain of chromosome 19 are often present in sporadic HBs; no other imbalances were found in VHL-associated HBs. Mutations of the *VHL* gene were detected in 31% of sporadic HBs and in all VHL-associated HBs. These findings indicate that inactivation of the *VHL* gene is probably not the most important molecular event in sporadic HBs, and that these tumors and VHL-associated HBs have a different genetic background. The pathogenetic pathway of sporadic HBs remains to be elucidated. Other than the *VHL* gene, TSGs on chromosome 3 and TSGs on other chromosomes might be instrumental in the development of these tumors.

Acknowledgements

The authors thank Bert van der Zwaag and Karin Wichers for technical assistance.

Chapter 4

Array-based comparative genomic hybridization analysis of sporadic hemangioblastomas

Johanna M.M. Gijtenbeek¹, Judith W.M. Jeuken², Simon V. Reijmersdal³, Sandra H.E. Boots-Sprenger², Eric F.P.M. Schoenmakers³, Pieter Wesseling², Johan M. Kros⁴, George W.A.M. Padberg¹, Roland Kuiper³

¹Department of Neurology,

²Department of Pathology and ³Department of Human Genetics, Nijmegen Centre for Molecular Life Sciences, Radboud University Nijmegen Medical Centre, The Netherlands

⁴Department of Pathology, Erasmus University Medical Center, Rotterdam, The Netherlands

Submitted

Abstract

Hemangioblastomas (HBs) are highly vascular, benign tumors of the central nervous system (CNS), which occur as sporadic tumors or as a manifestation of von Hippel-Lindau (VHL) disease. VHL disease is an autosomal dominant tumor syndrome, resulting from an inherited (germline) mutation in one allele of the *VHL* gene, a tumor suppressor gene (TSG) located at chromosome 3p25-26. Germline mutations of the *VHL* gene lead to several benign and malignant tumors, including, besides HBs, clear cell renal cell carcinomas (RCCs) and pheochromocytomas. Although the *VHL* gene also plays a role in the development of sporadic HBs and RCCs, biallelic inactivation of the gene is found in only a minority of sporadic tumors. Therefore, it has been suggested previously that additional genes are involved in the tumorigenesis of these tumors. Aiming at the identification of such genes, we analyzed five HBs, previously characterized with conventional comparative genomic hybridization (CGH) and *VHL* mutation analysis, with a 32K BAC array CGH to identify microdeletions or microamplifications, which may harbor causative genes. The array CGH used in this study enables interrogation of the entire human genome for submicroscopic genomic copy number alterations at over 32,000 loci with a resolution of less than 100kb. In three sporadic HBs, three subtle and de novo microdeletions were identified, within cytogenetic bands 2q14.1 (found in two tumors), 3q13.31, and 8p21.3, respectively. The subtle character of the genetic intervals affected (in the order of a few hundred kb) and, consequently, the limited number of genes residing within these deletion intervals, for the first time allows for a positional functional candidate approach, aiming at elucidating the oncogenetic triggers leading to HB (and/or RCC) development.

Introduction

Hemangioblastomas (HBs) are highly vascular, benign tumors of the central nervous system (CNS), predominantly located in the cerebellum and spinal cord, and account for 1-2.5% of all intracranial neoplasms.^{4,45} The majority of HBs occur as sporadic lesions. However, in approximately 25% of cases they are a manifestation of von Hippel-Lindau (VHL) disease. HBs are the most common tumors in VHL disease, occurring in 60-80% of patients.^{1,168}

VHL disease (OMIM #193300, <http://www.ncbi.nlm.nih.gov/entrez/query.fcgi?db=OMIM>) is an autosomal dominantly inherited disorder, which, besides CNS and retinal HBs, is characterized by the development of clear cell renal cell carcinomas (RCCs), pheochromocytomas, pancreatic islet cell tumors, endolymphatic sac tumors, and cysts and cystadenomas in the kidney, pancreas, epididymis, and broad ligament.^{1,27} VHL disease results from a heterozygous germline mutation in the *VHL* gene at 3p25-26, that can be identified in 100% of VHL families.^{60,62} The *VHL* gene is a tumor suppressor gene (TSG) that fits the two-hit model of Knudson of biallelic inactivation of TSGs.⁶⁶ Although the *VHL* gene is involved in the tumorigenesis (and/or early progression) of the sporadic counterparts of VHL-associated tumors, e.g. HBs and RCCs, its exact role in these tumors has not been fully elucidated.^{2,16,79,169} In sporadic HBs, inactivation of one allele of the *VHL* gene by somatic mutation, LOH, or hypermethylation, has been reported in only approximately 20-50% of tumors.^{38,61,75-77} Moreover, in only 10% of sporadic HBs biallelic inactivation of the *VHL* gene could be demonstrated.^{61,169} Other genes are thus likely to be involved in the development of sporadic HBs, but these gene(s) have not yet been identified. In previous studies on sporadic HBs, we showed multiple chromosomal aberrations by comparative genomic hybridization (CGH), including loss (-) of chromosomes 3, 6, 8, 9, 10, 18, and 22, and gain (+) of chromosomes 4(q), and 19.^{160,169} Loss of chromosome 3 (69%) and chromosome 6 (44%) were the most frequent DNA copy number changes found in these tumors.¹⁶⁹ Other studies confirmed the potential importance of (a gene on) chromosome 6(q) in the development of sporadic HBs, as loss of the 6q arm was found in 23% of the cases by CGH, and LOH at 6q was detected in the majority (in 83%) of the tumors included in these studies, with the minimal deleted region detected at 6q23-24.^{170,171} Up till now, loss of chromosome 8(q) has been reported in five of 34 (15%) HB cases, including three of our own series.^{14,169,170}

CGH is a useful technique for genome-wide screening of DNA copy number imbalances by hybridizing differentially labeled test and reference DNA to normal metaphase spreads. The main disadvantage of CGH, however, is its relatively low resolution of 2-5 Mb. One possibility to overcome this problem is offered by the application of array CGH in which differentially labeled reference and tumor DNAs are co-hybridized onto an array of bacterial artificial chromosome (BAC)-derived targets instead of chromosomes.^{143,144,172} Array CGH has in theory a practically unlimited genomic resolution, but the actual resolution of the slides used depends on the genomic size and spacing of the targets present on the array. We have the availability of full human genome coverage (so-called "Golden Path") arrays, currently containing over 32,000 well annotated and fully integrated BAC clones, altogether representing well over 99% of the sequenced human genome (at two-fold coverage). These "ultimate resolution" genomic arrays are capable of reliably detecting copy number imbalances affecting genomic intervals as small as 100 kb.^{145,146,173} In this study, we have used these tiling-resolution 32K BAC arrays for the identification of novel and small copy number changes in HBs that previously remained undetected by conventional CGH analysis. Based on our previous studies and reports from others, we were particularly interested in abnormalities on chromosomes 3, 6, and 8.^{169,171} Therefore, a subset of sporadic HBs from tumors previously analyzed with conventional CGH and *VHL* gene mutation analysis were selected in which these aberrations might be expected. This approach led to the identification of three novel candidate regions on chromosomes 2, 3, and 8 of which the corresponding genes may be associated with the development of HBs.

Material and Methods

Tumor samples

Five sporadic HBs obtained from patients treated at the Radboud University Nijmegen Medical Centre, The Netherlands (N241, N242), the Erasmus University Medical Center Rotterdam, The Netherlands (N365, N366), and the University Hospital Leuven, Belgium (N248) were analyzed in this study. Conventional CGH and *VHL* gene mutation analysis of these tumors have been performed previously (Tabel 1).¹⁶⁹

Table 1 Chromosomal imbalances by CGH and *VHL* gene mutations in sporadic hemangioblastomas

	Chromosomal imbalances by CGH	Mutation <i>VHL</i> gene
N241	-3	none
N242	-3	none
N248	-6, -8, -9, +15q	392delGGCC
N365	-3, -8	none
N366	-3, -8, -10, -11, -18, +19	none

Tiling-resolution array-based CGH

In this study, we have used a tiling-resolution microarray consisting of 32,447 overlapping BAC clones selected to cover the entire genome,^{145,174} which was prepared as previously described.^{146,175} In short, genomic target DNAs were isolated from bacterial cultures using an AutogenPrep 960 (Autogen, Holliston, MA) according to the manufacturer's instructions. Subsequently, 50 ng DNA from each of the clones was amplified using degenerate oligonucleotide-primed PCR (DOP-PCR), dissolved at a concentration of 1 µg/µl in 30% DMSO-containing spotting buffer, and spotted once on a single CMT-ultragaps coated glass slide (Corning) by use of an Omnigrid 100 arrayer (Genomic Solutions).

Labeling and hybridization

Tumor DNA was extracted from snap-frozen tissue samples using the DNeasy tissue kit (Qiagen). Subsequently hybridizations were performed basically as described elsewhere.¹⁷² In brief, 500 ng of genomic DNA from tumor sample and sex-matched reference pool were labeled by random-primed labeling with Cy3-dUTP or Cy5-dUTP (Amersham Biosciences), respectively. Labeled DNAs were mixed with 120 µg human Cot-1-DNA (Roche), co-precipitated, and re-suspended in hybridization solution (50% formamide; 10% dextran sulphate; 2 x sodium saline citrate (SSC); 4% SDS; 10 µg/µl tRNA (Invitrogen)). Slides were hybridized for 18 hours at 37°C with active circulation, followed by five wash cycles in 50% formamide, 2x SSC at 45°C, and five wash cycles in phosphate buffer at 20°C. Next, slides were dried by centrifugation and scanned on a Genepix Autoloader 4200AL laser scanner (Axon Instruments). Analysis of the microarray image files was performed with the GenePix Pro 5.0 software package (Axon Instruments), and all data were uploaded in a database for normalization and further analysis. Loss and gain regions were detected with

the aid of a standard hidden Markov model (HMM) as described previously.¹⁴⁶ Statistical analysis was performed using a Student *t* test. Chromosomal regions were considered as candidate regions for gain or loss when the average log₂ ratio of a chromosomal region of interest was significantly different from the average log₂ ratio of 15 flanking clones on each side (p-value below 0.01). All identified genomic copy number alterations were compared to both public and private databases of known disease-unrelated large-scale copy-number variations (CNVs) (<http://projects.tcag.ca/variation/>). Gene organization of the region involved was obtained from public databases (<http://genome.ucsc.edu> NCBI genome build 35, May 2004).

Results

In all five HB samples selected for this study multiple genomic copy number alterations were detected ranging from the gain or loss of complete chromosomes to regions as small as 0.26 Mb, although the average log₂ ratio differences were relatively small due to the expected presence of considerable amounts of non-tumor cells in the samples (Figure 1). Nevertheless, all chromosomal aberrations identified by conventional CGH (Table 1) could be confirmed by array CGH, and additional chromosomal gains and losses were also detected (e.g. loss of chromosome 18 and 21q11.2-21.3 in tumor N241, and gain of chromosome 15 in tumor N248; Figure 1). Tumor N366 revealed the most complex genomic profile, showing many chromosomes at intermediate copy number levels (Figure 1). In addition to whole chromosome alterations, submicroscopic copy number changes were found throughout the genome, ranging in size from 0.26-1.84 Mb. However, many of these genomic variations have previously been identified in healthy individuals and thus should be considered as disease-unrelated copy number variations (CNVs). On average, three to seven CNVs were identified per tumor with minimal sizes varying from 0.26 to 0.43 Mb, which illustrates the practical resolution that can be achieved with these tiling-resolution BAC arrays even in tumor samples with high levels of non-tumor cell contamination (of normal vascular cells, e.g. endothelial cells, pericytes).

In three of the five tumors, we detected in total four novel deletions (Table 2). A sub-megabase deletion on 2q13-14.1 was detected in two HB cases (N248

Table 2 Candidate microdeletions in hemangioblastomas detected by array CGH

Tumor No	Chromosome location	Size (Mb)	No of clones	Start clone	End clone	Candidate genes
N248	2q13-14.1	0.27	5	RP11-638N20	RP11-395L14	CBWD2, FOXD4L1, RABL2A
N365	8p21.3	1.38	12	RP11-563N12	RP11-135I5	FEZ1/LZTS1
N366	2q13-14.1	0.50	6	RP11-638N20	RP11-702P7	CBWD2, FOXD4L1,RABL2A
	3q13.31	0.67	9	RP11-170O17	RP11-33E19	LSAMP

and N366; Figure 2). However, this region appeared to be paralogous (>98% homology) to three regions on chromosome 9. Consequently, copy number changes in any of these loci, like for example the loss of chromosome 9 in tumor N248, will affect log₂ ratios in all paralogous regions. In addition, a putative 1.38 Mb deletion on 8p21.3 in tumor N365 and a 0.67 Mb deletion on 3q13.31 in tumor N366 were found. Both deletions would be homozygous in the tumor cells, since these tumors were known to have already a loss of one copy of these respective chromosomes (Table 1 and Figure 1). Although the log₂ ratio differences of these regions were not readily detected from the primary profile, these regions were detected by the hidden Markow algorithm (Materials and Methods section), and the average ratios were significantly lower relative to the surrounding clones and correlated very well with the extrapolated values that could be predicted on the basis of the average log₂ ratios corresponding to the loss of a single copy. Interesting candidate TSGs are present in both regions, namely *LSAMP* on 3q13.31 and *FEZ1/LZTS1* on 8p21.3 (Figure 2).

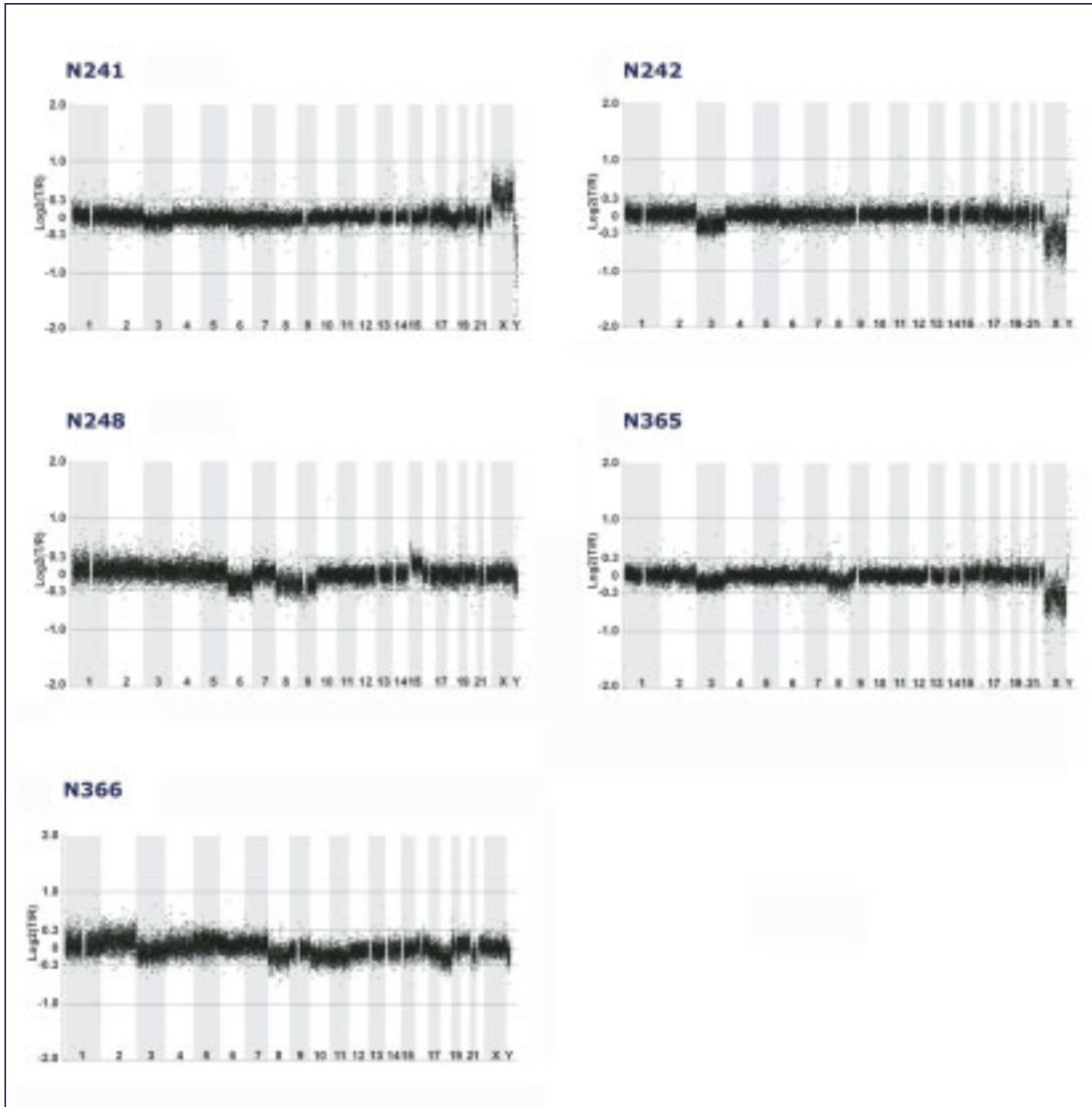


Figure 1 Genomic profiles of five hemangioblastomas. Array containing 32,447 human BAC clones (indicated by small circles representing the log₂-transformed and normalized test-over-reference intensity ratios), genomically ordered from 1pter to Yqter in the genome profile, and for individual chromosomes from pter to qter, all on the basis of the physical mapping positions obtained from the May 2004 freeze (build 35) of the UCSC genome browser. The profiles of tumors N241, N248, N365, and N366 are based on two merged experiments.

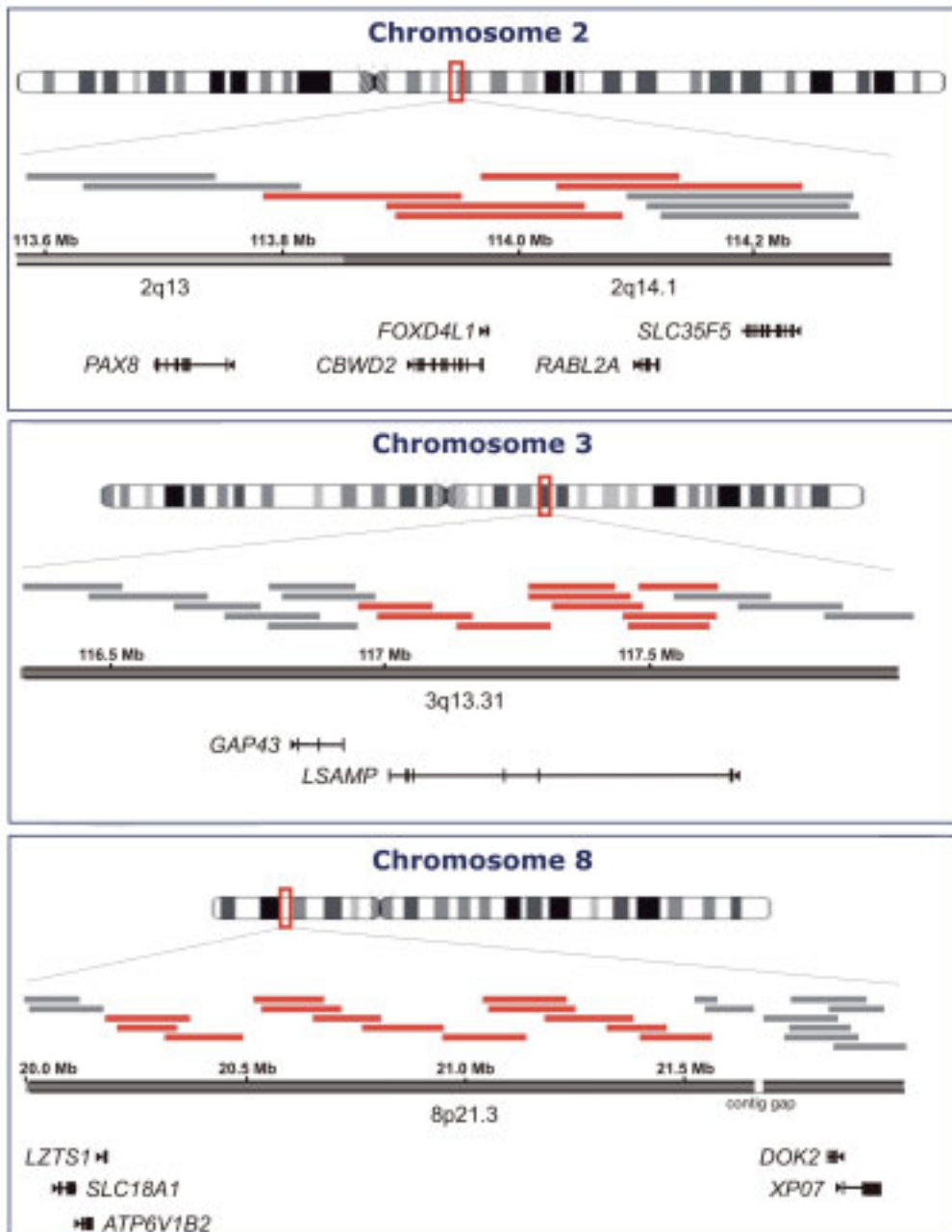


Figure 2 Schematic representation of the genomic organisation of the three identified deletions. Gray bars indicate BAC clones with normal ratios, red bars represent BAC clones with a significantly low ratio. Mapping positions obtained from the May 2004 freeze (build 35) of the UCSC genome browser.

Discussion

Since biallelic inactivation of the *VHL* gene at 3p25-26 is found in only a minority of sporadic HBs, we and others previously suggested that the development of these tumors may also be dependent on the (in)activation of other genes.^{61,169,171} To identify chromosomal regions of interest that might potentially harbor such genes, we previously screened the genomes of 16 sporadic HBs by conventional CGH.^{160,169} Multiple chromosomal aberrations were detected, supporting the hypothesis of the presence of an alternative, *VHL*-independent pathway.¹⁶⁹ Although CGH is a useful technique for detecting larger (> 5 Mb) copy number changes it is not particularly suitable for the detection of more subtle (smaller) deleted regions, which might contain putative TSGs or oncogenes. In order to identify such small copy number changes without focusing on specific known regions/genes, we used the high-resolution and high-throughput 32 K array CGH technique. In addition to previously described chromosomal copy number changes, we were able to detect various small copy number changes, ranging in size from 0.26-1.84 Mb. As could be expected, most of these genomic variations represent known, disease-unrelated CNVs. As HBs are extremely well-vascularized and only the stromal cells are neoplastic, the identification of novel copy number changes in HBs is hampered in both array CGH and conventional CGH by the relatively large amount of normal DNA in this tumor type. As a result, tumor-specific copy number changes were reflected by much lower test-versus reference ratio differences than those of chromosome X (in sex-matched hybridizations) and CNVs, which are present in all cells. Nevertheless, in three tumors we identified four potentially relevant microdeletions within cytogenetic bands 2q13-14.1 (found in two cases), 3q13.3, and 8p21.3 (Table 2). These regions were selected for further validation by interphase FISH for the following reasons: firstly, none of these copy number aberrations were known as recurrent disease-unrelated polymorphic regions. Secondly, although the ratio differences of the identified regions were only small, they were found to be significant and close to the values that could be expected in tumors that have a relatively high degree of non-tumor cell contamination. Finally, among the genes that may be affected by these microdeletions were several interesting candidate TSGs. No submicroscopic alteration were identified on chromosome 6, whereas in

another study LOH at 6q23-24 has been reported in 9 of 11 (82%) sporadic HBs.¹⁷¹ Abnormalities on other frequently lost chromosomes in sporadic HBs were not identified.

The putative homozygously deleted region on chromosome 3q13.3 contains one single gene, the *LSAMP* (limbic system-associated membrane protein) gene. *LSAMP* encodes a neuronal surface glycoprotein that belongs to the IgLON family of cell adhesion molecules and is distributed in the cortical and subcortical regions of the limbic system. During development of the limbic system, the encoded protein is found on axonal membranes and guides the formation of specific neuronal connections. Interestingly, *LSAMP* has been proposed previously as a TSG involved in the genetically related sporadic and familial clear cell RCCs.¹⁷⁶ *LSAMP* expression has also been reported to be negatively correlated with overall survival in sporadic epithelial ovarian tumors.¹⁷⁷ Similar mechanisms could apply for tumor N366, where the loss of chromosome 3 and a microdeletion on the remaining allele would result in biallelic inactivation of the *LSAMP* gene.

The short arm of chromosome 8 (8p) is frequently deleted in human cancer.¹⁷⁸⁻¹⁸¹ One of the genes originally mapped to 8p22 is *FEZ1/LZTS1* (leucine zipper, putative tumor suppressor 1), an apparently broadly acting TSG with altered expression in various cancers including breast, esophageal, gastric, lung, prostate, and urinary bladder carcinomas.^{182,183,184,185} *FEZ1/LZTS1* inhibits tumor cell growth through regulation of mitosis, and inactivation of the gene leads to an early exit from the M (mitosis) phase of the cell cycle (i.e. abrogation of the mitotic cell cycle checkpoint) and uncontrolled cell proliferation.¹⁸⁶ In the HB (N365) with loss of 8p21.3 the microdeletion may be the 'second hit' of inactivation of the TSG, as the other chromosome 8 was lost as well. Mutations of the gene have been reported.^{182,187}

A third region (2q13-14.1) with a submicroscopic deletion was observed in two of the five tumors. This region contains three annotated genes encoding the cobalamin synthetase W domain-containing protein 2 (*CBWD2*), the forkhead box D4-like 1 transcription factor (*FOXD4L1*), and the RAS oncogene family member *RABL2A*, respectively. Whereas the precise function of the proteins encoded by these genes is currently unknown, members of both the *FOX* and *RAB* families have been implied in cancer.¹⁸⁸⁻¹⁹³ The interpretation of this finding is complicated by the fact that the 2q13-14.1 deletion interval surrounds the site where two ancestral chromosomes fused to form chromosome 2. This

region is duplicated at several positions elsewhere in the human genome, primarily in subtelomeric and pericentromeric locations, thus multiple copies of these genes (low copy repeats; LCRs) have been found.^{188,189} For example, a LCR encompassing the *CBWD* and *FOXD4* genes has three extra copies located at the telomeric region of 9p and at two pericentromeric regions of chromosome 9 (9q13).^{188,189} A copy number loss in any of these regions, as in tumor N248 which has a loss of the entire chromosome 9, will result in lower ratios in our array CGH profiles at all respective loci, including the 2q13-14.1 region. However, since tumor N366 does not have a loss of chromosome 9, we cannot exclude a possible role for the genes within this LCR in HB development, and further detailed studies are required to elucidate this possibility.

In conclusion

This study is the first report on tiling resolution array CGH analysis of sporadic HBs. In three out of five tumors a total of three candidate microdeletions were identified; on 2q13-14.1, 3q13.31, and 8p21.3, of which the latter two appear to represent homozygous deletions. Several interesting TSGs (*LSAMP*, *FEZ1/LZTS1*) are located at these cytogenetic intervals. The possible role of these genes in sporadic HBs remains to be established, and validation of the array CGH results (by FISH analysis) is currently ongoing. Furthermore, investigation of a larger group tumors is needed in order to elucidate the full spectrum of putative genes involved in the tumorigenesis of sporadic HBs as well as to investigate the statistic validity of our findings for HB tumorigenesis in general.

Acknowledgement

The authors thank Raf Sciot and Frank van Calenbergh, Department of Pathology and Neurosurgery, University Hospital Leuven, Belgium for the HB samples.

Chapter 5

Cyclin D1 genotype and expression in sporadic hemangioblastomas

Johanna M.M. Gijtenbeek¹, Sandra H.E. Boots-Sprenger², Barbara Franke³,
Pieter Wesseling², and Judith W.M. Jeuken²

¹ Department of Neurology,

² Department of Pathology and ³Department of Human Genetics, Nijmegen Centre for
Molecular Life Sciences, Radboud University Nijmegen Medical Centre, The Netherlands

Abstract

Central nervous system (CNS) hemangioblastomas (HBs) are highly vascularized tumors occurring in sporadic form or as a manifestation of von Hippel-Lindau (VHL) disease. The VHL protein (pVHL) regulates various target genes, one of which is the *CCND1* gene, encoding cyclin D1, a protein that plays a critical role in the control of the cell cycle. Overexpression of cyclin D1 is found in many cancers. The *CCND1* gene contains a common G→A polymorphism (870G>A) that enhances alternative splicing of the gene. *CCND1* genotype is associated with clinical outcome in a number of cancers although prognostic significance varies with tumor type. In VHL disease, *CCND1* genotype has been suggested as a genetic modifier that influences susceptibility to HBs.

In order to analyze whether *CCND1* genotype plays a role in sporadic CNS HBs, we investigated *CCND1* genotype in tumor tissue of 17 sporadic and also in five VHL-associated HBs. In addition, in these tumors the extent and localization of cyclin D1 expression was investigated by immunohistochemistry. We found no deviation in *CCND1* genotype distribution and allele frequencies from expected values. Also, there was no correlation between age at onset and *CCND1* genotype. The expression of cyclin D1 as detected by immunohistochemistry was highly variable within and between tumors, without a clear correlation with *CCND1* genotype. We conclude that, whereas variable but sometimes high cyclin D1 expression is a feature of sporadic HBs, *CCND1* genotype is unlikely to be an important genetic modifier in the oncogenesis of these tumors.

Introduction

Central nervous system (CNS) hemangioblastomas (HBs) occur in sporadic form or as a manifestation of von Hippel-Lindau (VHL) disease. In VHL disease, germline mutations of the *VHL* tumor suppressor gene (TSG) and inactivation of the VHL protein (pVHL) are associated with a susceptibility to HBs, renal cell carcinomas (RCCs), pheochromocytomas, and multiple cysts in pancreas and kidney.¹ VHL protein targets the hypoxia-inducible transcription factor (HIF) for ubiquitin dependent proteolysis, and pVHL inactivation results in overexpression of HIF and HIF target genes including those involved in angiogenesis, energy metabolism and apoptosis.⁹⁸ Vascular endothelial growth factor (VEGF) is regarded as one of the most important targets of HIF because of its important role in tumor angiogenesis. However, up till now arguments for a role of VEGF in the neoplastic transformation of cells are scarce,¹⁹⁴ and other HIF-dependent or HIF-independent target genes of pVHL are likely to be involved.¹¹⁹ One of the recently reported target genes of pVHL is *CCND1*.^{123,126,127} *CCND1* encodes a protein (cyclin D1) that plays a critical role in the control of the cell cycle at the G1/S checkpoint, and that can function as an oncogene; overexpression of cyclin D1 can release a cell from its normal cell cycle controls and may thereby cause transformation to a neoplastic phenotype.^{124,125} Overexpression of cyclin D1 is a feature of many cancers,^{125,195} including VHL-associated RCC cell lines and tumors.^{123,126,127} Whether or not the upregulation of cyclin D1 alone following inactivation of the *VHL* gene is sufficient for tumorigenesis remains to be elucidated.¹²⁷

The *CCND1* gene contains a common G→A polymorphism (870G>A) within the splice donor region of exon 4 that modulates mRNA splicing. Transcripts originating from alleles containing an A appear less likely to be spliced than those containing a G. Splicing creates an altered carboxy-terminal domain in the protein, and the unspliced protein may have a longer half-life.¹⁹⁵ It has been suggested that DNA damage in cells with the A allele may bypass the G1/S checkpoint more easily compared to cells with the G allele.¹²⁹ A significant association between the *CCND1* A genotype (AA or AG) and early onset and progression has been reported in various tumors, like squamous cell carcinoma of the head and neck,¹³⁰ hereditary and sporadic colorectal cancer,^{129,131} prostate cancer,¹³² and sporadic pituitary adenomas.¹⁹⁶ However, an association between *CCND1* GG genotype and poorly differentiated tumors

and reduced disease-free interval in squamous cell carcinoma of the head and neck has also been reported.¹⁹⁷ Therefore, the effect of *CCND1* genotype is not clear and may differ between various tumors.

One study investigated the role of *CCND1* genotype as a possible modifier of VHL disease.¹²³ It was suggested that the functional effects of cyclin D1 upregulation due to *VHL* gene inactivation might be influenced by *CCND1* genotype.¹²³ The G allele was described to be associated with an increased susceptibility to retinal and CNS HBs, but not with RCCs.¹²³ In order to investigate whether *CCND1* genotype plays a role in sporadic CNS HBs we genotyped 17 sporadic HBs for the 870G>A polymorphism, as well as five VHL-associated HBs. Furthermore, as this *CCND1* polymorphism has been associated with protein turnover, the extent of cyclin D1 expression was investigated by immunohistochemistry.

Materials and Methods

Tumor samples were obtained from 22 patients who underwent resection of a cerebellar or spinal HB at the Radboud University Nijmegen Medical Centre, The Netherlands (N298, N241-N244, N341-N342, N379, N392), Erasmus University Medical Center Rotterdam, The Netherlands (N364-N367, N369), and University Hospital Leuven, Belgium (N245-N250, N373, N378). All tumors were histopathologically classified as HBs according to the World Health Organization classification.⁴⁵ Based on established clinical criteria,¹ 17 tumors were sporadic cerebellar HBs (Table 1). Five patients had von Hippel-Lindau disease (N364, N373, N378, N379, N392), which was confirmed by germline mutation analysis (S80R, L158V, N78S, T152P, C407T). Two of the examined VHL-associated HBs were spinal tumors (N364, N373). All VHL patients had multiple cerebellar and spinal HBs, and multiple cysts in abdominal organs. One VHL patient (N392) had extensive metastatic renal cell cancer.

***CCND1* genotyping**

DNA was isolated from fresh-frozen tumor material as described previously by a salting out procedure.¹⁵⁴ Formaline-fixed and paraffin-embedded tissue was

deparaffinized and washed in ethanol, air-dried, and incubated in P-buffer (50mM Tris-HCL pH 8.2, 100 mM NaCl, 1mM EDTA, 0.5% Tween-20, 0.5% NP40, 20 mM DTT) at 90°C for 15 minutes. Protein digestion was performed with 0.5 mg/ml proteinase K (Roche Diagnostics GmbH, Mannheim, Germany) at 37°C for one day. Subsequently, genomic DNA was isolated using DNeasy Tissue kit as described by the manufacturer (Qiagen GmbH, Hilden, Germany) The A>G polymorphism at position 870 (exon 4) of the coding sequence of the *CCND1* gene was analyzed using restriction fragment length polymorphism (RFLP) analysis. A *ScrFI* site that is present only in the G allele was used as described earlier.¹²³ Fragment amplification was performed in 50 µl reaction volume containing 100-200 ng genomic DNA, 5 ng of each primer (forward-5'-GTGAAGTTCATTTCCAATCCGC, reverse-5'-GGGACATCACCTCACTTAC), 10 mM Tris-HCl pH 9.0, 50 mM KCl, 1.5 mM MgCl₂, 0.1 % Triton X-100, 0.01 % (w/v) gelatin, 0.3 mM dNTPs and 2 U *Taq* DNA polymerase (Invitrogen, Breda, The Netherlands). Fragment amplification conditions in a PTC-200 (MJ-Research via Biozym, Landgraaf, The Netherlands) consisted of an initial 3 min at 94°C followed by 40 cycles of 1 min 94°C, 1 min of 63°C and 1 min of 72°C. An additional step of 3 min at 72°C concluded the program. The 167 bp PCR-product was purified on Multiscreen™ PCR plates (Millipore, Etten-Leur, The Netherlands) and taken up in a volume of 20 µl water. The identity of the PCR product was confirmed by direct sequencing on an ABI PRISM 3700 automated sequencer using the DyeDeoxy-terminator cycle sequencing kit according to the protocol of the manufacturer (Applied Biosystems, Nieuwerkerk a/d IJssel, The Netherlands). Ten µl of purified PCR-product was subsequently subjected to restriction analysis with the enzyme *ScrFI* in a total volume of 25 µl containing 2.5 µl of Buffer 4 (New England Biolabs, via Westburg, Leusden, The Netherlands) and 5 U of *ScrFI* (New England Biolabs, via Westburg). Digestion was performed overnight at 37°C after which the product was run on a 4 % agarose gel until distinction between cut (145 bp + 22 bp) and uncut (167 bp) bands could clearly be made. RFLP analysis of this *CCND1* variant was validated by direct sequence analysis for samples representing all three possible genotypes.

Immunohistochemistry

After genotyping of the HBs, immunohistochemistry for cyclin D1 was performed on 10 sporadic HBs (at least two cases of each genotype class) and, in addition, on two VHL-associated HBs. In brief, 5 μ m sections of paraffin-embedded tissue were dewaxed in xylol for 10 min and rehydrated through alcohol. Endogenous peroxidase was blocked with 3% hydrogen peroxide in phosphate-buffered saline (PBS) for 30 min. Subsequently the sections were rinsed in PBS and then pretreated by 3 cycles of microwave heating in citrate buffer (pH 6.0) for 5 min and subsequent cooling down for 20 min till room temperature. After washing with PBS, the primary antibody (cyclin D1; Progen Biotechnik, Heidelberg, Germany) was applied to the sections for 60 min. After washing with PBS for 10 min, the sections were incubated for 30 min with the secondary antibody (poly-HRP-GAM/R/R IgG; Immunologic, Duiven, The Netherlands). After washing the sections for 10 min in PBS again, the staining procedure was finished using the CARD method and DAB (5 min), the sections were rinsed in water, counterstained with hematoxylin, dehydrated and cover-slipped.

Statistical analysis

The Chi-square test for cross tables was used to test for differences in genotype distributions between the different control populations reported in the literature, between cases and the different control populations, and between cases and the combined control population. Hardy-Weinberg equilibrium (HWE) testing was performed using standard procedures.

Results

***CCND1* genotype**

CCND1 genotype distribution of 17 sporadic and five VHL-associated HBs is summarized in Table 1. Figure 1 shows the results of the RFLP analysis for several of the samples analyzed.

CCND1 AA genotype was found in 23.5%, AG genotype in 35.3% and GG genotype in 41.2% of sporadic HBs. Allele frequencies were: A = 0.41, and G = 0.59. In the five VHL-associated HBs *CCND1* AA genotype was found in

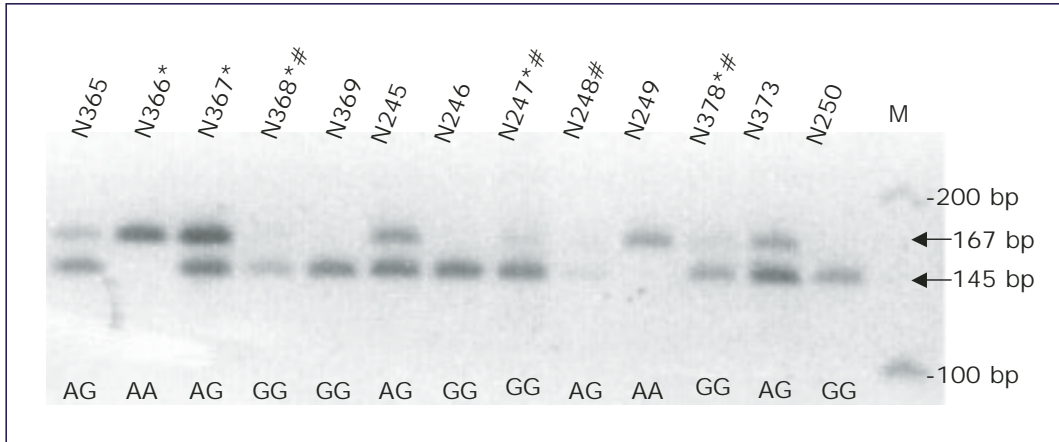


Figure 1 Products of the restriction fragment length polymorphism (RFLP) analysis of the G>A polymorphism at position 870 (exon 4) of the coding sequence of the *CCND1* gene. The band of 167 bp represents the A allele, the 145 bp band represents the G allele. Above the gel the identity of the sample is shown, below the genotype is indicated. (# analysis repeated; * verified by sequence analysis; M marker lane)

one case, and AG and GG phenotype each in two cases. Allele frequencies were: A = 0.4, and G = 0.6. These frequencies showed no deviation from HWE. Several studies have reported the *CCND1* genotype distribution in European, Japanese, and American control populations.^{130-132,196} Since statistical analysis showed no significant difference between the genotype distribution in these populations (n = 1087) (data not shown), we have used the combined data from these reports in the present study. In the controls, the overall genotype distribution was AA 17.2%, AG 51.1%, and GG 31.7%. There was no statistical significant difference between *CCND1* genotype in sporadic HBs and the control population (Table 2), or between the combined sporadic and VHL-associated HBs and the control population (data not shown). Also, the allele frequencies in our study showed no difference compared to the combined controls (A=0.43, G=0.57).

The mean age of the patients with sporadic HBs was 49 years versus 33 years for patients with VHL-associated HBs. No correlation was found between age at diagnosis and *CCND1* genotype or presence of an A or G allele in sporadic HBs: patients with AA, AG, or GG genotype had a mean age of 54, 42, and 52 years, patients with an A allele had a mean age of 47 years, with a G allele 48 years. Also, no correlation was found between age and *CCND1* genotype or

Table 1 *CCND1* 870G>A genotype, age at presentation, and cyclin D1 expression in central nervous system hemangioblastomas (HBs)

HB	<i>CCND1</i> genotype	HB nr (patient age)	Cyclin D1				
			Cytoplasmatic Extent ^a	Intensity ^b	Nuclear Extent	Intensity	
Sporadic	AA	N241 (34)	++	++	+	++	
		N342 (48)	-	-	-	-	
		N366 (69)	++	+++	++	++	
		N249 (66)					
	AG	N242 (56)	++	++	+	+	
		N244 (60)	+++	++	+	+	
		N365 (14)	+++	+	+++	++	
		N245 (31)					
		N248 (52)					
	GG	N243 (48)	+++	++	+++	+++	
		N298 (51)	+++	+++	++	+++	
		N341 (60)	++	++	-	-	
		N369 (28)	++	++	++	+++	
		N246 (56)					
	VHL	AA	N392 (46)				
		AG	N379 (28)	++	++	++	+++
			N373 (21)				
GG		N364 (45)	+	++	+	++	
		N378 (36)					

^a Extent: - = no expression; + = focal; ++ = dispersed; +++ = extensive

^b Intensity: - = no expression; + = low; ++ = moderate; +++ = high.

Not all samples were available for immunohistochemistry.

Table 2 Comparison of *CCND1* 870G>A genotype frequencies in patients with sporadic hemangioblastomas and the combined control population

		genotype			total
		AA	AG	GG	
Hemangioblastoma patients	n ^a	4	6	7	17
	%	23.5%	35.3%	41.2%	100%
Combined control population ^b	n	187	555	345	1087
	%	17.2%	51.1%	31.7%	100%

^a n = number of hemangioblastomas or controls.

^b ref^{130-132,196}.

The p-value (=0.433, Chi-square test: 1.865; degrees of freedom: 2) was nonsignificant.

presence of an A or G allele in VHL-associated HBs. The only patient with VHL disease and *CCND1* AA genotype (N392) had multiple cerebellar HBs and died of extensive metastatic renal carcinoma. The other VHL patients had less extensive disease.

Immunohistochemistry

Staining for cyclin D1 was variable within and between tumors with regard to intensity, extent, and localization. The staining results are summarized in Table 1 and examples are shown in Figure 2. The majority of HBs showed partial cyclin D1 staining in both nucleus and cytoplasm. In some cases, cyclin D1 expression was found almost exclusively in the cytoplasm (Figure 2). No correlation between genotype and immunohistochemical cyclin D1 expression was found (Table 1).

Discussion

Cyclin D1 is an important nuclear protein required for progression of cells through the G1 phase of the cell cycle.¹²⁴ Cyclin D1 has recently been reported as a target of pVHL, and overexpression, due to inactivation of the *VHL* gene

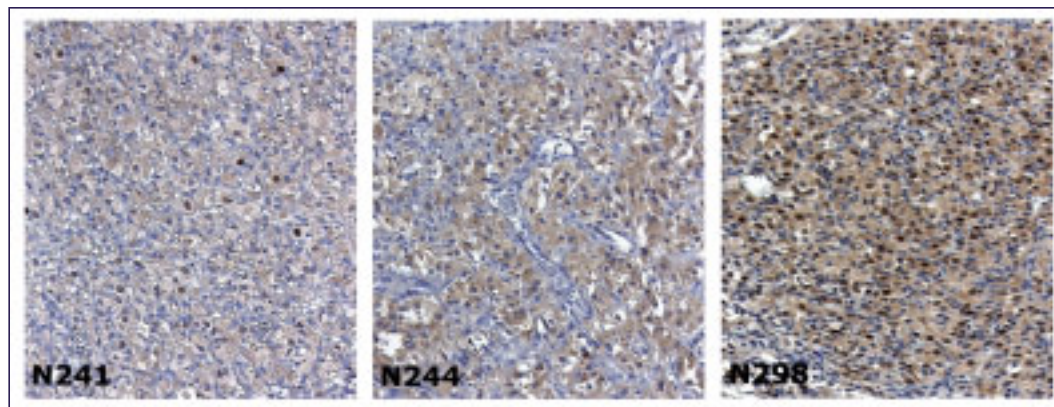


Figure 2 Examples of cyclin D1 expression in three hemangioblastomas as detected by immuno-histochemistry. As described in the Results section, there was a high intra- and inter-tumor variability in intensity, extent, and location of cyclin D1 staining without clear-cut correlation with the cyclin D1 genotype of tumors. Most tumors showed a combination of nuclear and cytoplasmic staining, see e.g. N241 (AA genotype) and N298 (GG genotype), while in some other tumors staining was predominantly cytoplasmic (see e.g. N244, AG genotype).

and subsequent loss of pVHL, might be a key factor in tumorigenesis of VHL-associated tumors.^{123,126,127}

Polymorphic variation in *CCND1* might influence prognosis in various tumors,^{129-132,196,197} as well as the phenotypic expression of VHL disease.¹²³ In most studies, a significant association was found between the *CCND1* AA^{129-132,196} and AG^{129,131} genotypes and early age at onset as well as poor prognosis of various cancers. However, the GG genotype was also suggested to be associated with poorly differentiated tumors and reduced disease-free survival.¹⁹⁷ In VHL disease, genetic modifiers may play a role in phenotypic expression, e.g. the risk of occurrence of RCCs, retinal and cerebellar HBs, and pheochromocytomas.¹²³ It has been suggested that the genetic variant 870G>A in *CCND1* is such a modifier; the number of retinal HBs was significantly higher in patients possessing the G allele compared with AA homozygotes, and possession of one or two G alleles was described to be associated (not statistically significant) with an almost 2-fold earlier diagnosis of CNS HBs, and increased susceptibility to HBs. No association of RCC with *CCND1* genotype was found.¹²³ If the *CCND1* G allele increases susceptibility to HBs, one might expect to find a higher frequency of the G allele in HBs.

In our study of 17 sporadic HBs, no statistical difference was detected in *CCND1* genotype distribution compared to a control population. We also found no correlation between age at presentation and *CCND1* genotype. Because we analyzed only five VHL-associated HBs, statistical analysis for this small group alone is not conclusive. As might be expected, VHL patients were younger at diagnosis than the sporadic patients.

Interestingly, the only patient with VHL disease and the *CCND1* AA genotype (N392), had multiple cerebellar HBs, and died of extensive metastatic renal cell carcinoma. Possibly, this phenotype increases susceptibility to a more aggressive disease, as has been shown for other tumors.^{129-132,196} However, more studies in VHL patients will be necessary to prove this suggestion.

Cyclin D1 overexpression in tumor cells has been demonstrated predominantly in the nucleus of tumor cells. However, exclusive cytoplasmic localization has also been reported recently.¹⁹⁸ Normally, cyclin D1 oscillates during the cell cycle; the protein accumulates in the nucleus during G1 phase and exits into the cytoplasm during S phase.¹⁹⁹ Nuclear expression of cyclin D1 seems to be a factor predicting poor prognosis in colorectal tumors.¹⁹⁸ In this study of 17 sporadic CNS HBs, the results are too diverse to find statistical significant evidence of an unequivocal correlation between localization of expression and genotype. Whether the subcellular localization of cyclin D1 in HBs has prognostic implications has not been studied.

In conclusion

In this study of 17 sporadic CNS HBs, the results are too diverse to find statistical significant evidence of an unequivocal correlation between *CCND1* genotype and the occurrence of HBs, implicating that the *CCND1* genotype is unlikely to be an important genetic modifier in the oncogenesis of these tumors. Other factors responsible for the induction of sporadic HBs remain to be elucidated.

Acknowledgments

The authors thank Mirjam Smeets for her skilful support of the immunohistochemical part of this study, Suzanne Hanssen for genotyping, and Huub Straatman for statistical analysis.

Chapter 6

Molecular analysis as a tool in the differential diagnosis of VHL disease-related tumors

Johanna M.M. Gijtenbeek¹, Bram Jacobs¹, Sandra H.E. Boots-Sprenger², Anita Bonne³, Jacques W.M. Lenders⁴, Benno Küsters², Pieter Wesseling², Judith W.M. Jeuken²

¹ Department of Neurology

² Department of Pathology and ³ Department of Human Genetics, Nijmegen Centre for Molecular Life Sciences

⁴ Department of Internal Medicine, Radboud University Nijmegen Medical Centre, The Netherlands

Abstract

Von Hippel-Lindau (VHL) disease is an autosomal dominant tumor syndrome, in which hemangioblastomas (HBs), clear cell renal cell carcinomas (RCCs), and pheochromocytomas are the most frequently encountered tumors. The differential diagnosis of dedifferentiated tumors in general can be difficult, as standard histological and immunohistochemical investigations do not always allow a definitive diagnosis. We used molecular genetic analysis to resolve the differential diagnosis of sarcomatoid RCC versus pheochromocytoma of a (peri)renal tumor in a VHL patient. Germline mutation analysis identified the C407T mutation, which has been related to a VHL phenotype in which pheochromocytomas are rare. Chromosomal imbalances detected in the tumor by comparative genomic hybridization (CGH) showed a pattern typical for RCCs and not for pheochromocytomas. CGH analysis of the multiple tumors of this VHL patient revealed a comparable karyotype in the metastatic tumors and the (peri)renal tumor. Concordantly, although the germline mutation was detected in all analyzed tumors, loss of heterozygosity (LOH) at 3p was only detected in the (peri)renal mass and most metastases. Overall, based on all genetic data this tumor corroborated a diagnosis of metastatic sarcomatoid RCC. In line with these observations is the immunopositivity for the RCC specific RC38 detected in the (peri)renal mass and the metastases that was not detected in pheochromocytomas. The RCC specific marker G250 was uninformative as it stains positive in all types of VHL-tumors. This case report illustrates the promising role of genetic analysis in the differential diagnosis of histologically dedifferentiated tumors.

Introduction

Von Hippel-Lindau (VHL) disease is an autosomal dominant tumor syndrome that results from a germline mutation in the *VHL* tumor suppressor gene (TSG) located on chromosome 3p25. Manifestations of VHL disease include a variety of lesions in the central nervous system (CNS) and visceral organs including hemangioblastomas (HBs) in the CNS and retina, renal cell carcinomas (RCCs), pheochromocytomas, and pancreatic neuroendocrine tumors.¹ The prevalence of the tumor-types may differ among VHL families and a correlation between genotype and phenotype has been identified; type 1 without and type 2 with pheochromocytoma, each type being characterized by specific *VHL* mutations.^{1,30,64}

All VHL-associated tumors show a germline mutation of the *VHL* coding region whereas the majority harbor an additional loss of heterozygosity (LOH) or a somatic mutation of the wild-type allele.^{61,67,200} It has been suggested that TSGs on chromosome 3p other than the *VHL* gene also play a role in the tumorigenesis of VHL-associated tumors and their sporadic counterparts.^{61,73,79} Furthermore, aberrations other than those of chromosome 3 have been reported in VHL-associated tumors.⁸¹⁻⁸⁸ In low-grade VHL-associated RCCs only few cytogenetic aberrations have been identified, i.e. gains of chromosomes 7 and 10.⁸⁸ In high-grade sporadic RCCs^{81-85,87} and in cell lines of VHL-associated RCCs,^{87,88} the most frequent aberrations were loss of 3p, 4q, 6q, 8p, 9p, 14q, and gain of 5q, 7, 17q, and Xq. Prognostic significance of some of these chromosomal aberrations has been suggested for RCCs.^{83,87} The same chromosomal regions that are involved in primary RCC were found to be affected in their metastases but with different frequencies for a few regions.⁸² Interestingly, chromosomal aberrations detected in pheochromocytomas differ from those detected in RCCs and involve besides loss of chromosome 3, loss of chromosome 11 in VHL-associated tumors, and loss of 1q and 3q in sporadic pheochromocytomas.^{89,90} Also, sporadic HBs show -3, -6, -8, -9, -18 and +19 in contrast to VHL-HBs, which infrequently show chromosomal imbalances.^{169,170}

Immunohistochemical investigations of VHL-associated tumors are usually reliable. Although both HBs and metastases of RCC show a clear cell phenotype, the diagnosis is made by their different staining patterns for epithelial markers.⁴⁵ The differential diagnosis of RCC and pheochromocytoma can

usually be resolved by using an antibody panel including pan-keratin, epithelial membrane antigen (EMA), chromogranin, and synaptophysin (www.immunoquery.com). In addition, G250 and RC38 have been described in the literature as immunohistochemical markers for RCC.^{100,201} However, the differential diagnosis of dedifferentiated tumors in advanced VHL disease, as well as in advanced cancer in general, can be difficult, as dedifferentiated tumors lose the normal staining patterns.

We report a case of VHL disease in which molecular genetic analysis methods applied on tumor tissue aided in resolving the differential diagnosis of metastatic sarcomatoid RCC and metastatic pheochromocytoma.

Case report

A 44-year-old man presented with a generalized epileptic attack. Diagnostic workup revealed a cystic left cerebellar tumor, which on histological examination proved to be a HB. The family history was positive for VHL disease, and screening for other VHL-associated tumors revealed retinal HBs, establishing the clinical diagnosis of VHL disease in this patient. Identification of a *VHL* germline mutation (C407T, Ser65Leu) in a blood sample of the patient confirmed the diagnosis.

Multiple cerebellar HBs were discovered in the following years, and one left cerebellar tumor was removed. Seven years after presentation, two cystic lesions in the left kidney were found. A partial nephrectomy of the left kidney was performed because of growth of these lesions. Histological examination revealed a well-differentiated clear cell RCC. At that time, urinary excretion of normetanephrine was increased threefold, suggesting the presence of a pheochromocytoma. However, the excretion of metanephrine and catecholamines was normal, plasma catecholamines were not increased, and a meta-iodobenzylguanidine (¹²³MIBG) scintigraphy was negative.

One and a half years later, the patient was admitted to the hospital because of general malaise. There were no symptoms or signs indicating a pheochromocytoma; in particular, hypertension was absent. A large, recurrent tumor in the left (peri)renal region was found, with metastases in liver, lung, and subcutaneous tissue. Histological analysis of a needle biopsy of the subcutaneous lesion revealed a highly pleiomorphic, partly sarcomatoid tumor;

the tumor cells were positive for synaptophysin and negative for pan-keratin AE1/AE3 (consistent with pheochromocytoma), as well as negative for chromogranin but variably positive for EMA (consistent with dedifferentiated/sarcomatoid RCC). A second and third needle biopsy of this tumor did not contain representative tumor tissue for further (immuno)histological or electron microscopic analysis. The patient deteriorated and died 3 months after the first needle biopsy of the subcutaneous mass and 10 years after his first epileptic attack, at the age of 54 years.

Postmortem examination. General autopsy revealed a large tumor in the left (peri)renal region, of which, after the partial nephrectomy, the exact origin could not be identified anymore. Histologically, the tumor consisted of highly pleomorphic, often sarcomatoid tumor cells, and the differential diagnosis included a sarcomatoid pheochromocytoma and sarcomatoid dedifferentiation of a clear cell RCC. Additionally, extensive peritoneal carcinomatosis, peritoneal lymph node metastases, liver metastases (maximum diameter 6 cm), lung metastases (maximum diameter 2 cm), and cardiac metastases were found. Also, a well-differentiated pancreatic neuroendocrine tumor of unknown biological behavior was detected. The cause of death was fatal heart failure due to cardiac metastases.

Because of the difficult differential diagnosis on the subcutaneous tumor, as well as the fact that much more material became available of the different tumors in this patient after autopsy, we decided to investigate the potential additional diagnostic value of genetic analysis of (dedifferentiated) tumors in VHL patients.

Material and methods

Formaline-fixed and paraffin-embedded tissue of two left cerebellar HBs, collected during surgery in 1991 (N329), and 1994 (N332), and paraffin-embedded tissue of the well-differentiated clear cell RCC, obtained during nephrectomy in 1998 (N385), were available for further analysis. In addition, the following tumor tissues were collected during autopsy: a left cerebellar HB (N392), high grade, pleomorphic, sarcomatoid tumors in the left (peri)renal region (N393), heart (N394), lung (N395), liver (N396), and mesenterium (N397), snap frozen and stored at -80°C, and a pancreatic neuroendocrine

tumor (N386), a right cerebellar HB (N387), a left cerebellar HB (N389), and the cauda equina HB (N388), formalin-fixed and paraffin-embedded.

From fresh-frozen tumor material DNA was isolated as described previously.¹⁵⁴ Sections of paraffin-embedded tissues were deparaffinized, washed in ethanol, air-dried, and incubated in P-buffer (50mM Tris-HCl pH 8.2, 100 mM NaCl, 1mM EDTA, 0.5% Tween-20, 0.5% NP40, 20 mM DTT) 90°C for 15 minutes. Protein digestions were performed with 0.5 mg/ml proteinase K (Roche Diagnostics GmbH, Mannheim, Germany) at 37°C for one day. Subsequently, genomic DNA was isolated using a DNeasy Tissue kit following the instructions of the manufacturer (Qiagen GmbH, Hilden, Germany).

VHL gene mutation analysis was performed by direct sequencing, as described by Bodmer, et al.¹⁶¹ Five primer sets were used to amplify exons 1 (three overlapping primer sets), 2, and 3 of the *VHL* gene. The polymerase chain reaction (PCR) products were subsequently purified and sequenced, using the BigDye Terminator v2.0 Cycle sequencing kit and a 3730 DNA Analyzer (Applied Biosystems), after which the sequences were analyzed.

For loss of heterozygosity (LOH) analyses, markers on chromosome 3p were used, including the dinucleotide repeat polymorphic markers D3S1317 and D3S666, which are located close to the *VHL* locus at 3p25.3.^{165,202} PCRs, using 6-FAM labeled primers, were performed on DNA extracted from paraffin-embedded tissues or fresh-frozen tissue samples. The PCR cycles included: denaturation for 2 min at 94°C; 35 cycles of 30 sec at 94°C, 30 sec at 55°C, and 45 sec at 72°C; a final step of 72°C for 5 min. The PCR products were analyzed on a 3100 DNA Analyzer (Applied Biosystems, The Netherlands).

Comparative genomic hybridization (CGH) was performed on all tumors as described previously.¹⁵³ Briefly, control and tumor DNA were labeled by nick-translation with digoxigenin-dUTP and biotin-dUTP, respectively (Roche Molecular Biochemicals, The Netherlands), and precipitated in the presence of human COT-1-DNA (Gibco BRL Life Technologies, Inc., Gaithersburg, MD, USA) and herring sperm DNA. The probe and the metaphase slides were denatured simultaneously. After hybridization and post-hybridization washes, biotin and digoxigenin were detected using streptavidin-FITC and sheep-anti-digoxigenin-TRITC (Roche Molecular Biochemicals). The chromosomes were counterstained with 4,6'-diamino-2-phenylindole-dihydrochloride (DAPI) (Merck, Darmstadt, Germany) and the slides were mounted in Fluoroguard (Biorad, Veenendaal, The Netherlands). To test the quality of the CGH hybridizations, negative and

positive controls were included in each series of CGH hybridizations.¹⁵³ For CGH analysis Quips CGH software (Applied Imaging, United Kingdom) was used. Detection thresholds for losses and gains were set at 0.8 and 1.2, respectively. Tissues of all tumors were stained with hematoxylin and eosin for histological examination. Immunohistochemical staining using the G250 antibody (Department of Urology, University Medical Center Nijmegen, The Netherlands, dilution 1:10)²⁰³ and RC38 antibody (Department of Pathology, University Medical Center Nijmegen, The Netherlands, dilution 1:20)²⁰⁴ were performed on snap-frozen tissue obtained during autopsy, as well as on snap-frozen tissue of five archival (not of this patient) RCCs (including one colon metastasis), three archival pheochromocytomas (including one lung metastasis), and three archival VHL-associated HBs, as previously described. In short, air-dried frozen tissue sections were fixed with acetone, stained by a sensitive indirect immunoperoxidase procedure using G250 or RC38 as primary antibody and 3-3-Di-Amino-Benzidine (DAB) as substrate. Sections were counterstained with hematoxylin.

Results

VHL gene mutation and LOH

The *VHL* germline mutation previously detected in the white blood cells of this patient was C407T, Ser65Leu. Mutation analysis of all the *VHL* exons revealed this germline mutation in exon 1 in all tumors analyzed; however, no additional somatic mutations were detected (Table 1). In a minority of tumors of which only paraffin-embedded material was available (N332, N386, N388), mutation analysis was not performed due to lack of adequate material. LOH at chromosome 3p was found in only four of the nine tumors analyzed (N393, N394, N396, N397), including the dedifferentiated (peri)renal tumor and its metastases (Table 1).

In the lung metastasis (N395) no LOH at 3p was found, due to contamination of normal lung tissue in this sample, as confirmed by revising of the H&E slides.

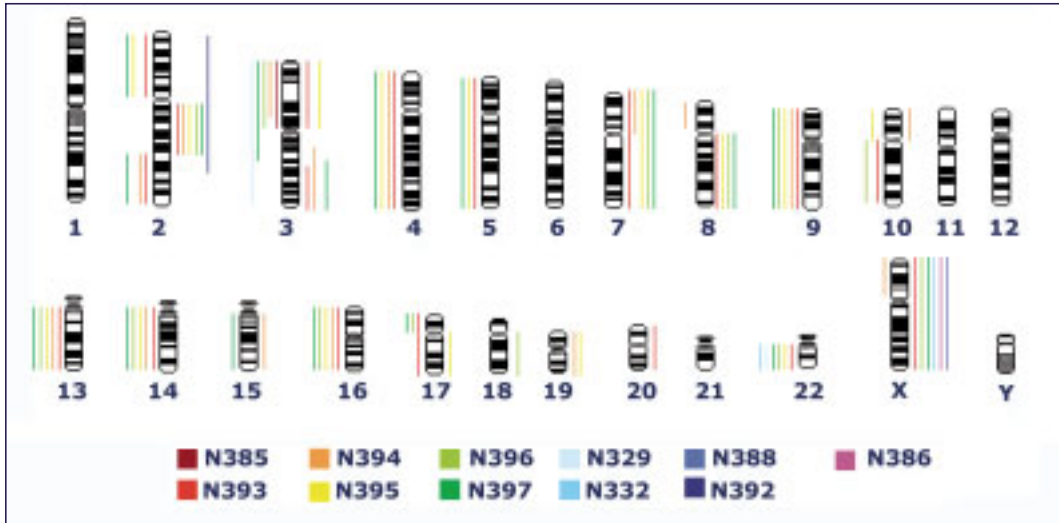


Figure 1 Chromosomal imbalances as detected by CGH in tumors of a patient with VHL disease. Lines on the left side of the chromosomes represent regions that are underrepresented in the tumor genome (losses), whereas lines on the right side of the chromosomes represent regions that are overrepresented (gains). For explanation of tumornumbers see Table 1.

Comparative genomic hybridization

The results of the CGH analysis are summarized in Table 1 and depicted in Figure 1. In five cerebellar HBs and one cauda equina HB, only few chromosomal aberrations were detected: loss of chromosome 3 (-3) in one (N329), -22 in two (N329, N332), gain of the X chromosome (+X) in two (N332, N388), and +2pter-q32 in one (N392). Two HBs (N387, N389) showed no chromosomal aberrations detectable by CGH. There was no increase of chromosomal imbalances in early HBs versus tumors removed at autopsy. The well-differentiated clear cell RCC (N385), removed by nephrectomy in 1998, showed only loss of chromosome 3p. The (peri)renal tumor at autopsy (N393) and the (metastatic) tumors in the heart, lung, liver and mesenterium (N394-N397) showed complex chromosomal aberrations (Table 1). Losses of chromosome 2p, 2q31-qter, 4, 9, 13q, 14q, 16, and 22, and gains of chromosome 2q11-24, 3q, 7, 8q, and X were most frequently found (present in at least three of these five tumors). The CGH results of the lung metastasis were less clear than those in the other tumors (visible with detection thresholds at 0.9 and 1.1, but not at 0.8 and 1.2), due to contamination with normal tissue. The pancreatic neuroendocrine tumor showed only +X.

Table 1 Germline mutation and chromosomal imbalances in tumors of a patient with VHL disease

Tumor No.	Tumor	Material analyzed*	Germline mutation* nt	AA	LOH*	Chromosomal imbalances	
						CGH losses	CGH gains
N329	HB	TP	C407T Ser65Leu		-	3,22	-
N332	HB	TP	nd		nd	22	X
N385	RCC	TP	C407T Ser65Leu		nd	3p	-
N386	Pancreatic tumor	AP	nd		nd	-	X
N387	HB	AP	C407T Ser65Leu		-	-	-
N388	HB cauda	AP	nd		nd	-	X
N389	HB	AP	C407T Ser65Leu		-	-	-
N392	HB	AF	C407T Ser65Leu		-	-	2pter-q32
N393	Renal tumor	AF	C407T Ser65Leu		LOH3p	2p,2q31-qter,4,5,9,10q,13q,14q,16,17,22	2q11-24,3p,3q24-qter,7,8q,20,X
N394	Metastasis heart	AF	C407T Ser65Leu		LOH3p	2q31-qter,3p13-pter,4,8p,9,13q,14q,16,Xp	2q11-24,3q21-qter,7p,10p,15q,19
N395	Metastasis lung	AF	C407T Ser65Leu		-	2p,4,5,9,10p,13q,14q,16,22	2q11-24,3p,7,8q,17q,19
N396	Metastasis liver	AF	C407T Ser65Leu		LOH3p	3p,9,10q,13q,14q,16,17p,22	2q11-24,7,8q,18q,X
N397	Metastasis mesenterium	AF	C407T Ser65Leu		LOH3p	2p,2q31-qter,3pter-q21 4,5,9,13q,14q,15q,16,17p,22	2q11-24,3q22-qter,7,8q,X

* HB = hemangioblastoma; RCC = renal cell carcinoma; T = biopsy/resection; A = autopsy; F = snap-frozen tissue; P = paraffin-embedded tissue; nt = nucleotide change; AA = aminoacid change, mutation name; nd = not done; LOH = loss of heterozygosity

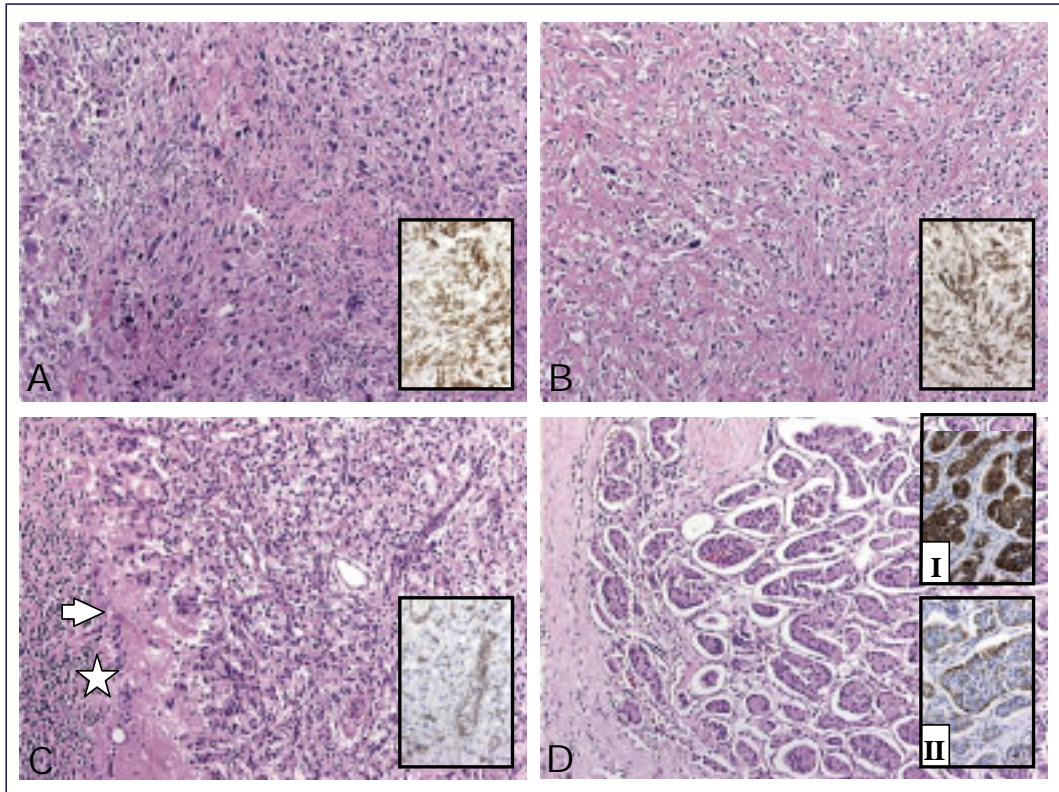


Figure 2 Histology (H&E staining) and immunohistochemistry (insets) of different tumors obtained by autopsy on a case of VHL disease: pleomorphic, sarcomatoid tumor in the left renal region (A) and liver (B); cerebellar hemangioblastoma (C); pancreatic neuroendocrine tumor (D). The tumor cells in A and B are extensively positive for RC38 (inset), while in C only the tumor microvasculature is RC38-positive (inset). The pancreatic tumor shows immunohistochemically both epithelial and neuroendocrine differentiation (Cam5.2 staining in I and Chromogranin staining in II, respectively). Note the transition between cerebellar cortex (asterisk) and hemangioblastoma in C (arrow indicates Purkinje cell). Original magnification in A-D x200.

Immunohistochemistry

Immunohistochemistry showed extensive staining of the tumor cell membranes of the (peri)renal tumor with RC38, as did the tumors from the heart (N394), lung (N395), liver (N396), and mesenterium (N397) (Figure 2) whereas in the cerebellar HB (N392) only the microvasculature stained positive (Figure 2). The same microvascular staining pattern was detected in all three archival VHL-associated HBs analyzed. As expected, G250 positivity was detected in all tumors

of this VHL patient. Furthermore, analyzing different tumors of other patients, extensive RC38 (and G250) staining was found in five archival non-VHL-associated RCCs, including one colon metastasis, whereas three archival non-VHL-associated pheochromocytomas, including one lung metastasis, showed RC38 expression only in the tumor microvasculature (and no G250 expression) (data not shown).

Discussion

HBs are the most common and usually early manifestation of VHL disease, occurring in up to 60% of patients, with a mean age at presentation of 25 years for retinal, and 33 years for CNS HBs.¹ The most frequent malignant tumor in VHL disease is clear cell RCC, occurring in up to 45% of patients, the mean age at presentation being 39 years.¹ Pheochromocytomas arise in 10-20% of patients; 5% of these are malignant. Pancreatic neuroendocrine tumors, or islet cell tumors, occur in 8-17% of VHL patients and have an uncertain malignant potential with the liver being the most common site of metastases.¹ We report on a VHL patient in which the differential diagnosis of a (peri)renal tumor as metastatic sarcomatoid RCC or pheochromocytoma was addressed using immunohistochemistry and molecular genetic analysis.

Although a well-differentiated clear cell RCC was diagnosed two years before, the nature of the recurrent (peri)renal mass was difficult to establish due to a completely dedifferentiated histology of the subcutaneous metastasis, and the ambiguous immunohistochemical staining results (synaptophysin+, pan-keratin AE1/AE3 -, consistent with pheochromocytoma; chromogranin -, EMA +, consistent with RCC; see also www.immunoquery.com). Pheochromocytoma could not be excluded because of the elevated urinary normetanephrine excretion and because the sensitivity of MIBG scanning is only 85%. At autopsy, a (peri)renal tumor was found, with pleiomorphic and sarcomatoid features on histological examination of which the origin (also due to the status post partial nephrectomy) could not be determined.

Genotype-phenotype correlations have been identified in families with VHL disease. In VHL type 1 patients pheochromocytomas are absent whereas VHL type 2 patients harbor pheochromocytoma.^{1,30,64} Specific germline mutations are associated with these different VHL types. The C407T germline mutation

detected in this patient has been associated with the VHL type 1 phenotype,^{30,31} making the diagnosis of a pheochromocytoma very unlikely.

As it has been reported that different tumor types show characteristic chromosomal imbalances, we used CGH analysis to screen for chromosomal imbalances in the (peri)renal tumor as well as the other tumors of this VHL patient. Most of the aberrations as detected by CGH in this (peri)renal tumor and its metastases have been previously detected in RCCs: -4q (reported in up to 28% of RCCs), -9p (29-47%), -14q (20-28%), +7 (15-28%), +X (20-28%).^{81,82,84,85} The tumor additionally showed LOH at 3p, which has been reported in 94% of RCCs.⁸⁷ Furthermore, typical aberrations found by CGH in VHL-associated pheochromocytomas, e.g. -3 (94%), and -11 (84%),⁹⁰ were not detected, nor were chromosomal aberrations less frequently found in (sporadic) pheochromocytomas such as -1p (17-83%), and -3q (39%).^{89,90} Overall, the CGH data of this (peri)renal tumor strongly favor a diagnosis of RCC over pheochromocytoma.

In previous reports, specific chromosomal rearrangements were suggested to have prognostic significance in RCCs; LOH on 8p or 9q, or loss of chromosome 9 may be a predictor of recurrence,^{85,87} whereas gain of chromosome 5q may predict a favorable outcome.⁸³ Indeed, in this patient, loss of chromosome 9 was found in the dedifferentiated renal tumor.

As a well-differentiated renal tumor was surgically removed from the left kidney before, we expect that the sarcomatoid RCC progressed from this earlier RCC rather than being a second primary RCC. However, a gain of 3p was found in the (peri)renal tumor and one of its metastases (the others showed -3p), whereas the early renal tumor (N385) showed -3p. Amplification of the only remaining allele during dedifferentiation of the renal tumor, probably as a result of a mitotic nondisjunction event, has been suggested to occur in primary RCCs and their metastatic tumors.⁸² The results of mutation analysis, LOH, and CGH confirmed that a mitotic nondisjunction event has occurred during progression of the well-differentiated RCC.

CGH was also used to analyze the genetic basis underlying the various tumors of VHL disease. In HBs, inactivation of the *VHL* gene by germline mutations and LOH at 3p has been reported in 62% of the patients.⁶¹ Few additional chromosomal aberrations have been found by CGH; loss of chromosome 6 in one of five VHL-associated HBs, and loss of chromosome 3 in one of seven VHL-HBs.^{160,169,170} Concordantly, we only detected a few chromosomal imbalances

in the HBs of this VHL patient. LOH at 3p was not detected in four of six HBs analyzed.

CGH revealed similarities in the patterns of aberrations detected in the (peri)renal tumor and the metastases analyzed. Loss of 2p (50%: 2/4 metastases), 2q3-qter (50%), 4 (75%), 5 (50%), 9 (100%), 13q (100%), 14q (100%), 16 (100%), 17p (50%), 22 (75%), and gains of 2q11-24 (100%), 3q (50%), 7(p) (100%), 8q (75%), and X (50%) were found in the metastases as well as in the (peri)renal tumor. This strongly suggests that these metastases all originate from the (peri)renal tumor. The clonal relationship between primary RCCs and their metastases has been analyzed in patients with paired specimens.⁸¹ Although most samples showed a high degree of concordance between primary tumors and their metastases, some metastases had no or little evidence of a clonal relationship.⁸¹

In the pancreatic tumor, we found a well-differentiated histological phenotype and only a gain of chromosome X. It was previously reported that genomic changes of neuroendocrine pancreatic tumors detected by CGH were more frequent in metastatic tumors, whereas non-metastatic tumors showed few aberrations.²⁰⁵ Although the liver metastasis showed + X as well, additional chromosomal aberrations were found in this metastasis. Moreover, as 11 of the 13 imbalances detected in this metastasis were also detected in the sarcomatoid RCC, it is most likely that it originates from the RCC.

To study the second hit of the *VHL* gene in the tumors of this VHL patient, mutation analysis of the *VHL* gene and LOH analysis of the *VHL* region were performed. The germline mutation C407T, Ser65Leu, was detected in all tumors analyzed, additional somatic mutations were not found. LOH at 3p, which is the common second hit,^{61,67} was found in four of nine tumors analyzed, including the metastasized renal tumor.

Overall, the post mortem molecular analysis by LOH and CGH indicated that this tumor was in fact a dedifferentiated, sarcomatoid RCC and not a pheochromocytoma. Immunohistochemical stainings using RCC specific antibodies are in line with this diagnosis. Immunohistochemistry showed extensive staining of RC38 of the tumor cell membranes of the (peri)renal tumor and the tumors of the mesenterium, heart, lung, and liver. RC38 recognizes aminopeptidase A, expressed in cells of the proximal tubulus of the kidney, in pericytes of angiogenic blood vessels, and in tumor cells of clear cell RCC.^{204,206} RC38 is a marker for RCCs, but has not been analyzed previously in

pheochromocytomas.^{201,206} We found RC38 expression only in the microvasculature of three archival pheochromocytomas, whereas five archival RCCs showed extensive staining of tumor cell membranes, indicating that RC38 can be used to differentiate between pheochromocytoma and RCC. The staining pattern in this patient favors a diagnosis of metastatic RCC. Interestingly, RC38 was also positive in the tumor vasculature, but not in the stromal cells of the analyzed HB of this patient (Figure 2) and in three archival VHL-associated HBs.²⁰⁴

Although G250 (CA IX) is a marker for clear cell RCC,²⁰³ it does not differentiate between RCC and pheochromocytoma in VHL disease, because G250 is overexpressed in all VHL-associated tumors. This overexpression is attributed to the absence of pVHL, which regulates the degradation of hypoxia-inducible factors (HIF) 1 and 2, and their target genes including the G250 gene.¹⁰⁰

In conclusion

In this patient with VHL disease, the combination of mutation analysis, CGH, and immunohistochemistry further clarified the differential diagnosis of metastatic sarcomatoid RCC versus pheochromocytoma. The germline mutation indicating a VHL type 1 phenotype, the genetic analysis by CGH, and the immunohistochemical staining of the tumors with RC38, led to the diagnosis of metastatic RCC. This case illustrates that, now that information on the genetic background of tumors is rapidly increasing, genetic analysis can be a powerful tool in establishing a final diagnosis, especially in situations where histology and immunohistochemistry are not conclusive. In this way, the management of individual patients can be optimized.

Chapter 7

Three-dimensional reconstruction of tumor microvasculature: Simultaneous visualization of multiple components in paraffin-embedded tissue

Johanna M.M. Gijtenbeek¹, Pieter Wesseling², Cathy Maass²,
Lambert Burgers², Jeroen A.W.M. van der Laak²

¹ Department of Neurology

² Department of Pathology, Nijmegen Centre for Molecular Life Sciences,
Radboud University Nijmegen Medical Centre, The Netherlands

Abstract

Three-dimensional (3D) visualization of microscopic structures may provide useful information about the exact 3D configuration, and offers a useful tool to examine the spatial relationship between different components in tissues. A promising field for 3D investigation is the microvascular architecture in normal and pathological tissue, especially because pathological angiogenesis plays a key role in tumor growth and metastasis formation. This paper describes an improved method for 3D reconstruction of microvessels and other microscopic structures in transmitted light microscopy. Serial tissue sections were stained for the endothelial marker CD34 to highlight microvessels and corresponding images were selected and aligned. Alignment of stored images was further improved by automated non-rigid image registration, and automated segmentation of microvessels was performed. Using this technique, 3D reconstructions were produced of the vasculature of the normal brain. Also, to illustrate the complexity of tumor vasculature, 3D reconstructions of two brain tumors were performed: a hemangioblastoma (HB) and a glioblastoma multiforme (GBM). The possibility of multiple component visualization was shown in a 3D reconstruction of endothelium and pericytes of normal cerebellar cortex and a HB, using alternate staining for CD34 and α -smooth muscle actin in serial sections, and of a GBM using immunohistochemical double staining. In conclusion, the described 3D reconstruction procedure provides a promising tool for simultaneous visualization of microscopic structures.

Introduction

The microscopic features of tissues are generally assessed in two-dimensional (2D) histological slides, which for most purposes suffices. However, the actual three-dimensional (3D) shape of microscopic structures cannot be extrapolated on the basis of examination of 2D sections alone. In some situations, 3D reconstruction may provide useful information about the exact 3D configuration of microscopic structures. Moreover, 3D reconstruction offers a useful tool to examine the spatial relationship between different components in tissues.²⁰⁷ Several applications of 3D visualization of histological features have already proved valuable in different areas of pathology.²⁰⁷⁻²¹³ For example, 3D reconstruction was used to visualize intraductal extension of invasive breast carcinomas,²¹⁴ bone marrow vascularity in acute lymphoblastic leukaemia,²¹⁵ and bone marrow infiltration of non-Hodgkin's lymphoma.²¹⁶

As pathological angiogenesis plays a key role in tumor growth and metastasis formation, 3D visualization may be a powerful tool to investigate the microvascular architecture in normal and pathological tissue. The structural and functional abnormalities of tumor vessels are likely to determine the efficacy of anti-angiogenic therapies in cancer.²¹⁷ Microvascular parameters like microvessel density have been shown to be a predictive factor for metastasis formation and survival in various tumors.^{210,218}

For many years, vascular corrosion casting in combination with scanning electron microscopy, and confocal laser scanning microscopy have been used to investigate 3D vascular patterns of normal and pathological tissues.^{208,209,219,220} Vascular corrosion casting is a complex technique, requiring fresh material, and quantitative data need to be interpreted with care.²²⁰ Confocal laser scanning microscopy needs immunofluorescent staining, and its use is limited to tissue samples no thicker than 30-40 μm .^{209,212}

Several techniques for automated 3D reconstruction using serial sections have recently been developed.^{210,212,213} The use of serial histological sections has the advantage that standard (immuno)histochemical staining can be applied on archival, paraffin-embedded material for recognition of the elements of interest, and that the thickness of the tissue that can be examined is not restricted by technical limits. Important considerations for automated 3D reconstruction are: tissue preparation (e.g. paraffin-embedded or fresh-frozen material) and sectioning, staining and counterstaining procedures, the

use of semi or fully automated segmentation of the structure(s) of interest, alignment of the serial sections (image registration), and the reconstruction method.^{207,210,212,213}

The aim of our investigation was to develop a technique for 3D reconstruction of microvessels (and other structures) in the brain from serial sections of archival material, to allow visualization and analysis of complex vascular patterns in tumors, and to visualize the relationship between different components, e.g. between endothelium and activated pericytes.

Paraffin-embedded tissue was used because of superior morphology, and serial tissue sections of 3 or 4 μm were cut using a section method allowing for minimal distortion and minimalization of section loss. Standard and double immunohistochemical staining methods were performed to highlight the structures of interest.

Materials and methods

Tissue preparation

Paraffin-embedded samples of cerebral white and neocortical grey matter and of cerebellar cortex of a normal human brain obtained by autopsy, as well as samples of a cerebellar hemangioblastoma (HB) and of glioblastoma multiforme (GBM) were selected from the archives of the Department of Pathology, Radboud University Nijmegen Medical Centre.

To allow for the serial sectioning of the paraffin block with equal thickness and minimal distortion and loss of sections, sectioning was performed on an electronic, motorized, rotary microtome (Microm HM 355S, MICROM International GmbH, Walldorf, Germany) (Figure 1). In this microtome, the block holder is replaced with a freezing device, which enables fast cooling of specimens to -45°C . A Section Transfer System (Microm STS, MICROM International GmbH) was mounted directly on the microtome to guide the sections via a continuous laminar flow of water from the knife-edge into the heated water bath without manual manipulation. The paraffin-blocks were attached to the fast freezing unit with acid free vaseline and rapidly cooled to -45°C . As soon as the block was firmly attached to the freezing unit the temperature was raised to -15°C , resulting in a firm paraffin-block with a stable temperature and allowing for the cutting of sections with identical thickness.

We chose to produce serial sections with a thickness of 3 or 4 μm at a low speed (1,5 mm/s) on a disposable blade carrier (including a Feather S22 blade, Klinipath, Duiven, The Netherlands) with laminar flow of warm water (45°C) between cutting edge and heated water bath. In this situation, section stretching occurs immediately and in a reproducible way after contact of the section with the water as a result of water surface tension. During the continuous sectioning and based on the size of the selected paraffin-embedded tissue block, we chose to separate rows of 5 sections from each other with a razorblade in case of single component analysis. These 5-section rows were transported over the water bridge to the water bath, after which they were dragged up on Menzel Superfrost Plus slides (Boom, Meppel, The Netherlands). Visualization of multiple components was performed in two different ways. First, alternating tissue sections were stained for two different components using standard immunohistochemistry with two monoclonal antibodies. For this purpose, even and uneven numbered 3 μm sections were separated from each other and dragged up on different slides. Alternatively, an immuno-double staining was performed on serial 4 μm sections. For single component analysis also 4 μm sections were used.

Fifty serial sections of normal cerebral white matter and neocortex, and of a HB and GBM, were stained for endothelial cells with a MAb to CD34 (mouse monoclonal, 1: 750, Neomarkers, Fremont, USA). Additionally, 60 serial sections of normal cerebellar cortex and 20 sections of a HB were stained alternately for CD34 and α -smooth muscle actin (mouse monoclonal, 1:15,000, Sigma Chemical Co, St. Louis, USA). Alpha-smooth muscle actin is a marker for activated pericytes in the tumor microvasculature, while quiescent pericytes are α -smooth muscle negative, and vascular smooth muscle cells in the wall of larger blood vessels constitutively express this protein. Immuno-double staining was performed on 49 sections of a GBM using the same two antibodies. Immunostaining was performed using the avidin-biotin-complex method, the chromagen used to highlight vessels was 3,3'-Diaminobenzidine tetrahydrochloride (DAB), resulting in a brown product. For the immuno-double staining, activated pericytes were stained using DAB and the endothelium was visualized using Fast Blue. In order to improve the signal to noise ratio during image acquisition, no counterstaining was used.

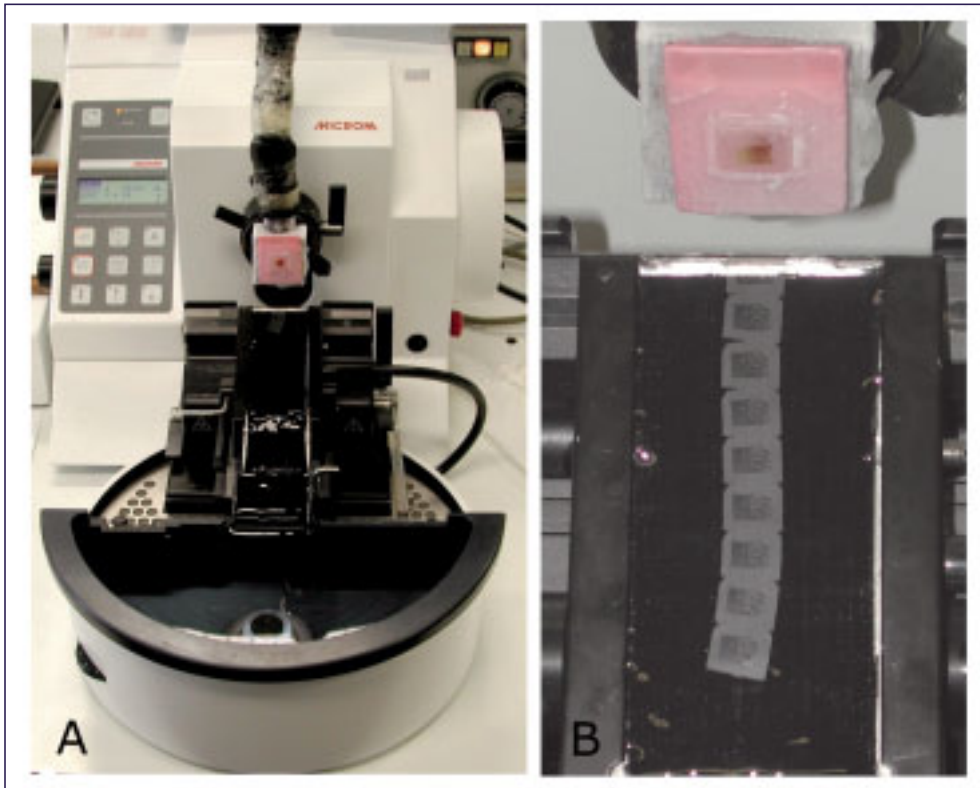


Figure 1. The electronic, motorized rotary microtome (A) that was used for preparation of high-quality serial sections (see Materials and Methods for more details). The holder of the paraffin-block is replaced by a fast freezing device, which enables fast cooling of the specimen to -45°C . The serial sections are guided via a continuous laminar water flow directly from the knife-edge into the heated water-bath without manual manipulation (B), after which the sections can be mounted on a glass slide.

Image acquisition and segmentation

Red-green-blue (RGB) color images of consecutive serial sections were acquired using a 3 CCD RGB camera (Sony DXC950P, Sony Corporation, Japan), attached to a conventional transmitted light microscope (AxioSkop 2 Imaging, Carl Zeiss, Germany). Images were grabbed using a frame grabber (Matrox Meteor II MC, Matrox Electronic Systems Ltd, Dorval, Canada) installed in a Microsoft Windows pc. Image acquisition, segmentation and interactive correction were facilitated by custom written macros in KS400 image analysis software (version 3.0, Carl Zeiss, Germany). Images of consecutive sections were manually aligned (image registration) using the revolving stage of the

microscope, by comparing a live color image of the section under examination with contours of vascular profiles from the previous section in an overlay display. Images were acquired using a 10x objective (Plan Neofluar, n.a.=0.30; specimen level pixel size $1.3 \times 1.3 \mu\text{m}^2$) for single component analysis and a 20x objective (Plan Aplanachromat, n.a. = 0.6; specimen level pixel size $0.65 \times 0.65 \mu\text{m}^2$) for double component analysis, and stored as 24 bit RGB TIFF images (size 760×571 pixels). Prior to acquisition of a series of images of serial sections, an image of an empty microscopic field was acquired for shading correction. All subsequently grabbed images were corrected for unequal illumination using this empty field image. All acquired images were averaged over 4 grabbed images to reduce camera noise.

Automatic recognition of CD34 positive stained vascular profiles was performed by applying a fixed threshold value to the ratio between the log-converted red and green image channels (multiplied by a constant). In case of multiple component visualization in double-immuno stained sections, the second component (stained using the Fast Blue precipitate) was recognized using the ratio between the log-converted red and blue image channels. Objects in the resulting binary image were dilated, holes in objects were filled and the objects were eroded back to their original size.²²¹ This resulted in almost perfect discrimination between endothelium or pericytes and background, with objects representing entire vascular profiles (including the lumen).

Subsequently, results of the automatic segmentation were shown as an overlay in the original color images after which interactive correction of segmentation errors was possible. Interactive correction was necessary only in cases with very weakly stained endothelium or in some cases where artifacts were present. A similar procedure was used for the α -smooth muscle actin stained slides.

Image registration

Alignment of consecutive serial sections (image registration) was a two-step process. First, during image acquisition the revolving microscope stage was used to perform a 'rough' initial registration, correcting for shifts and rotations of sections on the glass slides. Correction for stretching of sections is not possible during this phase. The subsequent automated registration procedure is used for more accurate alignment, including correction for stretching of sections. Automatic registration was performed using the Insight Segmentation

and Registration Toolkit (ITK version 1.4, open source software developed as an initiative of the US National Library of Medicine, freely available at www.itk.org). This software enables image registration using a variety of techniques.

Automated image registration can be formulated as a mathematical problem, in which a cost function is minimized by finding the optimal combination of parameter values for the selected transform. In the present study, a centered affine transform was used for projection of pixels from the image to be registered onto a fixed image. This transform corrects for rotational and translational as well as stretching effects between consecutive images, and is parameterized with 8 parameters: a 2 x 2 transformation matrix defining both scaling and rotation, 2 parameters defining the center of rotation (x,y) and 2 parameters defining a translation (x,y).

A normalized correlation metric was used as cost function, determining the 'goodness of fit' of a set of transform parameter values. This function is defined as the pixel wise cross-correlation normalized by the square root of the autocorrelation. This metric is very accurate for small misalignments between images, which is well suited for images in this study because of the manual pre-alignment. As the normalized correlation metric is only defined for monochromatic images, RGB color images were transformed to monochromatic images by averaging the R, G and B values. Application of the affine transform may map pixels (which represent discrete intensity values at fixed grid positions) to non-grid positions. An interpolation is required to calculate intensity values for grid positions after the transform. In the present study a 3rd order B-spline interpolation was used.

An optimization algorithm was used for minimizing the cost function. The 'One plus one evolutionary optimizer' (information available from Image Science Lab, Zurich, Germany) was used for this purpose, which was found to be both efficient and robust for our purpose. The efficiency of this optimizer highly depends on the choice of optimizer parameters: the so-called grow and shrink values were both set to -0.05, initial radius to 1. These values were empirically chosen, based on optimization of a number of test images. The translation was initialized with the center of the image as the center of rotation, and the unity matrix as transformation matrix. A maximum of 75 iterations was allowed. The optimal ('best fit') transform was applied to the monochromatic image used in the optimization as well as to the corresponding segmented (binary) image.

To reduce the possibility of erroneous transformations, images were processed in a pair wise fashion in the following manner. Image 2 was fit to image 1, next image 4 was fit to 3, then 3 was fit to 2 and the resulting transform was applied to both images 3 and 4. In this way transformation steps were kept as small as possible.

Three-dimensional reconstruction

KS400 was used to cut sub images (size 380 x 285 pixels) from the binary images resulting from the registration procedure. Also, all binary objects in an image without connection with corresponding objects in adjacent images were removed.

Three-dimensional surface rendering was performed using the Visualization Toolkit (VTK version 4.2, an open source software mainly developed by Kitware Inc, freely available at www.vtk.org). VTK procedures were written in Tcl/Tk (Version 8.3, Scriptics Corp; precompiled windows binaries freely available through www.tcl.tk). For each type of tissue, a volume consisting of 50 binary images was read from TIFF files, with (relative) pixel spacing for single component analysis set to 1 x 1 x 3.1. Using VTK, the 3D binary volume was first eroded (kernel size 3 x 3 x 1) after which a Gaussian smoothing was applied (standard deviation 3 x 3 x 1 pixels). A second binary erosion was applied (kernel size 5 x 5 x 1) after thresholding the output of the Gaussian smoother (lower bound 200). These filter steps and parameters were selected in such a way that the complexity of the 3D surface was reduced without compromising on the image quality. Based on visual inspection of a number of test images, filter parameters were selected that preserve the original size of the 3D structures.

Next, the VTK Marching Cubes function was used to construct a set of iso-surfaces encompassing the binary vascular 3D structure. The 3D structure was visualized using VTK surface rendering, calculating a 2D projection of the 3D surface structure with emulation of a light and camera standpoint. Also, the RGB image of the first tissue section was rendered in the same scene to facilitate comprehension of the 3D structure.

Multiple component visualization

Simultaneous visualization of two components was performed mainly as described above. Sections were immunohistochemically stained using two different antibodies. In case of alternate staining of two components, manual alignment and image acquisition was first performed for one component (storing images of sections 1, 3, 5, etc), based on contours of structures in the previous section in the overlay. Images of the second component were then manually aligned based on the stored images of the first component.

Image segmentation and registration were performed as described above for a single component. Visualization using VTK was performed for both components independently. The opacity and color of the two components could be determined independent of each other. For alternately stained sections, subimage size 179 x 193 pixels was used for the HB sections and subimage size 450 x 390 pixels for the normal cerebellar cortex. As each section is 3 μm thick, the resolution in z-direction now becomes 6 μm , resulting in relative pixel spacing 1 x 1 x 9.2. For immuno-double stained, 4 μm sections of a GBM, subimages of size 662 x 477 pixels were used, with relative pixel spacing 1 x 1 x 6.2.

Results

The vasculature of white and neocortical grey matter of the normal brain was reconstructed from serial sections stained for CD34 (Figure 2C and D). Examples of corresponding 2D histological sections are shown in Figure 2A and B. To visualize the differences in pathological vessel architecture in brain tumors, one HB and one GBM were analyzed. (Figure 3A and B show 2D slides, 3C and D show 3D reconstructions). HBs are highly vascularized, and although 2D histological sections stained for CD34 already show this phenomenon (Figure 3A), the complexity of the vascular architecture can only be truly appreciated by 3D visualization of the vessels (Figure 3C). Glomeroid microvascular proliferations are a pathological hallmark of GBM. As shown in Figure 3B and D, the spatial presentation of this aberrant vasculature is much easier to comprehend in 3D than in 2D images.

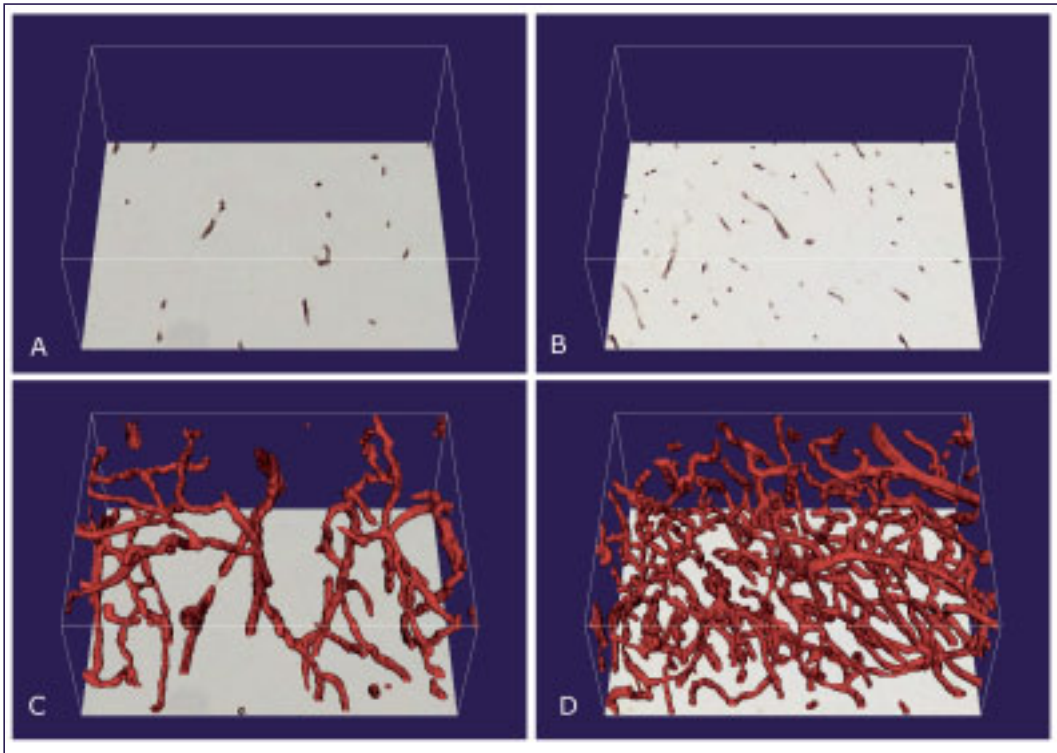


Figure 2 2D histological sections of normal cerebral white (A) and neocortical grey matter (B) stained for endothelium with antibodies to CD34. Corresponding 3D reconstructions of the microvascular architecture (C and D). The 3D reconstructions are based on analysis of a stack of 50 serial sections, the first of which is shown in A and B. Volume indicated by box: 494 x 370 x 200 μm .

To show the interrelation of two different components, microvessels of normal cerebellar cortex, a HB, and a GBM are reconstructed. The relation between endothelium and surrounding activated pericytes is shown in Figure 4 and 5. Alternately stained sections were used for a HB and normal cerebellar cortex, a doublestaining technique was used for a GBM. In contrast to normal cerebellar tissue (Figure 4C), in the area of GBM shown in Figure 5 very few activated pericytes are present in the wall of capillary vessels. An occasional larger blood vessel (arteriole/venule) in the sample of normal cerebellar cortex and of the GBM contains α -smooth muscle actin positive vascular smooth muscle cells in its wall. In the HB, almost all tumor capillaries show extensive coverage of α -smooth muscle actin positive pericytes, demonstrating the activated state of the vessels in this tumor (Figure 4D).

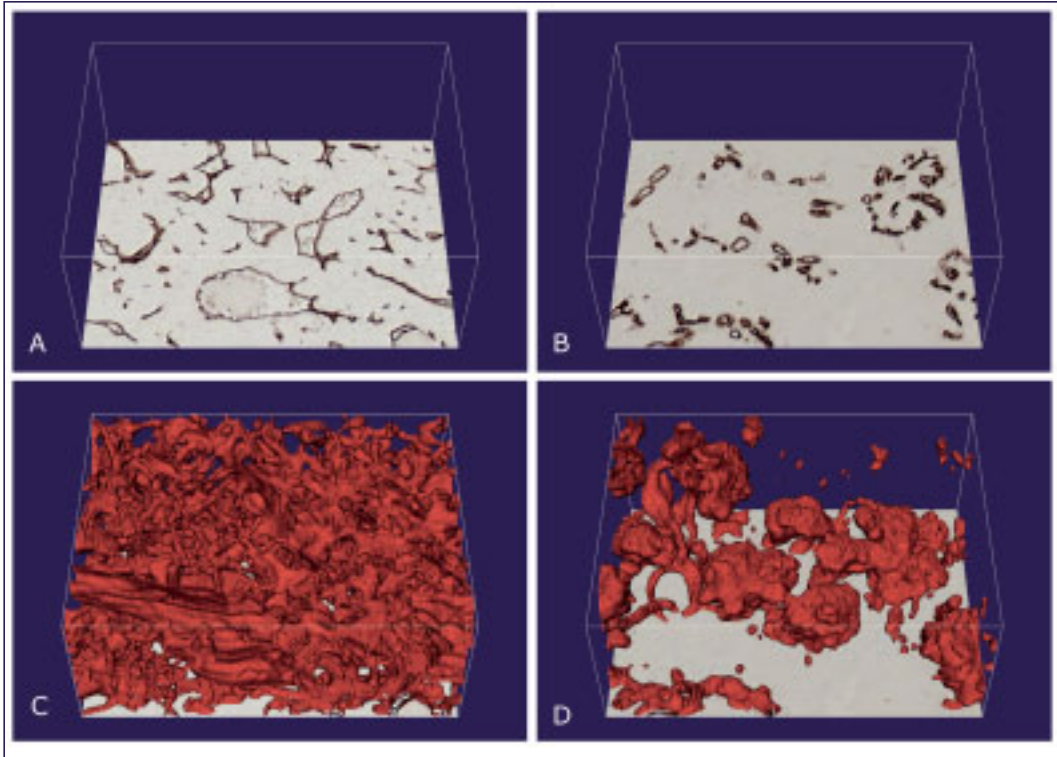


Figure 3 2D histological sections of a hemangioblastoma (A) and a glioblastoma multiforme (B) stained for endothelium with antibodies to CD34. Corresponding 3D reconstructions of the microvascular architecture (C and D). Note the extremely high vascular density in a hemangioblastoma, and the glomeruloid microvascular proliferation in a glioblastoma. Volume of box: 494 x 370 x 200 μm .

Manual alignment, performed for all samples, proved to be accurate and relatively fast (up to 3 minutes to align a complicated image). After automated segmentation, manual interactive correction of segmentation errors was necessary only in a few cases with very weakly stained endothelium or in a few cases when artefacts were present. Although manual alignment proved to be accurate, automated fine-alignment was used because this reduces possible observer bias. Automated alignment of an image took 15 minutes computer time (PC 2.4 GHz). Using alternately stained sections for simultaneous visualization of two components hampers the z-resolution, because only half of the sections are stained for each component. To reduce this problem, slightly thinner sections were used for this technique. In contrast, using immuno-double

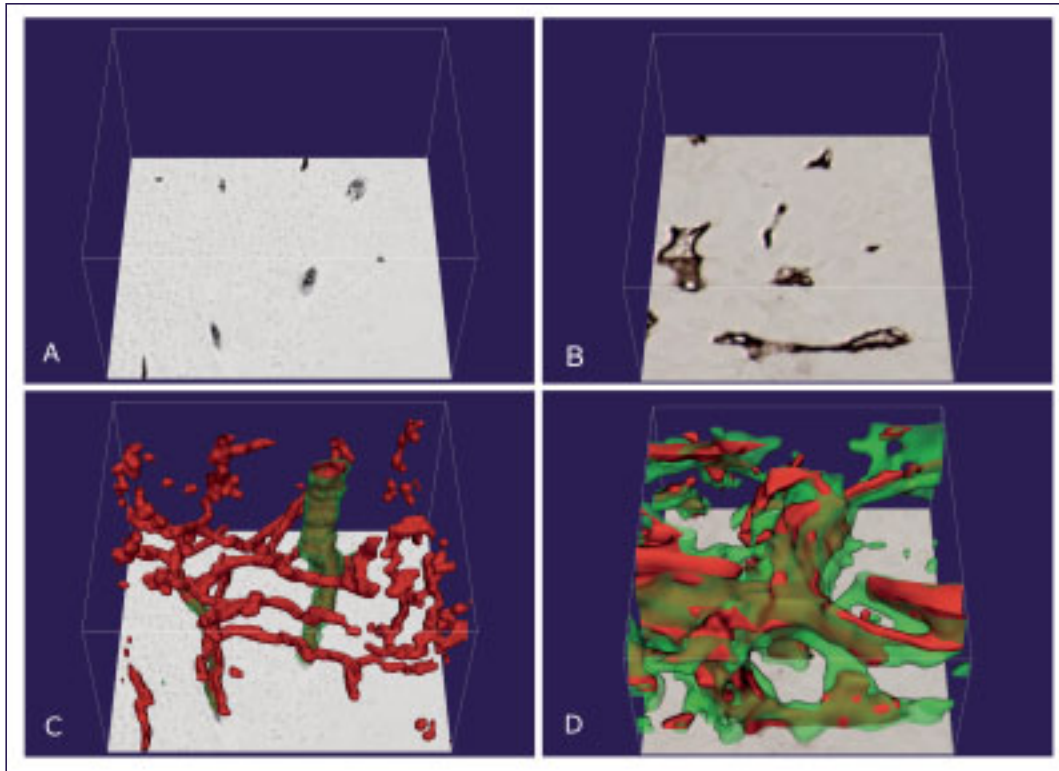


Figure 4 2D histological section (CD34 staining) of normal cerebellar cortex (A) and a hemangioblastoma (B). For this study the sections were alternately stained for endothelium with antibodies to CD34 and for activated pericytes with antibodies to α -smooth muscle actin. The spatial relationship between endothelium (red) and activated pericytes (transparent green) is shown in C and D. Because of the extremely intricate architecture of the microvasculature in a hemangioblastoma (see also fig. 3C), in figure 4B,D a more detailed image is presented showing the different cellular components of its microvasculature. Volume of box in A and C: $293 \times 254 \times 180 \mu\text{m}$, in B and D: $116 \times 125 \times 60 \mu\text{m}$. Note the extensive presence of activated pericytes in capillaries of a hemangioblastoma, while in normal cerebellar cortex α -smooth muscle actin positive cells are only found in the wall of somewhat larger vessels (consistent with vascular smooth muscle cells in arterioles or venules which are known to constitutively express α -smooth muscle actin).

staining results in full resolution for both components. This latter technique is however technically somewhat more challenging in terms of immunohistochemistry and image analysis.

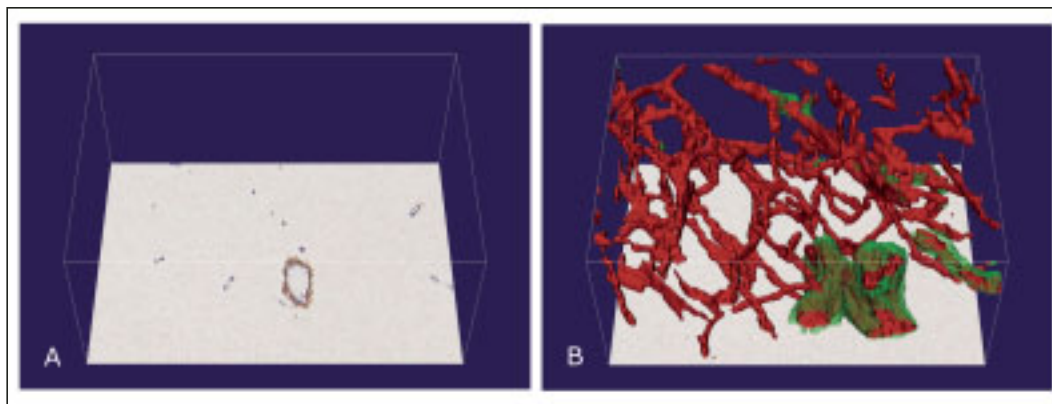


Figure 5 2D histological section of a glioblastoma multiforme (A) doublestained for endothelium with antibodies to CD34 (blue) and for activated pericytes with antibodies to α -smooth muscle actin (brown). Corresponding 3D reconstruction in B, with endothelium in red and activated pericytes as well as vascular smooth muscle cells in transparent green. Volume of box: 430 x 310 x 196 μm . In contrast to the area shown in fig. 3B and 3D, in this area of a glioblastoma the microvascular architecture is still relatively normal. Apart from α -smooth muscle actin positive vascular smooth muscle cells in the wall of a larger blood vessel, also dispersed α -smooth muscle actin positive cells indicating activated pericytes are present in the capillaries (the latter are not found in the normal cerebellar microvasculature as seen in fig. 4C).

Discussion

We describe a novel method for 3D visualization of microscopic structures in normal brain and in brain tumors. The method was found to be reliable and robust, and is applicable on archival, paraffin-embedded material. Besides 3D reconstruction of normal vessels in neocortical and white matter of the cerebrum, reconstructions were made of two well-vascularized brain tumors: a HB and a GBM. HBs are benign tumors, characterized by stromal cells and a very rich capillary network.⁴⁵ GBMs, on the other hand, are high-grade malignant glial tumors, with florid, and sometimes glomeruloid microvascular proliferations as a major histopathological hallmark.^{222,223} The microvascular patterns in both tumors are routinely assessed in 2D slides, and 3D images of the microvasculature in these tumors have only sporadically been published before. Furthermore, we present examples of the spatial relationship between endothelium and activated pericytes in the capillary walls in normal cerebellar cortex, a HB, and a GBM.

For 3D reconstruction, archival paraffin-embedded samples were serially sectioned at 3 or 4 μm using a unique section method in order to limit loss and distortion of sections to a minimum. Other serial section techniques may account for a loss of sections of up to 5%, such lost sections may be replaced with interpolated images.²¹³ However, automated interpolating of lost images raises concern about unforeseen distortions to align the sections. In our procedure, segmentation was easy and accurate because of high quality of the histological sections and the bright immunohistochemical staining without counterstaining; manual correction of the segmentation was only sporadically necessary, this in contrast to other methods that need manual correction of obvious errors,^{210,212} occurring in approximately 5% of sections.²¹⁰

In 3D reconstruction using serial histological sections, accurate alignment of the sections is a major challenge. Therefore, a number of techniques have been described which circumvent the use of sections. Use of confocal laser scanning microscopy makes use of optical sections, eliminating the need for registration.^{207,209} However, due to optical limitations this technique is limited to 50-100 μm thick tissue fragments.²⁰⁷ A second method to prevent image distortion caused by cutting sections is by using the cut face of the tissue block instead of the sections themselves.²²⁴ Images are recorded by using the autofluorescence of the tissue. A major drawback of this technique is that no specific visualization of microscopic structures can be applied (such as immunohistochemistry), enabling only reconstruction of gross structures. In the present study, image registration was a two-step process. During image acquisition, manual alignment was performed to correct for shifts and rotations of the tissue as much as possible, without the possibility to correct for tissue stretching. Next, a fully automated registration procedure was used, which optimized the alignment accuracy of the manual method. Only slight improvement was seen comparing the results of automated and manual alignment. Still, as we are studying microstructures, even this slight improvement may be critical. Manually and automated alignment procedures have been compared previously, and similar results have been reported.^{213,225} Fully automated methods of alignment eliminates the bias introduced by manual alignment.^{207,210,212,213,225}

The endothelium of capillaries is surrounded by pericytes, which are regarded as the microvascular equivalent of smooth muscle cells. The functions of these cells are variable and complex. Activated pericytes may play a role in the

formation of angiogenic sprouts during the early phases of both normal and pathologic angiogenesis.^{226,227} In later phases of neovascularization, major functions of pericytes are participation in stabilization of vessel walls and regulation of several endothelial functions, such as permeability, proliferation, and vascular branching.²²⁸ Pericyte coverage may differ between tumors and normal vessels. The amount of activated pericytes on vessels in different tumor types is reported to be highly variable, e.g. extensive in florid microvascular proliferations in GBMs, but little in renal cell carcinomas.^{226,229} In cerebellar HBs pericyte coverage as detected by electron microscopy and computerized morphometric techniques, is described to range from 30-97% (mean 69%), which is much higher compared to normal cerebral grey matter.⁴⁹ To visualize the coverage by activated pericytes in the complex vasculature of HBs and GBMs we performed 3D visualization of serial sections stained for CD34 and α -smooth muscle actin. Our 3D reconstruction showed nearly complete coverage of α -smooth muscle actin positive pericytes in a HB. A 3D reconstruction model of the relation between endothelium and pericytes in capillaries using electron micrographs of serial sections has been published before.²³⁰ However, computer based techniques were not available at that time. Although in the present study resolution in the z-direction (6 μ m) was less when multiple components were visualized using the alternate staining approach, accurate visualization could still be obtained. The use of immuno-double staining, however, greatly facilitates the 3D reconstruction of different components in the same tissue sections.

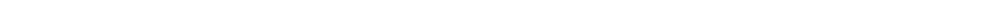
In conclusion

The results of the 3D reconstruction as described shed unprecedented light on morphological features of normal and pathological microvasculature. The procedure is applicable on serial sections of all kinds of tissues and structures. The potential of the procedure is mainly limited by the possibility to specifically visualize the object(s) of interest by immunohistochemical or other techniques, and the quality and thickness of the serial sections. We are currently assessing the 3D morphology of the microvasculature in a series of other human brain tumors, as well as using this approach to monitor the (sometimes subtle) changes after chemotherapeutic (e.g. anti-angiogenic) treatment in murine

intracerebral xenograft models for human malignant melanoma and GBM.^{231,232} Finally, we expect the information obtained by our 3D reconstruction method to significantly contribute to a better understanding of the radiological images of brain tumors, e.g. in situations where the effect of anti-angiogenic treatment of experimental brain tumors is monitored by radiology.²³³

Chapter 8

Summary and general discussion



Hemangioblastomas (HBs) of the central nervous system (CNS) are benign tumors with unique histological and molecular genetic features. The genetic pathways underlying the development of sporadic HBs are currently not completely clear. Therefore, the goal of our studies was to elucidate the genetic background of sporadic HBs. We screened the genome of these tumors for chromosomal abnormalities, and tried to identify putative genes involved in the development of these tumors. Since inactivation of the *VHL* tumor suppressor gene (TSG) underlies the development of hereditary HBs, we discussed the role of this gene in the tumorigenesis of both hereditary and sporadic tumors. As the cyclin D1 gene (*CCND1*) is a target gene of pVHL, we analyzed cyclin D1 expression and *CCND1* genotype in order to evaluate whether *CCND1* genotype influences the susceptibility to HBs.

The *VHL* gene, *VHL* protein, and target genes

HBs are a major manifestation of VHL disease, and a germline mutation of the *VHL* gene at 3p25-26 can be determined in all patients with a VHL-associated HB.⁶² A critical role of the *VHL* gene in the development of these tumors is well established, as inactivation of both alleles of the *VHL* gene has been reported in 62-66% of VHL-associated HBs.^{67,61} According to Knudson's two-hit hypothesis, biallelic inactivation is expected in 100% tumors, but limitations of the common molecular genetic techniques hamper detection of biallelic inactivation in some of these tumors. To date it is not clear whether mutations of other genes are required for HB development. Unraveling of the molecular basis of VHL disease and the functions of the VHL protein (pVHL) provided insight into the pathobiology of VHL-associated tumors. The main function of pVHL is its critical role in the oxygen-sensing pathway of the cell by regulation of hypoxia-inducible factor (HIF-1).⁹⁷ HIF-1 has a key role in the cellular response to hypoxia, including the regulation of genes involved in cellular metabolism, angiogenesis and apoptosis.²³⁴ Loss of function of the pVHL induces upregulation of HIF-1 and, subsequently, overexpression of angiogenic and growth factors, like vascular endothelial growth factor (VEGF) and platelet-derived growth factor (PDGF-B). The presence of such factors explains the hypervascularity of HBs and renal cell carcinomas (RCCs), because they are potent mitogens for endothelial cells and pericytes.

However, the overexpression of angiogenic factors does not explain tumor initiation. Therefore, other pathways than HIF regulation are likely to be involved in the processes that lead to the development of tumors in VHL disease. Moreover, genotype-phenotype correlations in VHL disease suggest that pVHL has functions other than the regulation of HIF; e.g. in type 2C VHL disease (pheochromocytomas only) the ability to regulate HIF is retained. Most mutations leading to type 2 VHL disease are missense mutations, whereas in type 1 families deletions, microdeletions/ insertions, splice site or nonsense mutations as well as missense mutations (in 27%) are found, leading to a truncated protein that has lost its normal function, or to complete lack of pVHL.⁶² In case of a specific missense mutation (in type 2C VHL) the change of one amino acid may lead to a pVHL gain of function, e.g. a pVHL that binds to and modulates other proteins than HIF.³⁹

Extensive investigations have been undertaken to elucidate the pathways of tumor development in VHL disease. Novel target genes of pVHL, regulated by both HIF-dependent and HIF-independent mechanisms, have been identified. In addition, pVHL has been implicated in various cellular processes including cell cycle control and extracellular matrix regulation. A review of the literature is provided in **Chapter 1**.

One of the target genes of pVHL is *CCND1*, encoding cyclin D1, a protein implicated in the control of the cell cycle at the G1/S checkpoint.^{123,124} Overexpression of cyclin D1 may release the cell from its normal cell cycle control, and may induce malignant transformation.¹²⁵ Overexpression of cyclin D1 is a feature of many cancers. In sporadic as well as in VHL-associated HBs we found variable, but sometimes high cyclin D1 expression (**Chapter 5**). The *CCND1* gene contains a common G→A polymorphism located within the splice donor region of exon 4 which modulates splicing of mRNA. The unspliced protein variant (transcripts from the A-allele) has a longer half-life, and DNA damage in cells with the unspliced protein may bypass the G1/S checkpoint more easily than cells with the spliced variant (transcripts from the G-allele). The G→A polymorphism influences age of onset and clinical outcome of various cancers. In most studies, the *CCND1* AA and AG genotypes are associated with early age of onset and poor prognosis. In VHL disease, genetic modifiers may play a role in phenotypic expression, e.g. the risk of occurrence of HBs, RCCs, and pheochromocytomas, and it has been suggested that the *CCND1* polymorphism

is one of these modifiers. In patients with VHL disease, the number of retinal HBs was significantly higher in patients harboring the G-allele compared to AA-homozygotes, and the presence of a G-allele was associated with an earlier diagnosis of CNS HBs by almost two-fold, whereas no increased susceptibility to RCCs was found.¹²³ If the *CCND1* G allele indeed increases susceptibility to HBs, a higher frequency of the G allele is to be expected in these tumors. Therefore, we analyzed 17 sporadic and five VHL-associated HBs for *CCND1* genotype. We found no deviation in *CCND1* genotype distribution and allele frequencies from expected values of normal populations (**Chapter 5**). Therefore, we could not confirm the suggested modifier effect of *CCND1* genotype for HBs. However, our study population was small, and a larger study is needed to draw firm conclusions.

Chromosomal imbalances in sporadic tumors

Inactivation of the *VHL* gene has been linked to the development of sporadic RCCs and HBs.² Somatic *VHL* mutations, hypermethylation of the promoter, or LOH at 3p have been found in the majority of sporadic RCCs.^{69-73,235} According to Knudson's two-hit hypothesis of TSGs, inactivation of both alleles of the *VHL* gene is required for tumor development. In most studies, biallelic inactivation is not established. In those studies reporting biallelic inactivation, the frequency was unexpectedly low; in 33-46% of tumors somatic mutation of one *VHL* allele combined with LOH at 3p was found,^{69,70} and 44% of tumors showed biallelic inactivation when results of somatic mutation, LOH, and hypermethylation were combined.⁷⁴ Therefore, *VHL*-independent pathways involving TSGs on 3p12-21 have been suggested to play a primary role in the tumorigenesis of RCCs.^{73,79} Genes on other chromosomes than 3p may be involved as well, because additional chromosomal aberrations are frequently reported, such as loss (-) of 4q, 6q, 8p, 9p, 14q, and gain (+) of 5q, 7, 17q, and Xq.^{81-85,87} Some of these chromosomal abnormalities may have prognostic significance; e.g. +5q is reported to be associated with a favourable prognosis, whereas LOH at 8p or 9p correlated with recurrence.^{83,87}

We screened the genome of 16 sporadic HBs by CGH for chromosomal aberrations. Aberrant chromosomal regions (with a loss or gain of DNA) might contain TSGs or oncogenes involved in the development of these tumors.

Interestingly, we detected multiple chromosomal abnormalities in these benign tumors (**Chapter 2 and 3**).

The most frequently detected aberrations were loss of chromosome 3 (-3) in 69% (11/16 tumors), -6 in 44% (7/16), -18 or -18q (designated 18(q)) in 31% (5/16), and -9, and +19 in 25% (4/16) (Figure 1). In 31% (5/16) of tumors combined -3 and -6 was detected, whereas an additional -8 was found in 3 tumors. Interestingly, the tumors with -8 had either -3 or a somatic *VHL* mutation, and two tumors had a normal constitution of chromosome 6. Overall, eight of 10 sporadic HBs with multiple chromosomal abnormalities had two of the following imbalances: -3, -6, or -8 (**Chapter 3**).

We compared the chromosomal imbalances in sporadic HBs with chromosomal imbalances in sporadic RCCs and pheochromocytomas as reported in the literature. The most common changes by CGH in pheochromocytomas include -1q, -3q, -6q, -11p, and +19q.^{89,236} Relatively common chromosomal imbalances in either RCCs or pheochromocytomas are also detected in sporadic HBs; -3p, -6(q), -9 for RCCs, -3q, -6(q), +19 for pheochromocytomas. Our findings may suggest a sequence of chromosomal imbalances in sporadic HBs; -3 (harboring the *VHL* gene) followed by -6, and then -18, and/or -9, and/or +19 (**Chapter 2**).

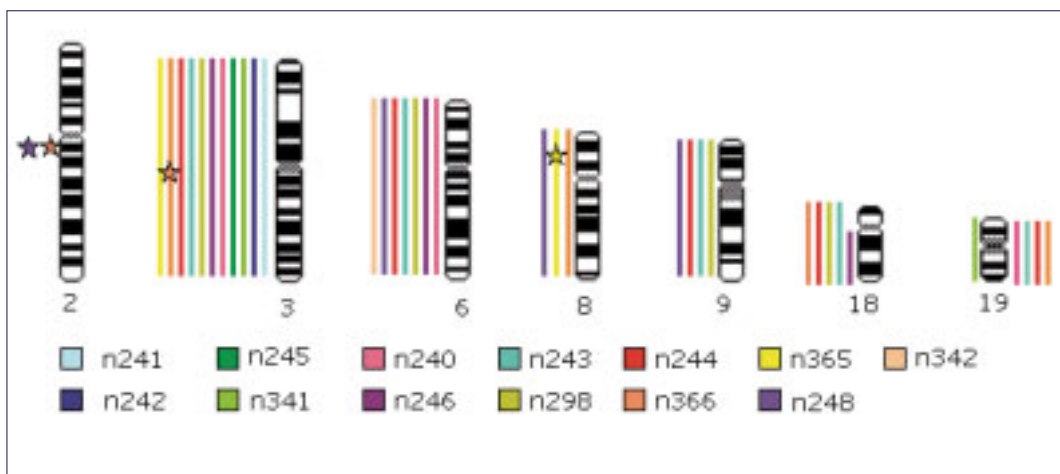


Figure 1 Map showing chromosomal imbalances most frequently detected by CGH. The asterisks indicate the additional aberrations identified by array CGH.

Inactivation of the *VHL* gene in sporadic HBs

The role of the *VHL* gene in the development of sporadic HBs is not clear, as somatic *VHL* gene inactivation by somatic mutation or LOH is found in only 20-50% of sporadic HBs (Table 1).^{38,61,75-77,171} Hypermethylation seems to be an infrequent feature of sporadic HBs, as it could not be demonstrated in two studies.^{61,77}

We found somatic mutations of the *VHL* gene in five sporadic HBs (31%), including three frameshift and two missense mutations, all of these had not been published before (**Chapter 3**). Similar frequencies of somatic mutations have been reported by others (Table 1). Two of the tumors with somatic mutations had also -3, two tumors had also -6, whereas in one tumor with a somatic mutation no additional losses or gains were detected by CGH. Additionally, in 5/16 (31%) of tumors combined -3 and -6 was found. Thus, all tumors with -6 had either -3, or a somatic mutation of the *VHL* gene (**Chapter 3**).

Table 1 Somatic *VHL* gene mutations, LOH at 3p, and hypermethylation of *VHL* promoter in sporadic Hbs

Author	<i>VHL</i> mutation	Loss of 3p (LOH* or CGH#)	Hypermethylation <i>VHL</i> promotor	Confirmed biallelic inactivation <i>VHL</i>
Kanno ⁷⁵	3/13 (23%)			
Oberstrass ³⁸	7/17 (41%)			
Tse ⁷⁷	2/5 (40%)	1/2 (50%)*	0/5	0/2
Lee ⁷⁶	2/20 (10%)	10/19 (53%)*		0/20
Glasker ⁶¹	3/13 (23%)	5/10 (50%)*	0/13	1/13 (8%)
Lemeta ¹⁷¹		11/11 (100%)*		
This thesis	5/16 (31%)	11/16 (69%)*		2/16 (13%)

In most studies, inactivation of both alleles of the *VHL* gene is not determined (Table 1). One recent study combined somatic mutation analysis, LOH, and hypermethylation analysis, and found biallelic inactivation in only one of 13 (8%) sporadic HBs.⁶¹ We could confirm biallelic inactivation in only two tumors (2/16; 13%). These tumors showed a somatic mutation combined with loss of chromosome 3 (**Chapter 3**). We did not perform LOH and hypermethylation analysis, so we might have underestimated the frequency of biallelic inactivation

in our studies. However, the results of our studies and those of other investigators suggest that biallelic inactivation of the *VHL* gene may not be a common mechanism in the development of sporadic HBs, and that the role of *VHL* is limited in these tumors. Therefore, other TSGs or oncogenes are likely involved in the oncogenesis of sporadic HBs. These genes may act in collaboration with *VHL* in the subset of sporadic HBs with monoallelic or biallelic inactivation of the *VHL* gene. Such genes involved in sporadic HBs might also act in collaboration with the *VHL* gene in VHL-associated tumors.

Genetic heterogeneity of sporadic and hereditary HBs

A striking contrast was found in CGH results of seven VHL-associated HBs; only one -3 was detected (**Chapter 3**), while in all tumors a *VHL* mutation was determined. Although no blood samples were available for most of these cases, these mutations were likely to be germline mutations. Since we did not perform LOH or hypermethylation analysis we could not determine the frequency of biallelic inactivation in VHL-associated HBs.

CGH analysis of six HBs of a single VHL-patient with a known *VHL* germline mutation also revealed few chromosomal abnormalities in the VHL-associated HBs; -3 and -22 in one HB, -22 and +X in a recurrence of this tumor, + X in a cauda equina HB, and +2pter-q32 in one HB obtained at autopsy. Two HBs did not show abnormalities by CGH (**Chapter 6**). There was no increase in chromosomal imbalances in HBs presenting early in the disease versus tumors removed at autopsy. LOH analysis for 3p was performed in four tumors (three without -3) and was found to be negative. The germline mutation could be determined in four tumors, and no somatic mutations were found (**Chapter 6**). In this patient, multiple chromosomal abnormalities were found in the renal tumor and its metastasis (**Chapter 6**).

The striking contrast of the multiple chromosomal aberrations in sporadic HBs with the low frequency of abnormalities in VHL-associated HBs as detected by CGH in our study underscores that their molecular genetic pathways are distinct. We investigated a subset of sporadic HBs for micro-deletions or amplifications by array CGH.

The role of putative TSGs in sporadic HBs

After the publication of our initial study, other investigators confirmed that loss of chromosome 6 (or 6q) might be of relevance in HBs. Loss of chromosome 6(q) was reported by them in 24% (four of 17; -6 in two, and -6q in two) sporadic, and in one of five VHL-associated HBs.¹⁷⁰ Additionally, -3 was found in two tumors with -6q, and another sporadic HB had only -8.¹⁷⁰ Twelve sporadic and four VHL-associated HBs had no chromosomal abnormalities detected by CGH, and the authors concluded that large deletions of 3p occur in a minority of tumors. These findings are in contrast with our results, as we found loss of a whole chromosome 3 in 69% of tumors, and multiple, additional abnormalities. These differences might be explained by the fact that we used snap-frozen material in the majority of tumors, while others used paraffin-embedded tissue, the latter generally leading to less robust CGH results.^{142,170} Furthermore, for those cases from which only paraffin-embedded tissue was available normal DNA also isolated from paraffin-embedded non-tumor tissue was used. In our experience, this leads to more reliable CGH results.

In subsequent LOH studies, LOH at 6q was found in 82% of 11 sporadic HBs, with a minimal deleted region at 6q23-24, and LOH at 3p was detected in all tumors.¹⁷¹ Based on our results, and confirmed by the studies of others,^{170,171} it seems likely that the development of sporadic HBs is dependent on the inactivation of TSGs on 3p and 6(q). However, in five sporadic HBs analyzed by array CGH we did not detect a microdeletion on chromosome 6 (**Chapter 4**).

We did not detect loss of chromosome 6 by CGH in VHL-associated HBs (Chapter 3 and 6). Others reported loss of chromosome 6 in only one of five VHL-associated HBs, and LOH at 6q in 2 of 4 VHL-associated HBs.^{170,171}

Similarly, -8, -9, -18q, and +19 are reported in a variety of tumors. Many putative TSGs have been suggested on these chromosomes, as well as on chromosome 3p apart from the *VHL* gene on 3p25-26.¹⁵⁶ An important role for candidate TSGs at 3p12-14, containing for instance the *FHIT* (fragile histidine triad) gene, and at 3p21.3, containing *RASSF1A* (RAS-association domain family 1) among others, has already been suggested in the tumorigenesis of sporadic and VHL-associated RCCs.^{73,79,237} TSGs at chromosome 6q23-24, for instance

LATS1 (large tumor suppressor 1), which suppresses tumor growth by regulating cell proliferation and survival, and *ZAC* (zinc finger protein), which inhibits tumor growth by induction of apoptotic cell death, have been speculated to be involved in the tumorigenesis of HBs.¹⁷¹ However, the role of these TSGs in HBs remains to be determined.

Array CGH of sporadic HBs

The results of our studies and reports in the literature, prompted us to extend our investigations in an attempt to find putative genes involved in the tumorigenesis of sporadic HBs.

Although GCH has the advantage of genome-wide screening of DNA copy number changes in a single experiment, the technique is limited by the detection limit of 2-5Mb, and especially small deletions are difficult to detect. Therefore, we analyzed HBs with 32K array CGH. Array CGH allows high-resolution screening of the genome for small chromosomal abnormalities with a detection limit of approximately 100 kb, by using thousands of genomic clones as targets for hybridization instead of whole chromosomes. Informative array CGH results were obtained from five sporadic HBs (**Chapter 4**). The study was hampered by the amount of normal tissue in HBs; the stromal cells are the neoplastic component, whereas the rich capillary network contains non-neoplastic endothelial cell and pericytes. Results of conventional CGH and mutation analysis of the *VHL* gene were available in all cases (**Chapter 3**). Overall, the abnormalities detected by CGH were also identified by array CGH. Some minor differences were found, several of which were in retrospect visible with conventional CGH. No additional abnormalities were detected at 6q23-24, nor at other regions of chromosome 6 or 3p.

In three tumors, candidate chromosomal microdeletions were detected, including 2q13-14.1 in two tumors, and 8p21.3 and 3q13.31 in one tumor each. The identified regions on 8p and 3q are of special interest as these chromosomes are frequently affected in HBs (**Chapter 3**). Both deletions would be homozygous, since these tumors had already loss of one copy of chromosome 8 and 3, respectively. The short arm of chromosome 8 (8p) is frequently deleted in cancer.¹⁷⁸⁻¹⁸¹ One of the genes located at this region is *FEZ1/LZTS1* (leucine zipper, putative tumor suppressor 1), a tumor suppressor gene that inhibits tumor growth through regulation of mitosis, and that has

been suggested to play a role in the development of various tumors including prostate, urinary bladder, breast, esophageal, and lung cancer.^{182-184,186} Chromosome 3q13 is also an interesting region, as it contains *LSAMP* (limbic system-associated membrane protein), a gene that is a candidate TSG for clear cell RCCs, the other tumor type frequently associated with VHL disease.¹⁷⁶ *LSAMP* encodes a neuronal surface glycoprotein expressed in the limbic system, and regulates the formation of specific neuronal connections. The mechanism of suppression of tumor growth in RCCs is unclear.²³⁷ The results of array CGH are preliminary, as only five HBs were analyzed, and validation of the results (e.g. by FISH) is required.

Molecular genetic analysis and the differential diagnosis of tumors

The molecular genetic techniques used in our studies are described briefly in the introduction chapter of this thesis (**Chapter 1**). CGH, LOH, and mutation analysis are commonly used, and results of these techniques are complementary. VHL patients often harbor multiple tumors, and dedifferentiation of these tumors occurs often in the later stages of the disease. Dedifferentiated tumors can be difficult to characterize histologically. Nowadays, information on the genetic background of tumors is rapidly increasing. This information can aid in establishing a definitive diagnosis when standard histological and immunohistochemical investigations are not conclusive. This is illustrated in a patient with VHL disease in which molecular genetic analysis resolved the differential diagnosis of metastatic sarcomatoid RCC and pheochromocytoma (**Chapter 6**).

An extreme example of angiogenesis

HBs are histologically characterized by neoplastic stromal cells and a very rich capillary network. Histopathologically, sporadic and hereditary HBs are identical. The vasculature of HBs contains capillaries with endothelial cells and pericytes. The positive staining for α -smooth muscle actin indicates that the pericytes are activated; this might be due to the ongoing production of angiogenic and growth factors in these tumors.

We developed a novel method for simultaneous 3D visualization of multiple tissue components (**Chapter 7**). Since we were interested in tumor vasculature

we used the technique to reconstruct microvessels in both normal and pathological tissue. 3D images were reconstructed from 2D paraffin-embedded serial sections, using immunohistochemical staining with CD34 (for endothelium) and α -smooth muscle actin (for activated pericytes). HBs are an extreme example of angiogenesis, as is strikingly illustrated in the three dimensional images. Using this procedure, we were also able to demonstrate extensive coverage of the HB capillaries by activated pericytes (Figure 2). We will use the technique to assess the 3D morphology of the microvessels in other human brain tumors, as well as to monitor the microvascular changes after anti-angiogenic therapy in murine intracerebral xenograft models for different tumors, e.g. GBM and malignant melanoma.

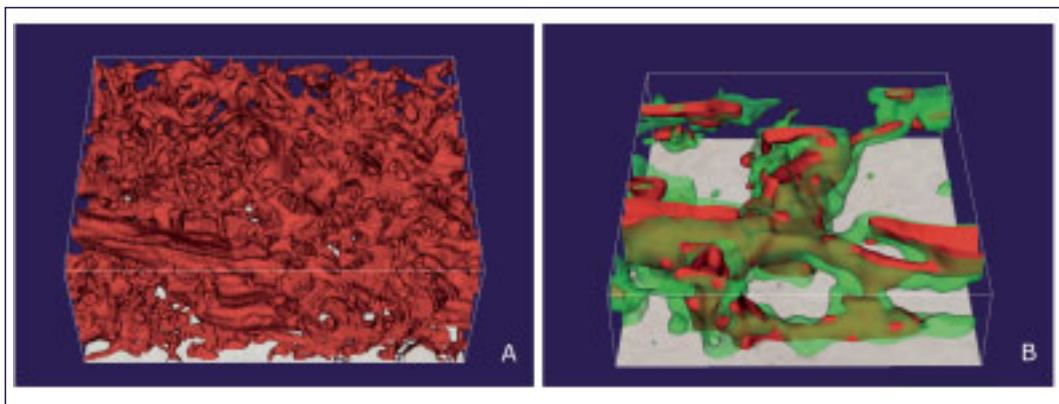


Figure 2 3D reconstruction of capillary network of a hemangioblastoma (A). Extensive coverage of capillaries by activated pericytes (B; detail of A).

In **summary**, the molecular genetic studies revealed that:

- Striking differences exist in frequency of chromosomal abnormalities detected by CGH between sporadic and VHL-associated HBs;
- Multiple chromosomal aberrations as detected by CGH are present in sporadic HBs, including -3, -6, -8, -9, -18, and +19
- Loss of a whole chromosome 3 is more frequently detected in sporadic HBs than in VHL-associated HBs (in VHL-associated HBs more often LOH)

- Loss of chromosome 6 is a frequent event in sporadic HBs and usually associated with -3 or a somatic mutation of the *VHL* gene, as well as with multiple other chromosomal imbalances
- Somatic *VHL* mutations occur in approximately 31% of sporadic HBs
- Three candidate microdeletions (on chromosome 2, 3, and 8) were identified by array CGH, which may be associated with HBs development

These findings indicate that inactivation of the *VHL* gene is not the most important molecular event in sporadic HBs, and that sporadic and *VHL*-associated HBs have a different genetic background.

Future perspectives

The results of the molecular genetic studies discussed in this thesis confirm our hypothesis of a distinct molecular pathway in sporadic HBs compared to *VHL*-associated HBs. However, many questions remain to be answered.

It is currently unknown why *VHL* mutations in *VHL* disease lead to the occurrence of only particular tumor types, nor is it clear why HBs preferentially occur in the cerebellum. Insight into p*VHL* functions other than inhibiting HIF, and the understanding of how these functions act together might provide answers to those questions. Evidence is accumulating that the *VHL* gene alone does not explain the tumorigenesis of sporadic and hereditary HBs, as biallelic inactivation is only found in part of the tumors. It will be important to identify other genes that cooperate with *VHL* inactivation to cause specific tumors such as HBs. We used a combination of molecular genetic techniques to further elucidate the genetic background of sporadic HBs. Although striking differences with *VHL*-associated HBs were found and a pathway of subsequent chromosomal abnormalities was suggested, the genes involved in the development of sporadic HBs remain to be identified. The technique we used in our studies, CGH, is a useful tool to screen for chromosomal abnormalities in tumors, and is currently used in our laboratory in a variety of tumors in experimental settings. Array-based CGH is a powerful tool to screen the genome for putative genes, and although promising results can be obtained, analysis

of the obtained large data sets and confirmation of the putative genes is still challenging. In HBs, array CGH is hampered by the relatively large amount of normal DNA. Laser microdissection methods may enhance the yield of array CGH. Gene expression profiling, e.g. transcriptional profiling analysis involving messenger RNAs (mRNA) or post-transcriptional profiling involving the recently discovered microRNAs, may be a promising alternative to identify candidate genes.^{238,239} MicroRNAs are thought to control gene expression at the post-transcriptional level by degrading target mRNA, and thereby reducing the amount of protein encoded by these mRNAs.²³⁹ Many oncogenes and TSGs are potentially regulated by microRNAs, and there is also evidence that microRNAs can act themselves as oncogenes or TSGs.²³⁹

Another novel approach to elucidate the pathways involved in various diseases including cancer is proteomics. Since inactivation or overexpression of genes ultimately lead to an altered expression of proteins, the identification of individual proteins or clusters of proteins expressed in various diseases may be more relevant for establishing the diagnosis, prognosis and therapeutic targets than the identification of genes alone. The identification of differences in protein patterns between different tumors, e.g. between sporadic HBs and VHL-associated HBs, may enhance the understanding of differences in pathways involved in these tumors.²⁴⁰ HBs can probably be identified by their protein pattern, since a study using selective tissue microdissection and proteomic profiling showed a markedly different protein profile between a HB and RCC in one VHL patient.²⁴¹

Finally, the technique of 3D reconstruction of the microvasculature will be further applied in the experimental setting to study different aspects of angiogenesis and anti-angiogenic therapy in intracerebral xenograft models of various tumors.

References

1. Lonser RR, Glenn GM, Walther M, Chew EY, Libutti SK, Linehan WM, Oldfield EH. Von Hippel-Lindau disease. *Lancet* 2003;361:2059-67.
2. Kim WY, Kaelin WG. Role of VHL gene mutation in human cancer. *J Clin Oncol* 2004;22:4991-5004.
3. Lindau A. Studien über kleinhirncysten. Bau, pathogenese und beziehungen zur angiomatosis retinae. *Acta Path Microbiol Scand (Suppl 1)* 1926;1-128.
4. Resche F, Moisan JP, Mantoura J, Kersaint-Gilly A, Andre MJ, Perrin-Resche I, Menegalli-Boggelli D, Lajat Y, Richard S. Haemangioblastoma, haemangioblastomatosis, and von Hippel-Lindau disease. *Adv Tech Stand Neurosurg* 1993;20:197-304.
5. Richard S, Graff J, Lindau J, Resche F. Von Hippel-Lindau disease. *Lancet* 2004;363:1231-4.
6. Kleihues P, Cavenee WK, eds. Pathology and genetics of tumours of the nervous system. Lyon: IARC Press, 2000.
7. Wizigmann-Voos S, Plate KH. Pathology, genetics and cell biology of hemangioblastomas. *Histol Histopathol* 1996;11:1049-61.
8. Bruner JM, Tien RD, McLendon RE. Tumors of vascular origin. Russell and Rubinstein's pathology of tumours of the nervous system. Sixth Edition. London: Arnold, 1998: 239-56.
9. Richard S, Campello C, Taillandier L, Parker F, Resche F. Haemangioblastoma of the central nervous system in von Hippel-Lindau disease. French VHL Study Group. *J Intern Med* 1998;243:547-53.
10. Neumann HP, Eggert HR, Weigel K, Friedburg H, Wiestler OD, Schollmeyer P. Hemangioblastomas of the central nervous system. A 10-year study with special reference to von Hippel-Lindau syndrome. *J Neurosurg* 1989;70:24-30.
11. Wanebo JE, Lonser RR, Glenn GM, Oldfield EH. The natural history of hemangioblastomas of the central nervous system in patients with von Hippel-Lindau disease. *J Neurosurg* 2003;98:82-94.
12. Richard S, David P, Marsot-Dupuch K, Giraud S, Beroud C, Resche F. Central nervous system hemangioblastomas, endolymphatic sac tumors, and von Hippel-Lindau disease. *Neurosurg Rev* 2000;23:1-22.
13. Glasker S, Berlis A, Pagenstecher A, Vougioukas VI, van Velthoven V. Characterization of hemangioblastomas of spinal nerves. *Neurosurgery* 2005;56:503-9.
14. Weil RJ, Vortmeyer AO, Zhuang Z, Pack SD, Theodore N, Erickson RK, Oldfield EH. Clinical and molecular analysis of disseminated hemangioblastomatosis of the central nervous system in patients without von Hippel-Lindau disease. Report of four cases. *J Neurosurg* 2002;96:775-87.
15. Niemela M, Lemeta S, Summanen P, Bohling T, Sainio M, Kere J, Poussa K, Sankila R, Haapasalo H, Kaariainen H, Pukkala E, Jaaskelainen J. Long-term prognosis of haemangioblastoma of the CNS: impact of von Hippel-Lindau disease. *Acta Neurochir (Wien)* 1999;141:1147-56.
16. Maher ER, Yates JR, Ferguson-Smith MA. Statistical analysis of the two stage mutation model in von Hippel-Lindau disease, and in sporadic cerebellar haemangioblastoma and renal cell carcinoma. *J Med Genet* 1990;27:311-4.
17. de la Monte SM, Horowitz SA. Hemangioblastomas: clinical and histopathological factors correlated with recurrence. *Neurosurgery* 1989;25:695-8.
18. Fisher PG, Tontiplaphol A, Pearlman EM, Duffner PK, Hyder DJ, Stolle CA, Vortmeyer AO, Zhuang Z. Childhood cerebellar hemangioblastoma does not predict germline or somatic mutations in the von Hippel-Lindau tumor suppressor gene. *Ann Neurol* 2002;51:257-60.
19. Glasker S, van Velthoven V. Risk of hemorrhage in hemangioblastomas of the central nervous system. *Neurosurgery* 2005;57:71-6.

20. S later A, Moore NR, Huson SM. The natural history of cerebellar hemangioblastomas in von Hippel-Lindau disease. *AJNR Am J Neuroradiol* 2003;24:1570-4.
21. Lonser RR, Vortmeyer AO, Butman JA, Glasker S, Finn MA, Ammerman JM, Merrill MJ, Edwards NA, Zhuang Z, Oldfield EH. Edema is a precursor to central nervous system peritumoral cyst formation. *Ann Neurol* 2005;58:392-9.
22. Filling-Katz MR, Choyke PL, Patronas NJ, Gorin MB, Barba D, Chang R, Doppman JL, Seizinger B, Oldfield EH. Radiologic screening for von Hippel-Lindau disease: the role of Gd-DTPA enhanced MR imaging of the CNS. *J Compt Assist Tomogr* 1989;743-55.
23. Lee SR, Sanches J, Mark AS, Dillon WP, Norman D, Newton TH. Posterior fossa hemangioblastomas: MR imaging. *Radiology* 1989;171:463-8.
24. Neumann HP, Eggert HR, Scheremet R, Schumacher M, Mohadjer M, Wakhloo AK, Volk B, Hettmansperger U, Riegler P, Schollmeyer P. Central nervous system lesions in von Hippel-Lindau syndrome. *J Neurol Neurosurg Psychiatry* 1992;55:898-901.
25. Maher ER, Iselius L, Yates JR, Littler M, Benjamin C, Harris R, Sampson J, Williams A, Ferguson-Smith MA, Morton N. Von Hippel-Lindau disease: a genetic study. *J Med Genet* 1991;28:443-7.
26. Maher ER, Yates JR, Harries R, Benjamin C, Harris R, Moore AT, Ferguson-Smith MA. Clinical features and natural history of von Hippel-Lindau disease. *Q J Med* 1990;77:1151-63.
27. Maher ER, Kaelin WG Jr. Von Hippel-Lindau disease. *Medicine (Baltimore)* 1997;76:381-91.
28. Chen F, Kishida T, Yao M, Hustad T, Glavac D, Dean M, Gnarr JR, Orcutt ML, Duh FM, Glenn G. Germline mutations in the von Hippel-Lindau disease tumor suppressor gene: correlations with phenotype. *Hum Mutat* 1995;5:66-75.
29. Maher ER, Webster AR, Richards FM, Green JS, Crossey PA, Payne SJ, Moore AT. Phenotypic expression in von Hippel-Lindau disease: correlations with germline VHL gene mutations. *J Med Genet* 1996;33:328-32.
30. Zbar B, Kishida T, Chen F, Schmidt L, Maher ER, Richards FM, Crossey PA, Webster AR, Affara NA, Ferguson-Smith MA, Brauch H, Glavac D, Neumann HP, Tisherman S, Mulvihill JJ, Gross DJ, Shuin T, Whaley J, Seizinger B, Kley N, Olschwang S, Boisson C, Richard S, Lips CH, Lerman M. Germline mutations in the Von Hippel-Lindau disease (VHL) gene in families from North America, Europe, and Japan. *Hum Mutat* 1996;8:348-57.
31. Crossey PA, Richards FM, Foster K, Green JS, Prowse A, Latif F, Lerman MI, Zbar B, Affara NA, Ferguson-Smith MA. Identification of intragenic mutations in the von Hippel-Lindau disease tumour suppressor gene and correlation with disease phenotype. *Hum Mol Genet* 1994;3:1303-8.
32. Neumann HP, Bender BU. Genotype-phenotype correlations in von Hippel-Lindau disease. *J Intern Med* 1998;243:541-5.
33. Hes F, Zewald R, Peeters T, Sijmons R, Links T, Verheij J, Matthijs G, Leguis E, Mortier G, van der TK, Rosman M, Lips C, Pearson P, van der LR. Genotype-phenotype correlations in families with deletions in the von Hippel-Lindau (VHL) gene. *Hum Genet* 2000;106:425-31.
34. Hes FJ, Hoppener JW, van der Luijt RB, Lips CJM. [De ziekte van Von Hippel-Lindau]. *Ned Tijdschr Oncol* 2005;2:83-90.
35. Glasker S, Bender BU, Apel TW, Natt E, van Velthoven V, Scheremet R, Zentner J, Neumann HP. The impact of molecular genetic analysis of the VHL gene in patients with haemangioblastomas of the central nervous system. *J Neurol Neurosurg Psychiatry* 1999;67:758-62.

36. Olschwang S, Richard S, Boisson C, Giraud S, Laurent-Puig P, Resche F, Thomas G. Germline mutation profile of the VHL gene in von Hippel-Lindau disease and in sporadic hemangioblastoma. *Hum Mutat* 1998;12:424-30.
37. Hes FJ, McKee S, Taphoorn MJ, Rehal P, Der Luijt RB, McMahon R, Der Smagt JJ, Dow D, Zewald RA, Whittaker J, Lips CJ, MacDonald F, Pearson PL, Maher ER. Cryptic von Hippel-Lindau disease: germline mutations in patients with haemangioblastoma only. *J Med Genet* 2000;37:939-43.
38. Oberstrass J, Reifenberger G, Reifenberger J, Wechsler W, Collins VP. Mutation of the Von Hippel-Lindau tumour suppressor gene in capillary haemangioblastomas of the central nervous system. *J Pathol* 1996;179:151-6.
39. Hes FJ, Hoppener JW, Lips CJ. Clinical review 155: Pheochromocytoma in Von Hippel-Lindau disease. *J Clin Endocrinol Metab* 2003;88:969-74.
40. Conway JE, Chou D, Clatterbuck RE, Brem H, Long DM, Rigamonti D. Hemangioblastomas of the central nervous system in von Hippel-Lindau syndrome and sporadic disease. *Neurosurgery* 2001;48:55-62.
41. Weil RJ, Lonser RR, DeVroom HL, Wanebo JE, Oldfield EH. Surgical management of brainstem hemangioblastomas in patients with von Hippel-Lindau disease. *J Neurosurg* 2003;98:95-105.
42. Niemela M, Lim YJ, Soderman M, Jaaskelainen J, Lindquist C. Gamma knife radiosurgery in 11 hemangioblastomas. *J Neurosurg* 1996;85:591-6.
43. Jawahar A, Kondziolka D, Garces YI, Flickinger JC, Pollock BE, Lunsford LD. Stereotactic radiosurgery for hemangioblastomas of the brain. *Acta Neurochir (Wien)* 2000;142:641-4.
44. Chang SD, Meisel JA, Hancock SL, Martin DP, McManus M, Adler JR. Treatment of hemangioblastomas in von Hippel-Lindau disease with linear accelerator-based radiosurgery. *Neurosurgery* 1998;43:28-34.
45. Bohling T, Plate KH, Haltia MJ, Alitalo K, Neumann HP. Von Hippel-Lindau disease and capillary hemangioblastoma. In: Kleihues P, Cavenee WK, eds. Lyon: IARC Press, 2000: 223-6.
46. Vortmeyer AO, Gnarr JR, Emmert-Buck MR, Katz D, Linehan WM, Oldfield EH, Zhuang Z. von Hippel-Lindau gene deletion detected in the stromal cell component of a cerebellar hemangioblastoma associated with von Hippel-Lindau disease. *Hum Pathol* 1997;28:540-3.
47. Stratmann R, Krieg M, Haas R, Plate KH. Putative control of angiogenesis in hemangioblastomas by the von Hippel-Lindau tumor suppressor gene. *J Neuropathol Exp Neurol* 1997;56:1242-52.
48. Reifenberger G, Reifenberger J, Bilzer T, Wechsler W, Collins VP. Coexpression of transforming growth factor-alpha and epidermal growth factor receptor in capillary hemangioblastomas of the central nervous system. *Am J Pathol* 1995;147:245-50.
49. Ho KL. Ultrastructure of cerebellar capillary hemangioblastoma. IV. Pericytes and their relationship to endothelial cells. *Acta Neuropathol (Berl)* 1985;67:254-64.
50. Lindau A. Discussion on vascular tumours of the brain and spinal cord. *Proc R Soc Med* 1931;24:363-70.
51. Chaudhry AP, Montes M, Cohn GA. Ultrastructure of cerebellar hemangioblastoma. *Cancer* 1978;42:1834-50.
52. Spence AM, Rubinstein LJ. Cerebellar capillary hemangioblastoma: its histogenesis studied by organ culture and electron microscopy. *Cancer* 1975;35:326-41.
53. Frank TS, Trojanowski JO, Roberts SA, Brooks JJ. A detailed immunohistochemical analysis of cerebellar hemangioblastoma: an undifferentiated mesenchymal tumor. *Mod Pathol* 1989;2: 638-51.

54. Kepes JJ, Rengachary SS, Lee SH. Astrocytes in hemangioblastomas of the central nervous system and their relationship to stromal cells. *Acta Neuropathol (Berl)* 1979;47:99-104.
55. Kamitani H, Masuzawa H, Sato J, Kanazawa I. Capillary hemangioblastoma: histogenesis of stromal cells. *Acta Neuropathol (Berl)* 1987;73:370-8.
56. Nemes Z. Fibrohistiocytic differentiation in capillary hemangioblastoma. *Hum Pathol* 1992;23:805-10.
57. Becker I, Paulus W, Roggendorf W. Histogenesis of stromal cells in cerebellar hemangioblastomas. An immunohistochemical study. *Am J Pathol* 1989;134:271-5.
58. Vortmeyer AO, Frank S, Jeong SY, Yuan K, Ikejiri B, Lee YS, Bhowmick D, Lonser RR, Smith R, Rodgers G, Oldfield EH, Zhuang Z. Developmental arrest of angioblastic lineage initiates tumorigenesis in von Hippel-Lindau disease. *Cancer Res* 2003;63:7051-5.
59. Vortmeyer AO, Yuan Q, Lee YS, Zhuang Z, Oldfield EH. Developmental effects of von Hippel-Lindau gene deficiency. *Ann Neurol* 2004;55:721-8.
60. Latif F, Tory K, Gnarr J, Yao M, Duh FM, Orcutt ML, Stackhouse T, Kuzmin I, Modi W, Geil L. Identification of the von Hippel-Lindau disease tumor suppressor gene. *Science* 1993;260:1317-20.
61. Glasker S, Bender BU, Apel TW, van Velthoven V, Mulligan LM, Zentner J, Neumann HP. Reconsideration of biallelic inactivation of the VHL tumour suppressor gene in hemangioblastomas of the central nervous system. *J Neurol Neurosurg Psychiatry* 2001;70:644-8.
62. Stolle C, Glenn G, Zbar B, Humphrey JS, Choyke P, Walther M, Pack S, Hurley K, Andrey C, Klausner R, Linehan WM. Improved detection of germline mutations in the von Hippel-Lindau disease tumor suppressor gene. *Hum Mutat* 1998;12:417-23.
63. Richards FM, Webster AR, McMahon R, Woodward ER, Rose S, Maher ER. Molecular genetic analysis of von Hippel-Lindau disease. *J Intern Med* 1998;243:527-33.
64. Kaelin WG Jr. Molecular basis of the VHL hereditary cancer syndrome. *Nat Rev Cancer* 2002;2:673-82.
65. Webster AR, Richards FM, MacRonal FE, Moore AT, Maher ER. An analysis of phenotypic variation in the familial cancer syndrome von Hippel-Lindau disease: evidence for modifier effects. *Am J Hum Genet* 1998;63:1025-35.
66. Knudson AG. Mutation and cancer: statistical study of retinoblastoma. *Proc Natl Acad Sci USA* 1971;68:820-3.
67. Prowse AH, Webster AR, Richards FM, Richard S, Olschwang S, Resche F, Affara NA, Maher ER. Somatic inactivation of the VHL gene in Von Hippel-Lindau disease tumors. *Am J Hum Genet* 1997;60:765-71.
68. Crossey PA, Foster K, Richards FM, Phipps ME, Latif F, Tory K, Jones MH, Bentley E, Kumar R, Lerman MI. Molecular genetic investigations of the mechanism of tumourigenesis in von Hippel-Lindau disease: analysis of allele loss in VHL tumours. *Hum Genet* 1994;93:53-8.
69. Shuin T, Kondo K, Torigoe S, Kishida T, Kubota Y, Hosaka M, Nagashima Y, Kitamura H, Latif F, Zbar B. Frequent somatic mutations and loss of heterozygosity of the von Hippel-Lindau tumor suppressor gene in primary human renal cell carcinomas. *Cancer Res* 1994;54:2852-5.
70. Foster K, Prowse A, van den BA, Fleming S, Hulsbeek MM, Crossey PA, Richards FM, Cairns P, Affara NA, Ferguson-Smith MA. Somatic mutations of the von Hippel-Lindau disease tumour suppressor gene in non-familial clear cell renal carcinoma. *Hum Mol Genet* 1994;3:2169-73.

71. Gnarr JR, Tory K, Weng Y, Schmidt L, Wei MH, Li H, Latif F, Liu S, Chen F, Duh FM. Mutations of the VHL tumour suppressor gene in renal carcinoma. *Nat Genet* 1994;7:85-90.
72. Herman JG, Latif F, Weng Y, Lerman MI, Zbar B, Liu S, Samid D, Duan DS, Gnarr JR, Linehan WM. Silencing of the VHL tumor-suppressor gene by DNA methylation in renal carcinoma. *Proc Natl Acad Sci USA* 1994;91:9700-4.
73. Clifford SC, Prowse AH, Affara NA, Buys CH, Maher ER. Inactivation of the von Hippel-Lindau (VHL) tumour suppressor gene and allelic losses at chromosome arm 3p in primary renal cell carcinoma: evidence for a VHL-independent pathway in clear cell renal tumourigenesis. *Genes Chromosomes Cancer* 1998;22:200-9.
74. Hamano K, Esumi M, Igarashi H, Chino K, Mochida J, Ishida AH, Okada K. Biallelic inactivation of the von Hippel-Lindau tumor suppressor gene in sporadic renal cell carcinoma. *J Urol* 2002;167:713-7.
75. Kanno H, Kondo K, Ito S, Yamamoto I, Fujii S, Torigoe S, Sakai N, Hosaka M, Shuin T, Yao M. Somatic mutations of the von Hippel-Lindau tumor suppressor gene in sporadic central nervous system hemangioblastomas. *Cancer Res* 1994;54:4845-7.
76. Lee JY, Dong SM, Park WS, Yoo NJ, Kim CS, Jang JJ, Chi JG, Zbar B, Lubensky IA, Linehan WM, Vortmeyer AO, Zhuang Z. Loss of heterozygosity and somatic mutations of the VHL tumor suppressor gene in sporadic cerebellar hemangioblastomas. *Cancer Res* 1998;58:504-8.
77. Tse JY, Wong JH, Lo KW, Poon WS, Huang DP, Ng HK. Molecular genetic analysis of the von Hippel-Lindau disease tumor suppressor gene in familial and sporadic cerebellar hemangioblastomas. *Am J Clin Pathol* 1997;107:459-66.
78. Bender BU, Gutsche M, Glasker S, Muller B, Kirste G, Eng C, Neumann HP. Differential genetic alterations in von Hippel-Lindau syndrome-associated and sporadic pheochromocytomas. *J Clin Endocrinol Metab* 2000;85:4568-74.
79. Martinez A, Fullwood P, Kondo K, Kishida T, Yao M, Maher ER, Latif F. Role of chromosome 3p12-p21 tumour suppressor genes in clear cell renal cell carcinoma: analysis of VHL dependent and VHL independent pathways of tumorigenesis. *Mol Pathol* 2000;53:137-44.
80. Alimov A, Kost-Alimova M, Liu J, Li C, Bergerheim U, Imreh S, Klein G, Zabarovsky ER. Combined LOH/CGH analysis proves the existence of interstitial 3p deletions in renal cell carcinoma. *Oncogene* 2000;19:1392-9.
81. Bissig H, Richter J, Desper R, Meier V, Schraml P, Schaffer AA, Sauter G, Mihatsch MJ, Moch H. Evaluation of the clonal relationship between primary and metastatic renal cell carcinoma by comparative genomic hybridization. *Am J Pathol* 1999;155:267-74.
82. Gronwald J, Storkel S, Holtgreve-Grez H, Hadaczek P, Brinkschmidt C, Jauch A, Lubinski J, Cremer T. Comparison of DNA gains and losses in primary renal clear cell carcinomas and metastatic sites: importance of 1q and 3p copy number changes in metastatic events. *Cancer Res* 1997;57:481-7.
83. Gunawan B, Huber W, Holtrup M, von Heydebreck A, Efferth T, Poustka A, Ringert RH, Jakse G, Fuzesi L. Prognostic impacts of cytogenetic findings in clear cell renal cell carcinoma: gain of 5q31-qter predicts a distinct clinical phenotype with favorable prognosis. *Cancer Res* 2001;61:7731-8.
84. Junker K, Weirich G, Amin MB, Moravek P, Hindermann W, Schubert J. Genetic subtyping of renal cell carcinoma by comparative genomic hybridization. *Recent Results Cancer Res* 2003;162:169-75.

85. Moch H, Presti JC, Jr., Sauter G, Buchholz N, Jordan P, Mihatsch MJ, Waldman FM. Genetic aberrations detected by comparative genomic hybridization are associated with clinical outcome in renal cell carcinoma. *Cancer Res* 1996;56:27-30.
86. Pavlovich CP, Padilla-Nash H, Wangsa D, Nickerson ML, Matrosova V, Linehan WM, Ried T, Phillips JL. Patterns of aneuploidy in stage IV clear cell renal cell carcinoma revealed by comparative genomic hybridization and spectral karyotyping. *Genes Chromosomes Cancer* 2003;37:252-60.
87. Presti JC, Jr., Wilhelm M, Reuter V, Russo P, Motzer R, Waldman F. Allelic loss on chromosomes 8 and 9 correlates with clinical outcome in locally advanced clear cell carcinoma of the kidney. *J Urol* 2002;167:1464-8.
88. Phillips JL, Ghadimi BM, Wangsa D, Padilla-Nash H, Worrell R, Hewitt S, Walther M, Linehan WM, Klausner RD, Ried T. Molecular cytogenetic characterization of early and late renal cell carcinomas in von Hippel-Lindau disease. *Genes Chromosomes Cancer* 2001;31:1-9.
89. Edstrom E, Mahlamaki E, Bord B, Kjellman M, Karhu R, Hoog A, Goncharov N, Tean Teh B, Backdahl M, Larsson C. Comparative genomic hybridization reveals frequent losses of chromosomes 1p and 3q in pheochromocytomas and abdominal paragangliomas, suggesting a common genetic etiology. *Am J Pathol* 2000;156:651-9.
90. Lui WO, Chen J, Glasker S, Bender BU, Madura C, Khoo SK, Kort E, Larsson C, Neumann HP, Teh BT. Selective loss of chromosome 11 in pheochromocytomas associated with the VHL syndrome. *Oncogene* 2002;21:1117-22.
91. Decker HJ, Klauk SM, Lawrence JB, McNeil J, Smith D, Gemmill RM, Sandberg AA, Neumann HH, Simon B, Green J. Cytogenetic and fluorescence in situ hybridization studies on sporadic and hereditary tumors associated with von Hippel-Lindau syndrome (VHL). *Cancer Genet Cytogenet* 1994;77:1-13.
92. Jordan DK, Patil SR, Divelbiss JE, Vemuganti S, Headley C, Waziri MH, Gurll NJ. Cytogenetic abnormalities in tumors of patients with von Hippel-Lindau disease. *Cancer Genet Cytogenet* 1989;42:227-41.
93. Kim W, Kaelin WG Jr. The von Hippel-Lindau tumor suppressor protein: new insights into oxygen sensing and cancer. *Curr Opin Genet Dev* 2003;13:55-60.
94. Kibel A, Iliopoulos O, DeCaprio JA, Kaelin WG Jr. Binding of the von Hippel-Lindau tumor suppressor protein to Elongin B and C. *Science* 1995;269:1444-6.
95. Stebbins CE, Kaelin WG Jr., Pavletich NP. Structure of the VHL-ElonginC-ElonginB complex: implications for VHL tumor suppressor function. *Science* 1999;284:455-61.
96. Pause A, Lee S, Worrell RA, Chen DY, Burgess WH, Linehan WM, Klausner RD. The von Hippel-Lindau tumor-suppressor gene product forms a stable complex with human CUL-2, a member of the Cdc53 family of proteins. *Proc Natl Acad Sci USA* 1997;94:2156-61.
97. Maxwell PH, Wiesener MS, Chang GW, Clifford SC, Vaux EC, Cockman ME, Wykoff CC, Pugh CW, Maher ER, Ratcliffe PJ. The tumour suppressor protein VHL targets hypoxia-inducible factors for oxygen-dependent proteolysis. *Nature* 1999;399:271-5.
98. Iliopoulos O, Levy AP, Jiang C, Kaelin WG Jr., Goldberg MA. Negative regulation of hypoxia-inducible genes by the von Hippel-Lindau protein. *Proc Natl Acad Sci USA* 1996;93:10595-9.
99. Flamme I, Krieg M, Plate KH. Up-regulation of vascular endothelial growth factor in stromal cells of hemangioblastomas is correlated with up-regulation of the transcription factor HRF/HIF-2alpha. *Am J Pathol* 1998;153:25-9.

100. Ivanov S, Liao SY, Ivanova A, Danilkovitch-Miagkova A, Tarasova N, Weirich G, Merrill MJ, Proescholdt MA, Oldfield EH, Lee J, Zavada J, Waheed A, Sly W, Lerman MI, Stanbridge EJ. Expression of hypoxia-inducible cell-surface transmembrane carbonic anhydrases in human cancer. *Am J Pathol* 2001;158:905-19.
101. Wiesener MS, Munchenhagen PM, Berger I, Morgan NV, Roigas J, Schwartz A, Jurgensen JS, Gruber G, Maxwell PH, Loning SA, Frei U, Maher ER, Grone HJ, Eckardt KU. Constitutive activation of hypoxia-inducible genes related to overexpression of hypoxia-inducible factor-1alpha in clear cell renal carcinomas. *Cancer Res* 2001;61:5215-22.
102. Los M, Zeamari S, Foekens JA, Gebbink MF, Voest EE. Regulation of the urokinase-type plasminogen activator system by the von Hippel-Lindau tumor suppressor gene. *Cancer Res* 1999;59:4440-5.
103. Wizigmann-Voos S, Breier G, Risau W, Plate KH. Up-regulation of vascular endothelial growth factor and its receptors in von Hippel-Lindau disease-associated and sporadic hemangioblastomas. *Cancer Res* 1995;55:1358-64.
104. Krieg M, Marti HH, Plate KH. Coexpression of erythropoietin and vascular endothelial growth factor in nervous system tumors associated with von Hippel-Lindau tumor suppressor gene loss of function. *Blood* 1998;92:3388-93.
105. Bohling T, Hatva E, Kujala M, Claesson-Welsh L, Alitalo K, Haltia M. Expression of growth factors and growth factor receptors in capillary hemangioblastoma. *J Neuropathol Exp Neurol* 1996;55:522-7.
106. Zagzag D, Zhong H, Scalzitti JM, Laughner E, Simons JW, Semenza GL. Expression of hypoxia-inducible factor 1alpha in brain tumors: association with angiogenesis, invasion, and progression. *Cancer* 2000;88:2606-18.
107. Cornford EM, Hyman S, Black KL, Cornford ME, Vinters HV, Pardridge WM. High expression of the Glut1 glucose transporter in human brain hemangioblastoma endothelium. *J Neuropathol Exp Neurol* 1995;54:842-51.
108. Hatva E, Bohling T, Jaaskelainen J, Persico MG, Haltia M, Alitalo K. Vascular growth factors and receptors in capillary hemangioblastomas and hemangiopericytomas. *Am J Pathol* 1996;148:763-75.
109. Benjamin LE, Hemo I, Keshet E. A plasticity window for blood vessel remodelling is defined by pericyte coverage of the preformed endothelial network and is regulated by PDGF- B and VEGF. *Development* 1998;125:1591-8.
110. Mandriota SJ, Turner KJ, Davies DR, Murray PG, Morgan NV, Sowter HM, Wykoff CC, Maher ER, Harris AL, Ratcliffe PJ, Maxwell PH. HIF activation identifies early lesions in VHL kidneys: evidence for site-specific tumor suppressor function in the nephron. *Cancer Cell* 2002;1:459-68.
111. de Paulsen N, Brychzy A, Fournier MC, Klausner RD, Gnarr JR, Pause A, Lee S. Role of transforming growth factor-alpha in von Hippel-Lindau (VHL)(-/-) clear cell renal carcinoma cell proliferation: a possible mechanism coupling VHL tumor suppressor inactivation and tumorigenesis. *Proc Natl Acad Sci USA* 2001;98:1387-92.
112. Clifford SC, Cockman ME, Smallwood AC, Mole DR, Woodward ER, Maxwell PH, Ratcliffe PJ, Maher ER. Contrasting effects on HIF-1alpha regulation by disease-causing pVHL mutations correlate with patterns of tumorigenesis in von Hippel-Lindau disease. *Hum Mol Genet* 2001;10:1029-38.

113. Ohh M, Yauch RL, Lonergan KM, Whaley JM, Stemmer-Rachamimov AO, Louis DN, Gavin BJ, Kley N, Kaelin WG, Jr, Iliopoulos O. The von Hippel-Lindau tumor suppressor protein is required for proper assembly of an extracellular fibronectin matrix. *Mol Cell* 1998;1:959-68.
114. Okuda H, Saitoh K, Hirai S, Iwai K, Takaki Y, Baba M, Minato N, Ohno S, Shuin T. The von Hippel-Lindau tumor suppressor protein mediates ubiquitination of activated atypical protein kinase C. *J Biol Chem* 2001;276:43611-7.
115. Knebelmann B, Ananth S, Cohen HT, Sukhatme VP. Transforming growth factor alpha is a target for the von Hippel-Lindau tumor suppressor. *Cancer Res* 1998;58:226-31.
116. Hergovich A, Lisztwan J, Barry R, Ballschiemter P, Krek W. Regulation of microtubule stability by the von Hippel-Lindau tumour suppressor protein pVHL. *Nat Cell Biol* 2003;5:64-70.
117. Pause A, Lee S, Lonergan KM, Klausner RD. The von Hippel-Lindau tumor suppressor gene is required for cell cycle exit upon serum withdrawal. *Proc Natl Acad Sci USA* 1998;95:993-8.
118. Lieubeau-Teillet B, Rak J, Jothy S, Iliopoulos O, Kaelin W, Kerbel RS. von Hippel-Lindau gene-mediated growth suppression and induction of differentiation in renal cell carcinoma cells grown as multicellular tumor spheroids. *Cancer Res* 1998;58:4957-62.
119. Wykoff CC, Pugh CW, Maxwell PH, Harris AL, Ratcliffe PJ. Identification of novel hypoxia dependent and independent target genes of the von Hippel-Lindau (VHL) tumour suppressor by mRNA differential expression profiling. *Oncogene* 2000;19:6297-305.
120. Wykoff CC, Sotiriou C, Cockman ME, Ratcliffe PJ, Maxwell P, Liu E, Harris AL. Gene array of VHL mutation and hypoxia shows novel hypoxia-induced genes and that cyclin D1 is a VHL target gene. *Br J Cancer* 2004;90:1235-43.
121. Jiang Y, Zhang W, Kondo K, Klco JM, St MT, Dufault MR, Madden SL, Kaelin WG, Jr, Nacht M. Gene expression profiling in a renal cell carcinoma cell line: dissecting VHL and hypoxia-dependent pathways. *Mol Cancer Res* 2003;1:453-62.
122. Maina EN, Morris MR, Zatyka M, Raval RR, Banks RE, Richards FM, Johnson CM, Maher ER. Identification of novel VHL target genes and relationship to hypoxic response pathways. *Oncogene* 2005;24:4549-58.
123. Zatyka M, da Silva NF, Clifford SC, Morris MR, Wiesener MS, Eckardt KU, Houlston RS, Richards FM, Latif F, Maher ER. Identification of cyclin D1 and other novel targets for the von Hippel-Lindau tumor suppressor gene by expression array analysis and investigation of cyclin D1 genotype as a modifier in von Hippel-Lindau disease. *Cancer Res* 2002;62:3803-11.
124. Sherr CJ. D-type cyclins. *Trends Biochem Sci* 1995;20:187-90.
125. Donnellan R, Chetty R. Cyclin D1 and human neoplasia. *Mol Pathol* 1998;51:1-7.
126. Bindra RS, Vasselli JR, Stearman R, Linehan WM, Klausner RD. VHL-mediated hypoxia regulation of cyclin D1 in renal carcinoma cells. *Cancer Res* 2002;62:3014-9.
127. Baba M, Hirai S, Yamada-Okabe H, Hamada K, Tabuchi H, Kobayashi K, Kondo K, Yoshida M, Yamashita A, Kishida T, Nakaigawa N, Nagashima Y, Kubota Y, Yao M, Ohno S. Loss of von Hippel-Lindau protein causes cell density dependent deregulation of CyclinD1 expression through hypoxia-inducible factor. *Oncogene* 2003;22:2728-38.
128. Baba M, Hirai S, Kawakami S, Kishida T, Sakai N, Kaneko S, Yao M, Shuin T, Kubota Y, Hosaka M, Ohno S. Tumor suppressor protein VHL is induced at high cell density and mediates contact inhibition of cell growth. *Oncogene* 2001;20:2727-36.

129. Kong S, Amos CI, Luthra R, Lynch PM, Levin B, Frazier ML. Effects of cyclin D1 polymorphism on age of onset of hereditary nonpolyposis colorectal cancer. *Cancer Res* 2000;60:249-52.
130. Zheng Y, Shen H, Sturgis EM, Wang LE, Eicher SA, Strom SS, Frazier ML, Spitz MR, Wei Q. Cyclin D1 polymorphism and risk for squamous cell carcinoma of the head and neck: a case-control study. *Carcinogenesis* 2001;22:1195-9.
131. Porter TR, Richards FM, Houlston RS, Evans DG, Jankowski JA, MacDonald F, Norbury G, Payne SJ, Fisher SA, Tomlinson I, Maher ER. Contribution of cyclin d1 (CCND1) and E-cadherin (CDH1) polymorphisms to familial and sporadic colorectal cancer. *Oncogene* 2002;21:1928-33.
132. Wang L, Habuchi T, Mitsumori K, Li Z, Kamoto T, Kinoshita H, Tsuchiya N, Sato K, Ohyama C, Nakamura A, Ogawa O, Kato T. Increased risk of prostate cancer associated with AA genotype of cyclin D1 gene A870G polymorphism. *Int J Cancer* 2003;103:116-20.
133. Fabbro D, Parkinson D, Matter A. Protein tyrosine kinase inhibitors: new treatment modalities? *Curr Opin Pharmacol* 2002;2:374-81.
134. Yang JC, Haworth L, Sherry RM, Hwu P, Schwartzentruber DJ, Topalian SL, Steinberg SM, Chen HX, Rosenberg SA. A randomized trial of bevacizumab, an anti-vascular endothelial growth factor antibody, for metastatic renal cancer. *N Engl J Med* 2003;349:427-34.
135. Aiello LP, George DJ, Cahill MT, Wong JS, Cavallerano J, Hannah AL, Kaelin WG, Jr. Rapid and durable recovery of visual function in a patient with von hippel-lindau syndrome after systemic therapy with vascular endothelial growth factor receptor inhibitor su5416. *Ophthalmology* 2002;109:1745-51.
136. Richard S, Croisille L, Yvart J, Casadeval N, Eschwege P, Aghakhani N, David P, Gaudric A, Scigalla P, Hermine O. Paradoxical secondary polycythemia in von Hippel-Lindau patients treated with anti-vascular endothelial growth factor receptor therapy. *Blood* 2002;99:3851-3.
137. Rogers LR, Kaelin W, Nadler P, Shields A F, LoRusso P. Response of cerebellar hemangioblastomas associated with von Hippel-Lindau disease to OSI-774 (TarcevaTM). ASCO Annual Meeting, 2002. Abstract
138. Piribauer M, Czech T, Dieckmann K, Birner P, Hainfellner JA, Prayer D, Fazeny-Dorner B, Weinlander G, Marosi C. Stabilization of a progressive hemangioblastoma under treatment with thalidomide. *J Neurooncol* 2004;66:295-9.
139. Niemela M, Maenpaa H, Salven P, Summanen P, Poussa K, Laatikainen L, Jaaskelainen J, Joensuu H. Interferon alpha-2a therapy in 18 hemangioblastomas. *Clin Cancer Res* 2001;7:510-6.
140. George DJ, Kaelin WG Jr. The von Hippel-Lindau protein, vascular endothelial growth factor, and kidney cancer. *N Engl J Med* 2003;349:419-21.
141. Jeuken JW, von DA, Wesseling P. Molecular pathogenesis of oligodendroglial tumors. *J Neurooncol* 2004;70:161-81.
142. Jeuken JW, Sprenger SH, Wesseling P. Comparative genomic hybridization: practical guidelines. *Diagn Mol Pathol* 2002;11:193-203.
143. Solinas-Toldo S, Lampel S, Stilgenbauer S, Nickolenko J, Benner A, Dohner H, Cremer T, Lichter P. Matrix-based comparative genomic hybridization: biochips to screen for genomic imbalances. *Genes Chromosomes Cancer* 1997;20:399-407.
144. Mantripragada KK, Buckley PG, de Stahl TD, Dumanski JP. Genomic microarrays in the spotlight. *Trends Genet* 2004;20:87-94.

145. Ishkanian AS, Malloff CA, Watson SK, DeLeeuw RJ, Chi B, Coe BP, Snijders A, Albertson DG, Pinkel D, Marra MA, Ling V, MacAulay C, Lam WL. A tiling resolution DNA microarray with complete coverage of the human genome. *Nat Genet* 2004;36:299-303.
146. de Vries BB, Pfundt R, Leisink M, Koolen DA, Vissers LE, Janssen IM, Reijmersdal S, Nillesen WM, Huys EH, Leeuw N, Smeets D, Sistermans EA, Feuth T, van Ravenswaaij-Arts CM, van Kessel AG, Schoenmakers EF, Brunner HG, Veltman JA. Diagnostic genome profiling in mental retardation. *Am J Hum Genet* 2005;77:606-16.
147. Burger PC, Scheithauer BW. Tumors of the central nervous system. In: Atlas of tumor pathology. Washington DC: Armed forces institute of pathology, 1994.
148. McKusick VA. Mendel inheritance in man: a catalogue of human genes and genetic disorders. Baltimore & London: The John Hopkins University Press, 1994.
149. Duan DR, Pause A, Burgess WH, Aso T, Chen DY, Garrett KP, Conaway RC, Conaway JW, Linehan WM, Klausner RD. Inhibition of transcription elongation by the VHL tumor suppressor protein. *Science* 1995;269:1402-6.
150. Pause A, Peterson B, Schaffar G, Stearman R, Klausner RD. Studying interactions of four proteins in the yeast two-hybrid system: structural resemblance of the pVHL/elongin BC/hCUL-2 complex with the ubiquitin ligase complex SKP1/cullin/F-box protein. *Proc Natl Acad Sci USA* 1999;96:9533-8.
151. Kallioniemi A, Kallioniemi OP, Sudar D, Rutovitz D, Gray JW, Waldman F, Pinkel D. Comparative genomic hybridization for molecular cytogenetic analysis of solid tumors. *Science* 1992;258:818-21.
152. du Manoir S, Speicher MR, Joos S, Schrock E, Popp S, Dohner H, Kovacs G, Robert-Nicoud M, Lichter P, Cremer T. Detection of complete and partial chromosome gains and losses by comparative genomic in situ hybridization. *Hum Genet* 1993;90:590-610.
153. Jeuken JW, Sprenger SH, Wesseling P, Macville MV, von Deimling A, Teepen HL, van Overbeeke JJ, Boerman RH. Identification of subgroups of high-grade oligodendroglial tumors by comparative genomic hybridization. *J Neuropathol Exp Neurol* 1999;58:606-12.
154. Miller SA, Dykes DD, Polesky HF. A simple salting out procedure for extracting DNA from human nucleated cells. *Nucleic Acids Res* 1988;16:1215.
155. Schraml P, Zhaou M, Richter J, Bruning T, Pommer M, Sauter G, Mihatsch MJ, Moch H. [Analysis of kidney tumors in trichloroethylene exposed workers by comparative genomic hybridization and DNA sequence analysis]. *Verh Dtsch Ges Pathol* 1999;83:218-24.
156. Knuutila S, Aalto Y, Autio K, Bjorkqvist AM, El Rifai W, Hemmer S, Huhta T, Kettunen E, Kiuru-Kuhlefelt S, Larramendy ML, Lushnikova T, Monni O, Pere H, Tapper J, Tarkkanen M, Varis A, Wasenius VM, Wolf M, Zhu Y. DNA copy number losses in human neoplasms. *Am J Pathol* 1999;155:683-94.
157. Bohling T, Turunen O, Jaaskelainen J, Carpen O, Sainio M, Wahlstrom T, Vaheri A, Haltia M. Ezrin expression in stromal cells of capillary hemangioblastoma. An immunohistochemical survey of brain tumors. *Am J Pathol* 1996;148:367-73.
158. Knuutila S, Bjorkqvist AM, Autio K, Tarkkanen M, Wolf M, Monni O, Szymanska J, Larramendy ML, Tapper J, Pere H, el-Rifai W, Hemmer S, Wasenius VM, Vidgren V, Zhu Y. DNA copy number amplifications in human neoplasms: review of comparative genomic hybridization studies. *Am J Pathol* 1998;152:1107-23.

159. Ivan M, Kaelin WG Jr. The von Hippel-Lindau tumor suppressor protein. *Curr Opin Genet Dev* 2001;11:27-34.
160. Sprenger SH, Gijtenbeek JM, Wesseling P, Sciort R, van Calenbergh F, Lammens M, Jeuken JW. Characteristic chromosomal aberrations in sporadic cerebellar hemangioblastomas revealed by comparative genomic hybridization. *J Neurooncol* 2001;52:241-7.
161. Bodmer D, Eleveld MJ, Ligtenberg MJ, Weterman MA, Janssen BA, Smeets DF, de Wit PE, van den BA, van den BE, Koolen MI, Geurts VK. An alternative route for multistep tumorigenesis in a novel case of hereditary renal cell cancer and a t(2;3)(q35;q21) chromosome translocation. *Am J Hum Genet* 1998;62:1475-83.
162. Beroud C, Joly D, Gallou C, Staroz F, Orfanelli MT, Junien C. Software and database for the analysis of mutations in the VHL gene. *Nucleic Acids Res.* 1998;26:256-8.
163. Brachmann RK, Vidal M, Boeke JD. Dominant-negative p53 mutations selected in yeast hit cancer hot spots. *Proc Natl Acad Sci USA* 1996;93:4091-5.
164. Fero ML, Randel E, Gurley KE, Roberts JM, Kemp CJ. The murine gene p27Kip1 is haplo-insufficient for tumour suppression. *Nature* 1998;396: 177-80.
165. Foster K, Crossey PA, Cairns P, Hetherington JW, Richards FM, Jones MH, Bentley E, Affara NA, Ferguson-Smith MA, Maher ER. Molecular genetic investigation of sporadic renal cell carcinoma: analysis of allele loss on chromosomes 3p, 5q, 11p, 17 and 22. *Br J Cancer* 1994;69:230-4.
166. Shiratsuchi T, Nishimori H, Ichise H, Nakamura Y, Tokino T. Cloning and characterization of BAI2 and BAI3, novel genes homologous to brain-specific angiogenesis inhibitor 1 (BAI1). *Cytogenet Cell Genet* 1997;79:103-8.
167. Holash J, Maisonpierre PC, Compton D, Boland P, Alexander CR, Zagzag D, Yancopoulos GD, Wiegand SJ. Vessel cooption, regression, and growth in tumors mediated by angiopoietins and VEGF. *Science* 1999;284:1994-8.
168. Glasker S. Central nervous system manifestations in VHL: genetics, pathology and clinical phenotypic features. *Fam Cancer* 2005;4:37-42.
169. Gijtenbeek JM, Jacobs B, Sprenger SH, Eleveld MJ, van Kessel AG, Kros JM, Sciort R, van Calenbergh F, Wesseling P, Jeuken JW. Analysis of von hippel-lindau mutations with comparative genomic hybridization in sporadic and hereditary hemangioblastomas: possible genetic heterogeneity. *J Neurosurg* 2002;97:977-82.
170. Lemeta S, Aalto Y, Niemela M, Jaaskelainen J, Sainio M, Kere J, Knuutila S, Bohling T. Recurrent DNA sequence copy losses on chromosomal arm 6q in capillary hemangioblastoma. *Cancer Genet Cytogenet* 2002;133:174-8.
171. Lemeta S, Pylikkanen L, Sainio M, Niemela M, Saarikoski S, Husgafvel-Pursiainen K, Bohling T. Loss of heterozygosity at 6q is frequent and concurrent with 3p loss in sporadic and familial capillary hemangioblastomas. *J Neuropathol Exp Neurol* 2004;63:1072-9.
172. Vissers LE, de Vries BB, Osoegawa K, Janssen IM, Feuth T, Choy CO, Straatman H, van d, V, Huys EH, van RA, Smeets D, van Ravenswaaij-Arts CM, Knoers NV, van dB, I, de Jong PJ, Brunner HG, van Kessel AG, Schoenmakers EF, Veltman JA. Array-based comparative genomic hybridization for the genomewide detection of submicroscopic chromosomal abnormalities. *Am J Hum Genet* 2003;73:1261-70.
173. Vissers LE, Veltman JA, van Kessel AG, Brunner HG. Identification of disease genes by whole genome CGH arrays. *Hum Mol Genet* 2005;14 Spec No. 2:R215-R223.

174. Krzywinski M, Bosdet I, Smailus D, Chiu R, Mathewson C, Wye N, Barber S, Brown-John M, Chan S, Chand S, Cloutier A, Girn N, Lee D, Masson A, Mayo M, Olson T, Pandoh P, Prabhu AL, Schoenmakers E, Tsai M, Albertson D, Lam W, Choy CO, Osoegawa K, Zhao S, de Jong PJ, Schein J, Jones S, Marra MA. A set of BAC clones spanning the human genome. *Nucleic Acids Res* 2004;32:3651-60.
175. Veltman JA, Yntema HG, Lugtenberg D, Arts H, Briault S, Huys EH, Osoegawa K, de JP, Brunner HG, Geurts van KA, van BH, Schoenmakers EF. High resolution profiling of X chromosomal aberrations by array comparative genomic hybridisation. *J Med Genet* 2004;41:425-32.
176. Chen J, Lui WO, Vos MD, Clark GJ, Takahashi M, Schoumans J, Khoo SK, Petillo D, Lavery T, Sugimura J, Astuti D, Zhang C, Kagawa S, Maher ER, Larsson C, Alberts AS, Kanayama HO, Teh BT. The t(1;3) breakpoint-spanning genes LSAMP and NORE1 are involved in clear cell renal cell carcinomas. *Cancer Cell* 2003;4:405-13.
177. Ntougkos E, Rush R, Scott D, Frankenberg T, Gabra H, Smyth JF, Sellar GC. The IglON family in epithelial ovarian cancer: expression profiles and clinicopathologic correlates. *Clin Cancer Res* 2005;11:5764-8.
178. Kagan J, Stein J, Babaian RJ, Joe YS, Pisters LL, Glassman AB, von Eschenbach AC, Troncoso P. Homozygous deletions at 8p22 and 8p21 in prostate cancer implicate these regions as the sites for candidate tumor suppressor genes. *Oncogene* 1995;11:2121-6.
179. El-Naggar AK, Coombes MM, Batsakis JG, Hong WK, Goepfert H, Kagan J. Localization of chromosome 8p regions involved in early tumorigenesis of oral and laryngeal squamous carcinoma. *Oncogene* 1998;16:2983-7.
180. Anbazhagan R, Fujii H, Gabrielson E. Allelic loss of chromosomal arm 8p in breast cancer progression. *Am J Pathol* 1998;152:815-9.
181. Wagner U, Bubendorf L, Gasser TC, Moch H, Gorog JP, Richter J, Mihatsch MJ, Waldman FM, Sauter G. Chromosome 8p deletions are associated with invasive tumor growth in urinary bladder cancer. *Am J Pathol* 1997;151:753-9.
182. Ishii H, Baffa R, Numata SI, Murakumo Y, Rattan S, Inoue H, Mori M, Fidanza V, Alder H, Croce CM. The FEZ1 gene at chromosome 8p22 encodes a leucine-zipper protein, and its expression is altered in multiple human tumors. *Proc Natl Acad Sci USA* 1999;96:3928-33.
183. Nonaka D, Fabbri A, Roz L, Mariani L, Vecchione A, Moore GW, Tavecchio L, Croce CM, Sozzi G. Reduced FEZ1/LZTS1 expression and outcome prediction in lung cancer. *Cancer Res* 2005;65:1207-12.
184. Cabeza-Arvelaiz Y, Sepulveda JL, Lebovitz RM, Thompson TC, Chinault AC. Functional identification of LZTS1 as a candidate prostate tumor suppressor gene on human chromosome 8p22. *Oncogene* 2001;20:4169-79.
185. Vecchione A, Ishii H, Baldassarre G, Bassi P, Trapasso F, Alder H, Pagano F, Gomella LG, Croce CM, Baffa R. FEZ1/LZTS1 is down-regulated in high-grade bladder cancer, and its restoration suppresses tumorigenicity in transitional cell carcinoma cells. *Am J Pathol* 2002;160:1345-52.
186. Ishii H, Vecchione A, Murakumo Y, Baldassarre G, Numata S, Trapasso F, Alder H, Baffa R, Croce CM. FEZ1/LZTS1 gene at 8p22 suppresses cancer cell growth and regulates mitosis. *Proc Natl Acad Sci USA* 2001;98:10374-9.
187. Vecchione A, Ishii H, Shiao YH, Trapasso F, Rugge M, Tamburrino JF, Murakumo Y, Alder H, Croce CM, Baffa R. FEZ1/LZTS1 alterations in gastric carcinoma. *Clin Cancer Res* 2001;7:1546-52.

188. Fan Y, Newman T, Linardopoulou E, Trask JB. Gene content and function of the ancestral chromosome fusion site in human chromosome 2q13-2q14.1 and paralogous regions. *Genome Res* 2002;12:1663-1672.
189. Wong A, Vallender EJ, Heretis K, Ilkin Y, Lahn BT, Lese Martin C, Ledbetter DH. Diverse fates of paralogs following segmental duplication of telomeric genes. *Genomics* 2004;84:239-247.
190. Carlsson P, Mahlapuu M. Forkhead transcription factors: key players in development and metabolism. *Dev Biol* 2002;250:1-23.
191. Katoh M, Katoh M. Human FOX gene family (Review). *Int J Oncol* 2004;25:1495-500.
192. Cheng KW, Lahad JP, Gray JW, Mills GB. Emerging role of RAB GTPases in cancer and human disease. *Cancer Res* 2005;65:2516-9.
193. Yoon SO, Shin S, Mercurio AM. Hypoxia stimulates carcinoma invasion by stabilizing microtubules and promoting the Rab11 trafficking of the alpha6beta4 integrin. *Cancer Res* 2005;65:2761-9.
194. Ehtesham M, Kabos P, Yong WH, Schievink WI, Black KL, Yu JS. Development of an intracranial ependymoma at the site of a pre-existing cavernous malformation. *Surg Neurol* 2003;60:80-2.
195. Betticher DC, Thatcher N, Altermatt HJ, Hoban P, Ryder WD, Heighway J. Alternate splicing produces a novel cyclin D1 transcript. *Oncogene* 1995;11:1005-11.
196. Simpson DJ, Fryer AA, Grossman AB, Wass JA, Pfeifer M, Kros JM, Clayton RN, Farrell WE. Cyclin D1 (CCND1) genotype is associated with tumour grade in sporadic pituitary adenomas. *Carcinogenesis* 2001;22:1801-7.
197. Holley SL, Parkes G, Matthias C, Bockmuhl U, Jahnke V, Leder K, Strange RC, Fryer AA, Hoban PR. Cyclin D1 polymorphism and expression in patients with squamous cell carcinoma of the head and neck. *Am J Pathol* 2001;159:1917-24.
198. Holland TA, Elder J, McCloud JM, Hall C, Deakin M, Fryer AA, Elder JB, Hoban PR. Subcellular localisation of cyclin D1 protein in colorectal tumours is associated with p21(WAF1/CIP1) expression and correlates with patient survival. *Int J Cancer* 2001;95:302-6.
199. Diehl JA, Cheng M, Roussel MF, Sherr CJ. Glycogen synthase kinase-3beta regulates cyclin D1 proteolysis and subcellular localization. *Genes Dev* 1998;12:3499-511.
200. Wait SD, Vortmeyer AO, Lonser RR, Chang DT, Finn MA, Bhowmick DA, Pack SD, Oldfield EH, Zhuang Z. Somatic mutations in VHL germline deletion kindred correlate with mild phenotype. *Ann Neurol* 2004;55:236-40.
201. Gohring B, Holzhausen HJ, Meye A, Heynemann H, Rebmann U, Langner J, Riemann D. Endopeptidase 24.11/CD10 is down-regulated in renal cell cancer. *Int J Mol Med* 1998;2:409-14.
202. Klauck SM, Yamakawa K, Seizinger BR. Dinucleotide repeat polymorphism at the D3S666 locus. *Hum Mol Genet* 1994;3:840.
203. Grabmaier K, Vissers JL, De Weijert MC, Oosterwijk-Wakka JC, Van Bokhoven A, Brakenhoff RH, Noessner E, Mulders PA, Merx G, Figdor CG, Adema GJ, Oosterwijk E. Molecular cloning and immunogenicity of renal cell carcinoma-associated antigen G250. *Int J Cancer* 2000;85:865-70.
204. Schlingemann RO, Oosterwijk E, Wesseling P, Rietveld FJ, Ruiter DJ. Aminopeptidase a is a constituent of activated pericytes in angiogenesis. *J Pathol* 1996;179:436-42.
205. Zhao J, Moch H, Scheidweiler AF, Baer A, Schaffer AA, Speel EJ, Roth J, Heitz PU, Komminoth P. Genomic imbalances in the progression of endocrine pancreatic tumors. *Genes Chromosomes Cancer* 2001;32:364-72.

206. van Dijk J, Oosterwijk E, van Kroonenburgh MJ, Jonas U, Fleuren GJ, Pauwels EK, Warnaar SO. Perfusion of tumor-bearing kidneys as a model for scintigraphic screening of monoclonal antibodies. *J Nucl Med* 1988;29:1078-82.
207. Salisbury JR. Three-dimensional reconstruction in microscopical morphology. *Histol Histopathol* 1994;9:773-80.
208. Malkusch W, Konerding MA, Klaphthor B, Bruch J. A simple and accurate method for 3-D measurements in microcorrosion casts illustrated with tumour vascularization. *Anal Cell Pathol* 1995;9:69-81.
209. Foreman DM, Bagley S, Moore J, Ireland GW, McLeod D, Boulton ME. Three dimensional analysis of the retinal vasculature using immunofluorescent staining and confocal laser scanning microscopy. *Br J Ophthalmol* 1996;80:246-51.
210. Kay PA, Robb RA, Bostwick DG. Prostate cancer microvessels: a novel method for three-dimensional reconstruction and analysis. *Prostate* 1998;37:270-7.
211. Duerstock BS, Bajaj CL, Pascucci V, Schikore D, Lin KN, Borgens RB. Advances in three-dimensional reconstruction of the experimental spinal cord injury. *Comput Med Imaging Graph* 2000;24:389-406.
212. Antiga L, Ene-Iordache B, Remuzzi G, Remuzzi A. Automatic generation of glomerular capillary topological organization. *Microvasc Res* 2001;62:346-54.
213. Brey EM, King TW, Johnston C, McIntire LV, Reece GP, Patrick CW Jr. A technique for quantitative three-dimensional analysis of microvascular structure. *Microvasc Res* 2002;63:279-94.
214. Ohtake T, Abe R, Kimijima I, Fukushima T, Tsuchiya A, Hoshi K, Wakasa H. Intraductal extension of primary invasive breast carcinoma treated by breast-conservative surgery. Computer graphic three-dimensional reconstruction of the mammary duct-lobular systems. *Cancer* 1995;76:32-45.
215. Perez-Atayde AR, Sallan SE, Tedrow U, Connors S, Allred E, Folkman J. Spectrum of tumor angiogenesis in the bone marrow of children with acute lymphoblastic leukemia. *Am J Pathol* 1997;150:815-21.
216. Salisbury JR, Deverell MH, Seaton JM, Cookson MJ. Three-dimensional reconstruction of non-Hodgkin's lymphoma in bone marrow trephines. *J Pathol* 1997;181:451-4.
217. Carmeliet P, Jain RK. Angiogenesis in cancer and other diseases. *Nature* 2000;407:249-57.
218. Weidner N. Intratumor microvessel density as a prognostic factor in cancer. *Am J Pathol* 1995;147:9-19.
219. Konerding MA, Malkusch W, Klaphthor B, van AC, Fait E, Hill SA, Parkins C, Chaplin DJ, Presta M, Denekamp J. Evidence for characteristic vascular patterns in solid tumours: quantitative studies using corrosion casts. *Br J Cancer* 1999;80:724-32.
220. Hossler FE, Douglas JE. Vascular Corrosion Casting: Review of Advantages and Limitations in the Application of Some Simple Quantitative Methods. *Microsc Microanal* 2001;7:253-64.
221. Serra J. *Image Analysis and mathematical Morphology*. London: Academic Press, 1982.
222. Kleihues P, Burger PC, Collins VP, Newcomb EW, Ohgaki H, Cavenee WK. Glioblastoma. In: Kleihues P, Cavenee WK, eds. *Lyon: IARC Press*, 2000: 29-39.
223. Wesseling P, van der Laak JA, Link M, Teepen HL, Ruiters DJ. Quantitative analysis of microvascular changes in diffuse astrocytic neoplasms with increasing grade of malignancy. *Hum Pathol* 1998;29:352-8.
224. Weninger WJ, Mohun T. Phenotyping transgenic embryos: a rapid 3-D screening method based on episcopic fluorescence image capturing. *Nat Genet* 2002;30:59-65.

225. Rydmark M, Jansson T, Berthold CH, Gustavsson T. Computer-assisted realignment of light micrograph images from consecutive section series of cat cerebral cortex. *J Microsc* 1992;165 (Pt 1):29-47.
226. Wesseling P, Schlingemann RO, Rietveld FJ, Link M, Burger PC, Ruiter DJ. Early and extensive contribution of pericytes/vascular smooth muscle cells to microvascular proliferation in glioblastoma multiforme: an immuno-light and immuno-electron microscopic study. *J Neuropathol Exp Neurol* 1995;54:304-10.
227. Ozerdem U, Stallcup WB. Early contribution of pericytes to angiogenic sprouting and tube formation. *Angiogenesis* 2003;6:241-9.
228. Sims DE. Diversity within pericytes. *Clin Exp Pharmacol Physiol* 2000;27:842-6.
229. Eberhard A, Kahlert S, Goede V, Hemmerlein B, Plate KH, Augustin HG. Heterogeneity of angiogenesis and blood vessel maturation in human tumors: implications for antiangiogenic tumor therapies. *Cancer Res* 2000;60:1388-93.
230. Furusato M, Wakui S, Suzuki M, Takagi K, Hori M, Asari M, Kano Y, Ushigome S. Three-dimensional ultrastructural distribution of cytoplasmic interdigitation between endothelium and pericyte of capillary in human granulation tissue by serial section reconstruction method. *J Electron Microsc* (Tokyo) 1990;39:86-91.
231. Bernsen HJ, Rijken PF, Peters H, Raleigh JA, Jeuken JW, Wesseling P, van der Kogel AJ. Hypoxia in a human intracerebral glioma model. *J Neurosurg* 2000;93:449-54.
232. Kusters B, Leenders WP, Wesseling P, Smits D, Verrijp K, Ruiter DJ, Peters JP, van der Kogel AJ, De Waal RM. Vascular endothelial growth factor-A(165) induces progression of melanoma brain metastases without induction of sprouting angiogenesis. *Cancer Res* 2002;62:341-5.
233. Leenders WP, Kusters B, Verrijp K, Maass C, Wesseling P, Heerschap A, Ruiter D, Ryan A, de WR. Antiangiogenic therapy of cerebral melanoma metastases results in sustained tumor progression via vessel co-option. *Clin Cancer Res* 2004;10:6222-30.
234. Semenza GL. Hypoxia-inducible factor 1: master regulator of O₂ homeostasis. *Curr Opin Genet Dev* 1998;8:588-94.
235. Kondo K, Yao M, Yoshida M, Kishida T, Shuin T, Miura T, Moriyama M, Kobayashi K, Sakai N, Kaneko S, Kawakami S, Baba M, Nakaigawa N, Nagashima Y, Nakatani Y, Hosaka M. Comprehensive mutational analysis of the VHL gene in sporadic renal cell carcinoma: relationship to clinicopathological parameters. *Genes Chromosomes Cancer* 2002;34:58-68.
236. Dannenberg H, Speel EJ, Zhao J, Saremaslani P, van Der HE, Roth J, Heitz PU, Bonjer HJ, Dinjens WN, Mooi WJ, Komminoth P, de Krijger RR. Losses of chromosomes 1p and 3q are early genetic events in the development of sporadic pheochromocytomas. *Am J Pathol* 2000;157:353-9.
237. Morrissey C, Martinez A, Zatyka M, Agathangelou A, Honorio S, Astuti D, Morgan NV, Moch H, Richards FM, Kishida T, Yao M, Schraml P, Latif F, Maher ER. Epigenetic inactivation of the *RASSF1A* 3p21.3 tumor suppressor gene in both clear cell and papillary renal cell carcinoma. *Cancer Res* 2001;61:7277-81.
240. Furuta M, Weil RJ, Vortmeyer AO, Huang S, Lei J, Huang TN, Lee YS, Bhowmick DA, Lubensky IA, Oldfield EH, Zhuang Z. Protein patterns and proteins that identify subtypes of glioblastoma multiforme. *Oncogene* 2004;23:6806-14.
241. Vortmeyer AO, Weil RJ, Zhuang Z. Proteomic applications for differential diagnosis of histologically identical tumors. *Neurology* 2003;61:1626-7.

Nederlandse samenvatting

Achtergrond bij dit proefschrift

Hemangioblastomen (HBs) zijn goedaardige tumoren van het centrale zenuwstelsel, die vooral voorkomen in de kleine hersenen. De bijzondere histologische kenmerken van HBs en de intrigerende genetische achtergrond zijn de aanleiding geweest om de studies te verrichten die in dit proefschrift staan beschreven.

In het merendeel van de HBs is er sprake van een sporadische tumor, dat wil zeggen dat er geen associatie is met andere tumoren in het lichaam. Bij ongeveer 25% van de patiënten met een HBs blijkt er echter sprake te zijn van de ziekte van Von Hippel-Lindau (VHL), een erfelijke aandoening die wordt veroorzaakt door een kiembaanmutatie in het *VHL* tumor suppressor gen. Het *VHL*-gen speelt ook een rol in de sporadische tumoren. Er zijn echter verschillende aanwijzingen dat naast het *VHL*-gen andere genen belangrijk zijn voor het ontstaan van sporadische HBs.

We hebben ervoor gekozen ons met name te richten op sporadische HBs, omdat die het meest frequent voorkomen en omdat de genetische achtergrond van deze tumoren niet is opgehelderd. Ontrafeling van de genetische gebeurtenissen die leiden tot HBs kan inzicht geven in de mechanismen die betrokken zijn bij het ontstaan van tumoren in het algemeen, en kan uiteindelijk leiden tot nieuwe behandelstrategieën.

Naast genetische studies worden in dit proefschrift een aantal andere onderzoeken beschreven die betrekking hebben op HBs. Om de achtergrond van de studies uit dit proefschrift beter te begrijpen volgt in het kort een beschrijving van de klinische verschijnselen van HBs en van de ziekte van Von Hippel-Lindau.

Hemangioblastomen

HBs zijn vrij zeldzaam; ze maken ongeveer 2% van alle tumoren in de hersenen uit. HBs bestaan uit tumorcellen waartussen talrijke bloedvaatjes gelegen zijn. De tumor zelf is meestal klein, maar kan een grote cyste vormen (zie **Figuur 1** in Hoofdstuk 1). De tumor met cyste neemt veel ruimte in en veroorzaakt klachten, die bepaald worden door de precieze plaats van de tumor. Omdat HBs vaak voorkomen in de kleine hersenen zijn de meest optredende klachten coördinatiestoornissen, o.a. bij lopen. Daarnaast kan

door druk op de vierde ventrikel een hydrocephalus ontstaan, met klachten van hoofdpijn, misselijkheid en braken. Deze situatie is soms levensbedreigend. De behandeling bestaat uit chirurgische verwijdering van de tumor. In geval van een sporadisch HB is de patiënt met deze ingreep definitief te genezen.

De ziekte van Von Hippel-Lindau

VHL is genoemd naar de Duitse oogarts Eugen von Hippel, die begin twintigste eeuw een HB in het netvlies beschreef, en naar de Zweedse patholoog Arvid Lindau, die in 1926 onderkende dat HBs in netvlies en hersenen samen met bepaalde andere tumoren in het lichaam voorkomen in het kader van één syndroom. VHL is een autosomaal dominant overervende aandoening, gekenmerkt door vaatrijke tumoren en cysten in verschillende organen.

De meest voorkomend zijn HBs in netvlies, kleine hersenen en ruggenmerg, niercelcarcinomen, feochromocytomen (tumoren van de bijnieren), goedaardige tumoren/cysten in nieren, alveesklier, bijbal, bindweefsel rond de baarmoeder en tumoren van het binnenoor.

VHL komt bij ongeveer 1:36.000 personen voor. HBs in het netvlies of in het centrale zenuwstelsel zijn vaak de eerste manifestatie van VHL en openbaren zich gemiddeld op een leeftijd van ongeveer 30 jaar. De meeste patiënten overlijden uiteindelijk aan de gevolgen van een niercelcarcinoom of van een HB in de kleine hersenen. De diagnose VHL is meestal te stellen doordat een patiënt verschillende bij VHL voorkomende tumoren heeft, en omdat de ziekte in zijn familie voorkomt.

Het *VHL*-gen is een tumor suppressor gen, een gen dat in actieve vorm het ontstaan van tumoren onderdrukt. Dit gen is gelokaliseerd op de korte arm van chromosoom 3 (3p25-26). Met DNA diagnostiek kunnen tegenwoordig bijna alle gevallen van VHL worden geïdentificeerd. Hierdoor is een vroege diagnose mogelijk, zelfs voordat een patiënt klachten krijgt. Er zijn richtlijnen opgesteld over welke patiënten voor genetische screening in aanmerking komen. Omdat in 40% van de gevallen een HB de eerste manifestatie van VHL is, wordt geadviseerd om bij alle patiënten met een HB onder de 50 jaar (ook bij afwezigheid van andere tumoren) genetische screening te verrichten. VHL patiënten en patiënten met een hoog risico op VHL, maar bij wie de aandoening nog niet is vastgesteld, dienen volgens vastgestelde richtlijnen

regelmatig onderzocht te worden op het ontstaan van (nieuwe) tumoren, o.a. middels een MRI scan van de hersenen en het ruggenmerg. De verwachting is dat met vroegtijdige opsporing en behandeling van VHL tumoren de levensverwachting toeneemt en de kwaliteit van leven aanzienlijk wordt verbeterd.

Sporadische versus VHL-geassocieerde hemangioblastomen

Histologisch zijn er geen verschillen tussen sporadische HBs en HBs in het kader van VHL. VHL-geassocieerde HBs ontstaan op jongere leeftijd (gemiddeld 33 jaar), komen meestal multipel voor en zijn vaak gelokaliseerd op verschillende plaatsen in het centrale zenuwstelsel (kleine hersenen, hersenstam, ruggenmerg). Bovendien komen bij deze patiënten dikwijls tumoren in andere organen voor, en recidiveren HBs vaker na operatie. De gemiddelde leeftijd van patiënten met een sporadisch HB is 45 jaar. Bij deze patiënten is de tumor meestal gelokaliseerd in de kleine hersenen en worden geen andere tumoren gevonden. De genetische verschillen tussen sporadische en VHL-geassocieerde HBs zijn onderwerp van dit proefschrift.

Genetische achtergrond

Het *VHL*-gen is een tumor suppressor gen, dat in actieve toestand de vorming van tumoren tegengaat. Wanneer het gen niet meer functioneert krijgen normale cellen de kans te transformeren tot een tumorcel. Een gen is gelegen op een chromosoom en omdat een celkern van elk chromosoom (behalve van het Y-chromosoom) twee exemplaren bevat, komt een gen in tweevoud voor (één allel per chromosoom). Volgens de '2-hit' hypothese van Knudson moeten beide allelen geïnactiveerd worden voordat een tumor suppressor gen volledig is uitgeschakeld. Een patiënt met VHL erft van één van zijn ouders een afwijkend (gemuteerd) allel (eerste 'hit'), dat in alle cellen voorkomt (kiembaanmutatie). In de loop van de tijd kan spontaan in het andere allel een afwijking (een zogenaamde somatische mutatie) optreden (tweede 'hit'), zodat beide allelen zijn uitgeschakeld en de cellen ongeremd kunnen gaan groeien. Een persoon met een kiembaanmutatie ontwikkelt niet altijd tumoren, maar loopt daarop wel een grote kans.

Bij patiënten met een sporadische tumor (die dus geen afwijkend allel geërft

hebben) moet er in het loop van het leven tweemaal een 'hit' optreden, die leidt tot twee afwijkende allelen en daardoor inactivatie van het *VHL*-gen. Meestal treedt in het ene allel een mutatie op en gaat het andere allel verloren door verlies van een groter chromosoomdeel waarop dit allel gelegen is. Afwijkingen in het *VHL*-gen worden ook aangetroffen in sporadische HBs, echter minder frequent. In 20-50% van de sporadische HBs wordt een mutatie of verlies van één allel van het *VHL*-gen aangetoond. Inactivatie van beide allelen kan tot nu toe echter maar in ongeveer 10% van de HBs worden aangetoond. Daarom wordt vermoed dat in sporadische HBs andere genen een (grote) rol spelen.

De functies van het VHL-eiwit

Het *VHL*-gen codeert voor een eiwit dat als belangrijkste functie de regulatie van een transcriptie-factor heeft, de 'hypoxia-inducible factor' (HIF-1 α). In tijden van zuurstoftekort in de cellen (hypoxie) stimuleert HIF-1 α de expressie van allerlei genen die ervoor zorgen dat de cellen efficiënt met de beschikbare zuurstof omgaan en dat er extra bloedvaatjes worden gevormd. De vorming van nieuwe bloedvaatjes (angiogenese) wordt o.a. veroorzaakt door verhoogde expressie van 'vasculaire endotheliale groeifactor' (VEGF). Tijdens normale zuurstof-concentraties bindt HIF aan het VHL-eiwit en wordt dan afgebroken door het proteosoom (een enzymcomplex dat eiwitten afbreekt). Indien het *VHL*-gen geïnactiveerd is wordt er geen VHL-eiwit gevormd en wordt HIF-1 α niet afgebroken. De cel gedraagt zich dan alsof er onvoldoende zuurstof aanwezig is en produceert o.a. VEGF. Dit verklaart waarom VHL-geassocieerde tumoren zoals HBs en niercelcarcinomen zo vaatrijk zijn. Andere genen die verhoogd tot expressie worden gebracht reguleren o.a. het suikermetabolisme en de groei van cellen. Het VHL-eiwit reguleert ook de productie van eiwitten die betrokken zijn bij de afbraak van de extracellulaire matrix en bij de regulatie van de cel cyclus (o.a. cycline D1). Het is tot op heden echter nog niet volledig duidelijk of afwezigheid van het VHL-eiwit voldoende verklaring is voor het ontstaan van de VHL-geassocieerde tumoren. Diverse studies suggereren dat andere genen ook belangrijk zijn voor de ontwikkeling van HBs, niercelcarcinomen en feochromocytomen.

Om de genetische achtergrond van sporadische HBs te verduidelijken hebben we gebruik gemaakt van een moleculair genetische techniek 'comparative genomic hybridization' (CGH), waarmee het mogelijk is alle 46 chromosomen van tumorcellen te screenen op afwijkingen. Met CGH kan verlies (loss) of winst (gain) van (een deel van) een chromosoom worden aangetoond. Zo'n (deel van een) chromosoom kan een gen bevatten dat een rol speelt bij het ontstaan van de tumor.

Samenvatting van het proefschrift

In **Hoofdstuk 1** worden het doel en de inhoud van het proefschrift omschreven. Daarnaast bevat het hoofdstuk een overzicht van de klinische verschijnselen en de histopathologische karakteristieken van HBs. De huidige inzichten met betrekking tot de moleculair genetische aspecten van VHL-geassocieerde HBs komen uitgebreid aan de orde. Een verkorte vorm van het literatuur overzicht is in deze Nederlandse samenvatting weergegeven. De moleculair genetische technieken waarvan we gebruik hebben gemaakt in de studies staan kort beschreven in het laatste deel van hoofdstuk 1.

Het genoom van 10 sporadische HBs werd mbv CGH gescreend op afwijkingen in de chromosomen. In **Hoofdstuk 2** worden de resultaten van deze analyse beschreven. In 8 van de 10 tumoren werden chromosomale afwijkingen gevonden; 5 tumoren hadden zelfs afwijkingen op meerdere chromosomen. In 7 van de 10 HBs (70%) werd een verlies van een heel chromosoom 3 (-3) gedetecteerd, in 50% was er sprake van -6, in 30% van -18 of -9, en winst (+) van chromosoom 19 werd eveneens in 30% van de HBs aangetoond. De studie beschreven in hoofdstuk 2 is de eerste studie van zijn soort geweest die CGH analyse van sporadische HBs rapporteert. Op grond van de resultaten hebben we geopperd dat in sporadische HBs een patroon van achtereenvolgende afwijkingen van chromosomen optreedt: verlies van chromosoom 3 (waar het *VHL*-gen zich bevindt), gevolgd door -6, en daarna -9 en/of -18 en/of +19. Dit patroon vertoont gelijkenissen met chromosomale afwijkingen zoals die in de literatuur gerapporteerd zijn in sporadische niercelfcarcinomen en feochromocytomen, tumoren die net als HBs ook kunnen voorkomen in het kader van VHL.

Omdat uit ons eerste onderzoek naar voren kwam dat in sporadische HBs mogelijk andere chromosomale regio's dan chromosoom 3 (met het *VHL*-gen) mede betrokken zijn bij het ontstaan van deze tumoren, hebben we het onderzoek in die richting uitgebreid en een grotere groep sporadische HBs vergeleken met *VHL*-geassocieerde HBs. De CGH resultaten zoals besproken worden in **Hoofdstuk 3** bevestigen de eerder gevonden frequenties van chromosomale afwijkingen: 69% van de 16 sporadische HBs had verlies van chromosoom 3, -6 werd aangetoond in 44% van de tumoren, -18 (of 18q) in 31%, -9 en +19 elk in 25%, en -8 in 19%. Daarnaast kwamen meerdere andere chromosomale afwijkingen voor (**Tabel 1**, Hoofdstuk 3). Er was een opvallend verschil met de 7 *VHL*-geassocieerde HBs; slechts in één tumor werd een -3 gedetecteerd. In deze studie werd ook mutatie analyse van het *VHL*-gen verricht. In alle *VHL*-geassocieerde HBs kon een (kiembaan)mutatie worden aangetoond, zoals verwacht op grond van het feit dat patiënten met *VHL* de geërfde mutatie in alle cellen meedragen. Inactivatie van beide allelen van het *VHL*-gen is nodig om het gen uit te schakelen. In één allel treedt meestal een mutatie op, het andere allel gaat vaak verloren. Zo'n verlies kan alleen worden aangetoond met CGH als een groter deel van het chromosoom verloren gaat. In één *VHL*-geassocieerd HB was een geheel chromosoom 3 verloren gegaan (inclusief het *VHL*-gen), en in die tumor kon dus met zekerheid inactivatie van het *VHL*-gen worden aangetoond. In 5 sporadische HBs (31%) werd een somatische mutatie in het *VHL*-gen gedetecteerd. Omdat 2 van deze tumoren ook verlies van chromosoom 3 (met o.a. het andere *VHL*-allel) hadden, kon uiteindelijk in 2 van de 16 sporadische HBs inactivatie van beide allelen van het *VHL*-gen worden aangetoond. In de andere tumoren met -3 werden geen somatische mutaties gevonden. Het grote verschil in chromosomale afwijkingen en mutaties wijst erop dat sporadische HBs een andere genetische achtergrond hebben, dat wil zeggen dat naast het *VHL*-gen op chromosoom 3 andere genen een rol spelen, terwijl in *VHL*-geassocieerde HBs het *VHL*-gen de belangrijkste factor is in het ontstaan.

Om te kunnen achterhalen welke genen op de afwijkende chromosomen belangrijk zijn in het ontstaan van sporadische HBs, werd in **Hoofdstuk 4** array CGH analyse verricht. Met array CGH kunnen chromosomen op kleine afwijkingen worden gescreend, gedetailleerder dan met conventionele CGH

mogelijk is. Een afwijkend gebiedje kan één of meerdere genen bevattend die betrokken zijn bij het ontstaan van de tumor. In 5 sporadische HBs werden 3 regio's gevonden die mogelijk relevante genen bevatten. Twee genen zijn met name interessant: het *LSAMP* gen (limbic system-associated membrane protein) dat op chromosoom 3q13.3 ligt en mogelijk een rol speelt bij het niercelcarcinoom, en het *FEZ1/LZTS1* gen (leucine zipper, putative tumor suppressor 1) op chromosoom 8p22 dat betrokken is bij de celdeling en dat de groei van verschillende typen tumoren blijkt te beïnvloeden. De resultaten van de array CGH analyse dienen nog te worden bevestigd.

In de afgelopen jaren is aangetoond dat het VHL-eiwit behalve HIF-1 α ook een aantal andere genen reguleert, waaronder het *CCND1* gen dat codeert voor het eiwit cycline D1. Dit eiwit is betrokken bij de regulatie van de celcyclus en de celdeling. Overexpressie van cycline D1 leidt tot ongecontroleerde celgroei en de vorming van tumoren. In **Hoofdstuk 5** hebben we onderzocht of in HBs een verhoogde expressie van cycline D1 aanwezig was. In sporadische HBs vonden we een zeer wisselende en soms sterk verhoogde aanwezigheid van cycline D1. Het *CCND1* gen bevat een veel voorkomend G \rightarrow A polymorfisme (normaal voorkomende variant), dat geassocieerd is met een vroeg ontstaan en een slechte prognose van verschillende maligniteiten. In de literatuur is gesuggereerd dat VHL patiënten met een of twee G-allelen meer HBs in het netvlies en een verhoogde gevoeligheid voor HBs in het zenuwstelsel hebben dan patiënten met A-allelen. Dit zou betekenen dat in HBs vaker een G-allel wordt aangetroffen dan op grond van de verdeling in de algemene populatie mag worden verwacht. In onze (kleine) studie was dat niet het geval, zodat we niet kunnen bevestigen dat het *CCND1* genotype het voorkomen van HBs beïnvloedt.

Er zijn verschillende moleculair genetische technieken beschikbaar om afwijkingen op chromosomen of in genen aan te tonen. Een kleine afwijking in een gen, zoals een kiembaanmutatie, wordt met mutatie analyse aangetoond. Verlies van (een deel van) een chromosoom kan worden aangetoond met CGH of met LOH (loss of heterozygosity). Deze technieken staan kort beschreven in het eerste hoofdstuk. In **Hoofdstuk 6** beschrijven we een patiënt met VHL die in de loop der jaren verschillende tumoren ontwikkelde, waaronder meerdere HBs en een niercelcarcinoom. Aan het eind van zijn

leven was er sprake van een grote weinig gedifferentieerde tumor in de nier-regio met meerdere uitzaaiingen, waarvan niet duidelijk was of het oorspronkelijk een niercelcarcinoom betrof of een feochromocytoom (een tumor uitgaande van de bijnieren). Gedifferentieerde tumoren zijn soms moeilijk histologisch te categoriseren. Omdat tegenwoordig steeds meer informatie beschikbaar komt over de specifieke genetische afwijkingen die in tumoren worden gevonden, hebben we de tumoren van deze patiënt gekarakteriseerd met behulp van CGH, LOH en mutatie analyse van het *VHL*-gen. De resultaten van de moleculair genetische analyses bevestigden dat deze patiënt een gedifferentieerd niercelcarcinoom had. Deze casus illustreert dat moleculair genetisch onderzoek een waardevol hulpmiddel kan zijn bij het stellen van een diagnose wanneer dat met standaard histologisch en immunohistochemisch onderzoek niet mogelijk is. Het stellen van de juiste diagnose kan leiden tot eerdere en betere behandeling van de patiënt.

In **Hoofdstuk 7** wordt een nieuwe computer methode beschreven waarmee microscopische weefselstructuren 3-dimensionaal in beeld gebracht kunnen worden. In series van (2D) histologische coupes wordt met een (immunohistochemische) marker de structuur waarvan een 3D reconstructie moet worden gemaakt geaccentueerd. Vervolgens worden deze beelden één voor één opgeslagen en verwerkt tot een 3D figuur.

Wij hebben ons, vanwege onze interesse in bloedvatvorming in tumoren, vooral gericht op de 3D reconstructie van bloedvaatjes. In tumoren worden continu nieuwe bloedvaatjes gevormd (angiogenese), omdat tumorcellen voor hun groei afhankelijk zijn van voldoende aanvoer van zuurstof en voedingsstoffen. Angiogenese is een belangrijk onderzoeksgebied voor de ontwikkeling van nieuwe middelen tegen tumoren, en medicamenten die bloedvatnieuwvorming tegengaan worden momenteel bij de behandeling van patiënten met bepaalde tumoren toegepast.

De wand van de bloedvaten is opgebouwd uit endotheelcellen, die omgeven zijn door steuncellen, de pericyten. Beide onderdelen van de vaatwand werden zichtbaar gemaakt met specifieke markers (anti-CD34 voor endotheelcellen; α -smooth muscle actin voor geactiveerde pericyten). Er werden 3D reconstructies gemaakt van het vaatbed van normale witte en grijze stof van de hersenen, van een HB en van een glioblastoma multiforme (GBM). Een GBM is een kwaadaardige hersentumor die o.a. gekenmerkt wordt door de

aanwezigheid van bijzondere vaatstructuren, zogenaamde 'glomeröide microvasculaire proliferaties'. De 3D reconstructies illustreren de typische vasculaire netwerken van beide tumoren (zie **Figuur 2**, Hoofdstuk 7) en geven meer inzicht in de microvascularisatie van tumoren.

Met deze nieuwe methode is het tevens mogelijk van meerdere microscopische structuren simultaan een 3D reconstructie te vervaardigen. De onderlinge 3-dimensionale samenhang tussen verschillende structuren worden daardoor zichtbaar gemaakt. Voorbeelden hiervan zijn de relatie tussen endotheelcellen en geactiveerde pericyten (gladde spiercellen) in de vaatwandjes van de normale cerebellaire grijze stof, in een HB en in een GBM (**Figuur 4 en 5**, Hoofdstuk 7). Opvallend is de uitgebreide aanwezigheid van geactiveerde pericyten rondom de endotheelcellen in het HB, hetgeen past bij een actief proces van bloedvatnieuwvorming.

In **Hoofdstuk 8** ten slotte wordt een samenvatting van de studies gegeven en worden de resultaten bediscussieerd.

Conclusies en toekomstig onderzoek

Samenvattend hebben de studies uit dit proefschrift het volgende aangetoond:

- Er bestaan grote verschillen in het voorkomen van chromosomale afwijkingen in sporadische HBs ten opzichte van VHL-geassocieerde HBs, aangetoond met CGH
- Er zijn multiële chromosomale afwijkingen aanwezig in sporadische HBs, met name verlies van chromosoom 3, 6, 8, 18, 9 en winst van chromosoom 19
- Verlies van een heel chromosoom 3 komt vaker voor in sporadische dan in VHL-geassocieerde HBs
- Verlies van chromosoom 6 is, na -3, de meest voorkomende afwijking in sporadische HBs

- Verlies van chromosoom 6 is geassocieerd met -3 of met een somatische mutatie van het *VHL*-gen, hetgeen zou kunnen duiden op een belangrijke rol van genen op dit chromosoom 6 in het ontstaan van sporadische HBs.
- Somatische VHL mutaties treden op in ongeveer 31% van sporadische HBs.
- Drie kandidaat chromosomale regio's, geïdentificeerd met behulp van array CGH, bevatten genen die mogelijk betrokken zijn bij HBs.

Deze resultaten wijzen erop dat inactivatie van het *VHL*-gen onvoldoende is voor het ontstaan van sporadische HBs, en dat VHL-geassocieerde HBs en sporadische HBs deels een andere genetische achtergrond hebben.

De studies beschreven in dit proefschrift hebben de moleculair genetische gebeurtenissen die ten grondslag liggen aan het ontstaan van sporadische HBs niet geheel kunnen ophelderen. Door de komst van nieuwe methoden om het pad van DNA (chromosoom/gen) naar RNA naar eiwit in kaart te brengen zijn er meerdere mogelijkheden voor verder onderzoek. Een veelbelovende methode om inzicht te krijgen in de processen die aanleiding geven tot tumorgroei is bijvoorbeeld proteomics, waarmee eiwitprofielen van tumoren kunnen worden gemaakt. Omdat het uiteindelijk de eiwitten zijn die een cel aansturen ligt het voor de hand te onderzoeken welke eiwitten in een bepaalde tumorcel al dan niet aanwezig zijn, en wat hun functie is. Verschillen in eiwitprofielen tussen sporadische en VHL-geassocieerde HBs kunnen mogelijk opheldering geven over de processen die leiden tot deze tumoren.

De door ons ontwikkelde techniek van 3D reconstructie van bloedvaatjes zal worden gebruikt voor het verder bestuderen van vaatnieuwvorming en het effect van (anti-angiogenese) therapie in experimentele tumormodellen.

Dankwoord

Dit proefschrift is tot stand gekomen dankzij de enthousiaste samenwerking van verschillende disciplines. Graag wil ik op deze plaats allen die een bijdrage hebben geleverd hartelijk bedanken.

Mijn promotor en hoofd van onze afdeling, George Padberg, ben ik zeer erkentelijk voor de ruimte en steun die ik heb gekregen bij het verrichten van de studies beschreven in dit proefschrift. Beste George, met onvermoeibare inzet probeer jij voor eenieder van ons de optimale werkomgeving te creëren, waarin alle ambities kunnen worden verwezenlijkt. Veel dank daarvoor, en voor je bereidheid mee te denken als de zaken vast dreigden te lopen.

Mijn copromotores Pieter Wesseling en Judith Jeuken ben ik veel dank verschuldigd. Zij zijn de inspirators van het onderzoek geweest. Beste Pieter, jouw fascinatie met de pathobiologie van hersentumoren en met hemangioblastomen in het bijzonder werkte zeer aanstekelijk. Dit proefschrift is het resultaat van de door jou aangezette poging het 'enigma' hemangioblastoom op te lossen. Heel veel dank voor je enthousiaste en uitstekende begeleiding.

Judith Jeuken en Sandra Boots-Sprenger, mijn 'co-copromotor', wil ik heel hartelijk danken voor de waardevolle lessen in de moleculaire genetica en in het verrichten van wetenschappelijk onderzoek. Beste Judith en Sandra, dank voor alle uren discussie over de valkuilen van de moleculair genetische diagnostiek. Veel dank voor alle arbeid in het lab en voor jullie onmisbare bijdragen aan de artikelen. Met jullie enthousiasme, doorzettingsvermogen en precisie zijn jullie een voorbeeld voor eenieder die wetenschappelijk onderzoek doet.

Alle coauteurs wil ik hartelijk danken voor hun waardevolle bijdragen. De expertise van de medeonderzoekers en de deskundigheid van de analisten op de afdelingen Pathologie en Antropogenetica zijn van onschatbare waarde geweest voor het onderzoek.

Enkele medeonderzoekers wil ik met name noemen, zonder de anderen te kort te willen doen. Bram Jacobs, beste Bram, dank voor je noeste arbeid in het lab. Pas achteraf realiseer ik me dat je het vast niet altijd makkelijk hebt

gehad met drie veeleisende dames op de achtergrond. Veel succes met je huidige onderzoek.

Cathy Maass verdient veel lof voor haar immunohistochemische kleuringen. Beste Cathy, je zag het steeds opnieuw als een uitdaging om aan onze hooggespannen verwachtingen tegemoet te komen, heel veel dank daarvoor.

Jeroen van der Laak, beste Jeroen, ik ben je veel dank verschuldigd voor je geduldige uitleg over het digitaliseren van de histologische coupes. De prachtige 3D beelden zijn voornamelijk aan jouw inventiviteit op software gebied te danken.

Roland Kuiper, beste Roland, dank voor je onmisbare expertise op het gebied van de array CGH. Het is prettig te beseffen dat we dit onderzoek voorlopig nog voort kunnen zetten.

De Nederlandse samenvatting is gecorrigeerd door Dorien Langenkamp. Beste Dorien, veel dank daarvoor en voor de uitstekende secretariële ondersteuning van jou en je collega's op de poli en vijfde verdieping.

Mijn collega's dank ik voor hun interesse in mijn proefschrift en voor het creëren van ruimte om het af te kunnen ronden. Beste collega's, dank voor de inspirerende, vriendschappelijke en collegiale sfeer op onze afdeling. De arts-assistenten dragen in belangrijke mate aan deze positieve werkomgeving bij. Dankzij jullie allen is onze afdeling Neurologie een fantastische plek om te werken, dank daarvoor. Mijn collega neuro-oncoloog Arnoud Kappelle wil ik in het bijzonder bedanken. Beste Arnoud, dank voor de uitstekende samenwerking en voor de vele uren (maanden) waarneming als ik om uiteenlopende redenen afwezig was.

Mijn paranimfen, Agnita Boon en Trudy Jonges, dank ik voor hun vriendschap en hun bereidheid mij tijdens de promotie bij te staan. Beste Agnita en Trudy, als vriendinnen, moeders van kleine kids, en als neuroloog respectievelijk patholoog, hebben we veel stof om regelmatig bij te praten. Ik hoop dat ik daarvoor nu iets meer tijd krijg.

Dit proefschrift is opgedragen aan mijn ouders, als blijk van mijn dank voor de liefdevolle zorg waarmee zij mij altijd hebben omringd. Lieve pa en ma, dankzij jullie grenzeloze steun en vertrouwen ben ik uiteindelijk neuroloog geworden, en heb ik dit proefschrift kunnen schrijven. Ik dank jullie voor alles.

Ten slotte dank ik mijn drie allerliefste mannen Hugo, Sem en Sander voor hun vertrouwen en hun liefde.

Curriculum vitae

Anja Gijtenbeek werd geboren op 30 juli 1962 te Halsteren. In 1980 behaalde zij haar eindexamen Gymnasium- β aan het St. Odulphuslyceum te Tilburg. In datzelfde jaar begon zij met de studie Geneeskunde aan de Universiteit van Amsterdam, alwaar zij het artsexamen behaalde in 1987. Daarna werkte zij als AGNIO neurologie in het Slotervaartziekenhuis te Amsterdam en in het Erasmus MC te Rotterdam, en vervolgens als AGNIO neurochirurgie in Rotterdam, in het UMC Groningen en in het VUmc te Amsterdam. Uiteindelijk startte zij in 1993 met de opleiding tot neuroloog in het MC Haaglanden (Westeinde Ziekenhuis) te Den Haag (opleider: J.Th.J. Tans). De aantekening klinische neurofysiologie werd in hetzelfde ziekenhuis behaald. Tevens werd tijdens de opleiding een stage neuro-oncologie gelopen in de Daniel den Hoed kliniek te Rotterdam.

Sinds 1 mei 1999 is zij geregistreerd als neuroloog en verbonden aan het Universitair Medisch Centrum St Radboud te Nijmegen. Haar aandachtsveld binnen de neurologie is de neuro-oncologie.

Anja is gehuwd en heeft twee zonen.

List of publications

- Gijtenbeek JM, Hop WC, Braakman R, Avezaat CJ. Surgery for intracranial meningiomas in elderly patients. *Clin Neurol Neurosurg* 1993;95:291-5.
- Gijtenbeek JM, van den Bent MJ, Vecht CJ. Cyclosporine neurotoxicity: a review. *J Neurol* 1999;246:339-46.
- Gijtenbeek JM, Gabreels-Festen AA, Lammens M, Zwarts MJ, van Engelen BG. Mononeuropathy multiplex as the initial manifestation of neurofibromatosis type 2. *Neurology* 2001;56:1766-8.
- Sprenger SH, Gijtenbeek JM, Wesseling P, Sciot R, van Calenbergh F, Lammens M, Jeuken JW. Characteristic chromosomal aberrations in sporadic cerebellar hemangioblastomas revealed by comparative genomic hybridization. *J Neurooncol* 2001;52:241-7.
- Gijtenbeek JM, Rosenblum MK, DeAngelis LM. Primary central nervous system T-cell lymphoma. *Neurology* 2001;57:716-8.
- Hofstee DJ, Gijtenbeek JM, Hoogland PH, van Houwelingen HC, Kloet A, Lotters F, Tans JT. Westeinde sciatica trial: randomized controlled study of bed rest and physiotherapy for acute sciatica. *J Neurosurg* 2002;96:45-9.
- Gijtenbeek JM, Brouwer HI, Boerman RH, Wiggenraad RG, Vecht CJ, Smitt PA. Extensive epidural cufflike growth of malignant pleural mesothelioma causing spinal cord compression. *J Thorac Cardiovasc Surg* 2002;124:200-2.
- Dorresteyn LD, Kappelle AC, Renier WO, Gijtenbeek JM. Anti-amphiphysin associated limbic encephalitis: a paraneoplastic presentation of small-cell lung carcinoma. *J Neurol* 2002;249:1307-8.
- Gijtenbeek JM, van Eck AT, van der Maazen RW, Koetsveld AC, Punt CJ. De behandeling van hersenmetastasen. *Ned Tijdschr Geneeskd* 2002;146:1724-9.

- Gijtenbeek JM, Jacobs B, Sprenger SH, Eleveld MJ, van Kessel AG, Kros JM, Sciot R, van Calenbergh F, Wesseling P, Jeuken JW. Analysis of von Hippel-Lindau mutations with comparative genomic hybridization in sporadic and hereditary hemangioblastomas: possible genetic heterogeneity. *J Neurosurg* 2002;97:977-82.
- Bienfait HP, Gijtenbeek JM, van den Bent MJ, de Bruin HG, Voogt PJ, Pillay M. Cerebral venous and sinus thrombosis with cerebrospinal fluid circulation block after the first methotrexate administration by lumbar puncture. *Neuroradiology* 2002;44:929-32.
- Hofstee DJ, Gijtenbeek JM, Hoogland PH, van Houwelingen HC, Kloet A, Lotters F, Tans JT. Bedrust en fysiotherapie geen meerwaarde bij acute lumbosacrale radiculare pijn; een gerandomiseerd, klinische studie. *Ned Tijdschr Geneesk* 2003;147:249-54.
- Gijtenbeek JM, Jacobs B, Boots-Sprenger S, Bonne A, Lenders J, Kusters B, Wesseling P, Jeuken JW. Molecular analysis as a tool in the differential diagnosis of VHL disease-related tumors. *Diagn Mol Pathol* 2005;14:115-20.
- Gijtenbeek JM, Boots-Sprenger SH, Franke B, Wesseling P, Jeuken JW. Cyclin D1 genotype and expression in sporadic hemangioblastomas. *J Neurooncol* 2005;74:261-6.
- Gijtenbeek JM, Wesseling P, Maass C, Burgers L, van der Laak JAWM. Three-dimensional reconstruction of tumor microvasculature: Simultaneous visualization of multiple components in paraffin-embedded tissue. *Angiogenesis* 2005;8:297-305.
- van de Langerijt B, Gijtenbeek JM, de Reus HPM, Geurts-Moespot A, Hendriks JCM, Kappelle AC, Verbeek MM. Cerebrospinal fluid vascular endothelial growth factor and tissue-type plasminogen activator as biomarkers for patients with leptomeningeal metastasis. Accepted for publication in *Neurology*.

